Palaeobiodiversity and Palaeoenvironments (2022) 102:383–418
https://doi.org/10.1007/s12549-021-00508-w

SENCKENBERG

ORIGINAL PAPER

The boundary between the Inthanon Zone (Palaeotropics) and the Gondwana-derived Sibumasu Terrane, northwest Thailand—evidence from Permo-Triassic limestones and cherts

Mongkol Udchachon[1] · Hathaithip Thassanapak[2] · Clive Burrett[1] · Qinglai Feng[3]

Received: 9 March 2021 / Revised: 29 April 2021 / Accepted: 14 July 2021 / Published online: 15 November 2021

Abstract

The boundary between tropical Permian faunas of the Inthanon Zone and Gondwana faunas in far NW Thailand has been long debated. Both the Late Devonian and the Permian Gondwanan platform margins lie a few kilometres west of the Mae Yuam/Mae Sariang Fault (MYMS FZ). In the Permian, the margin grades eastwards into hemipelagic radiolarites along the MYMS FZ and westwards into the Thitsiphin carbonate platform of Myanmar. The area west of the MYMS FZ is the Northern part of the West Thailand Region (NWTR). Quartz-rich limestones of Roadian age in the NWTR are succeeded by deep-water platform limestones in the NWTR and shallow-water carbonates in Myanmar and contain a distinctive fusulinid fauna including *Monodiexodina* which does not occur in palaeotropical terranes. A 300-m section of limestone 10 km west of the MYMS FZ contains Wordian microfauna and is placed in a deep shelf to slope environment. Carboniferous to Triassic continental margin, hemipelagic, non-hydrothermal, radiolarian cherts outcrop on either side of the Mae Yuam valley and were deposited on the upwelling margins of an ocean separating the Inthanon Zone and Sibumasu Terrane. The widely accepted allochthon model proposes that the Inthanon Zone Devonian-Triassic radiolarites were pelagic and deposited on a subducting ocean that supported seamounts with Visean to Permian tropical shallow-water carbonates lasting at least 90 my. We suggest an alternative hypothesis where the radiolarites of the Inthanon Zone were continental margin as shown by their geochemistry and deposited in deeper parts of small extensional basins with limited volcanism between long-lived, isolated carbonate platforms.

Keywords Limestone · Permian · Conodonts · Radiolarians · Triassic · Chert geochemistry

✉ Hathaithip Thassanapak
bthaithip@yahoo.com

Mongkol Udchachon
mongkol.c@msu.ac.th

Clive Burrett
cfburrett@gmail.com

Qinglai Feng
qinglaifeng@cug.edu.cn

[1] Palaeontological Research and Education Centre, Mahasarakham University, Maha Sarakham 44150, Thailand

[2] Applied Palaeontology and Biostratigraphy Research Unit, Department of Biology, Faculty of Science, Mahasarakham University, Maha Sarakham 44150, Thailand

[3] State Key Laboratory of Geological Processes and Mineral Resources, China University of Geosciences, Wuhan, Hubei 430074, People's Republic of China

Introduction

We summarise previous studies and provide new data on the Permian and Triassic sedimentary rocks and palaeontology of the area in northwest Thailand close to the north-south trending Mae Yuam Fault zone and assess these and previously published data on the boundary between the Gondwana-derived Sibumasu Terrane and the palaeo-tropical, Palaeotethyan, Carboniferous-Permian of the Inthanon Zone. We confirm that the Mae Yuam/Mae Sariang fault zone (MYMS FZ) traces the boundary between the Sibumasu Terrane and the Palaeotethyan Inthanon Zone, and we suggest a new and tentative model for the supposed late Palaeozoic allochthonous oceanic seamounts of the Inthanon Zone and their intervening cherts and underlying quartz-sandstones.

Extending the work of Ridd (1971, 1980), Stauffer (1974), Hutchison (1975) and Mitchell (1977), Bunopas (1982) and Bunopas and Vella (1983) divided most of mainland South-East Asia into the Shan-Thai and Indochina terranes, mainly

based on their very different late Carboniferous to early Permian histories with Shan-Thai having cool water, Gondwana faunal and sedimentological affinities and Indochina having tropical Tethyan (or 'Cathaysian') faunal affinities. It was established that the Shan-Thai Terrane was affected by Gondwana glaciation in the late Carboniferous and early Permian with marine faunas gradually becoming temperate and then tropical as the terrane rifted off Gondwana and drifted northwards during the middle to late Permian to become fully tropical by the late Permian (Baird et al. 1993; Shi and Archbold 1995; Fontaine et al. 2012; Angiolini et al. 2013; Thassanapak et al. 2020). Before 1980, the timing of the separation of the 'Thai-Malay Peninsula Block' (later 'Shan Thai' Terrane) from Gondwana and its collision with the Indochina block were unclear. Ridd (1980) documented for the first time that separation from Gondwana occurred in the middle-Palaeozoic and collision with Indochina was a Triassic event. Bunopas (1982) suggested that Shan-Thai rifted from the northwest Australian sector of Gondwana in the early Permian and collided with the composite Indochina Terrane in the Late Triassic (Norian). The Shan-Thai Terrane concept was explicitly expanded to include parts of western Yunnan Province, China, and Sumatra, Indonesia, and given the acronym Sibumasu (Metcalfe 1984) (Fig. 1). However, much of northern Thailand, previously included in the Shan-Thai and Sibumasu terrane concepts, was found to have tropical late Carboniferous to late Permian faunas characterised by diverse fusulinids, diverse calcareous algae and hermatypic corals (faunas variously biogeographically classified as Palaeotethyan, Tethyan, Cathaysian or Indochinese), associated with or overlying 'oceanic' basalts and was eventually interpreted as an allochthonous nappe or nappe pile emplaced on a Sibumasu autochthon or 'basement' in the Triassic and renamed the Inthanon Terrane or Inthanon Zone (Barr and MacDonald 1991; Caridroit et al. 1992; Fontaine et al. 1993, 2009; Ueno and Hisada 2001; Ueno 2003; Barber et al. 2011; Ueno and Charoentitirat 2011; Hara et al. 2021; Metcalfe et al. 2017) (Fig. 1).

In that widely accepted 'allochthon' model (summarised by Barber et al. (2011), fig. 19.15), the Inthanon Zone consists of autochthonous or para-autochthonous Sibumasu Cambrian to Permian sedimentary rocks over-thrust by strongly allochthonous Lower Devonian to Middle Triassic oceanic sediments, including 'pelagic' radiolarian cherts and mafic volcanics with tropical Carboniferous to possibly lower Triassic limestones capping oceanic volcanic seamounts (Barr and McDonald 1991; Caridroit et al. 1992; Ueno 1999, 2003; Feng et al. 2008; Kamata et al. 2009; Barber et al. 2011; Ridd 2015b; Metcalfe et al. 2017; Morley 2018).

Barber et al. (2011, their fig. 19.1) extended the Inthanon Zone to include part of eastern Thailand (west of the Klaeng Fault), and parts of southern Thailand and northern Malaysia. However, these areas have typically Sibumasu Terrane stratigraphy and faunas and do not contain the Devonian-Triassic mélange and palaeotropical Carboniferous-Permian carbonates, typical of the Inthanon Zone.

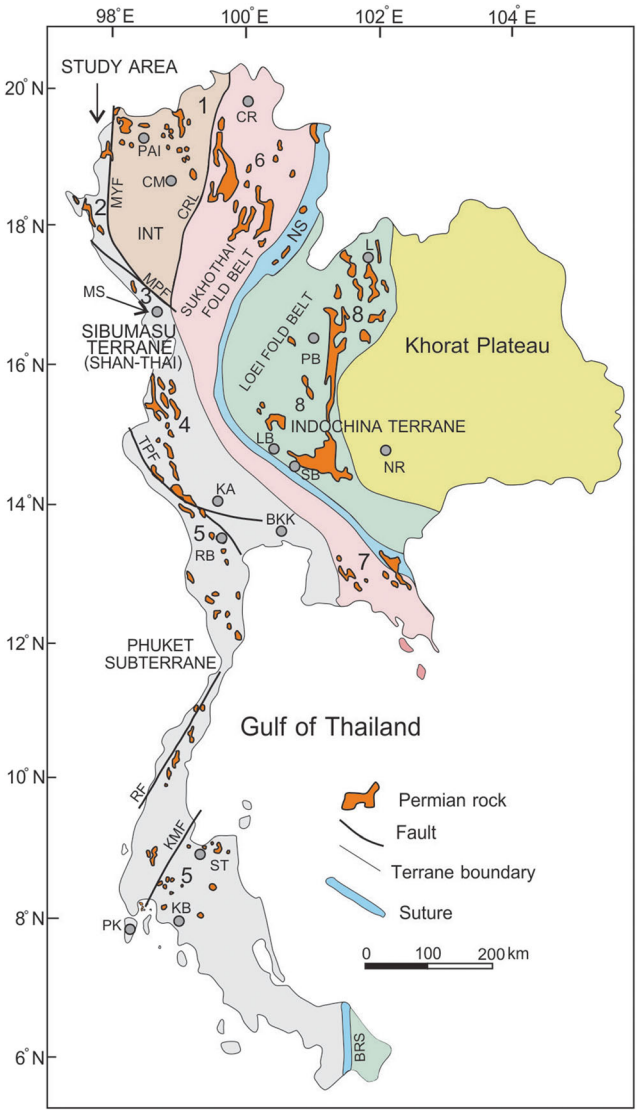

Fig. 1 Tectonic units in Thailand showing the distribution of Permian sedimentary rocks, from Thassanapak et al. (2020). Terranes from west to east are Sibumasu, Inthanon (or Zone) Sukhothai Terrane (? Carboniferous to Permian-Triassic volcanic arc with Triassic deep-water basins, Thassanapak et al. 2017), Nan (NS) (dismembered ophiolitic suture zone), Indochina (composite terrane with Ordovician to Triassic arc magmatism). This map also shows the distribution of Permian limestone units in Thailand. The Ratburi Group and its correlates are distributed across the Sibumasu Terrane, the Doi Chiang Dao Formation in the Inthanon Zone or Terrane, the Saraburi Group in the Indochina Terrane and the Ngao Group in the Sukhothai Terrane. *1* Doi Chiang Dao Formation, *2* Phawar Formation or Doi Pha War Fm, *3* Mae Tho Formation, *4* Khao Plukmu Formation, *5* Ratburi Group, *6* Pha Huat Formation (Ngao Group), *7* Khao Phrik 'unit', *8* Saraburi Group. Other abbreviations are *BKK* Bangkok, *BRS* Betong Raub Suture, *CM* Chiang Mai, *CR* Chiang Rai, *INT* Inthanon Zone, *KA* Kanchanaburi Province, *KB* Krabi, *KMF* Klong Marui Fault, *L* Loei, *LB* Lopburi, *MS* Mae Sot, *NR* Nakhon Ratchisima (Khorat), *NS* Nan Suture, *PB* Phetchabun, *PK* Phuket, *RB* Ratburi, *RF* Ranong Fault Zone, *SB* Saraburi, *ST* Surat Thani, *TPF* Three Pagodas Fault

Ridd (2015a) reviewed the literature relevant to the boundary between the main Sibumasu Terrane and the Inthanon Zone. He emphasised that the autochthonous lower to middle Palaeozoic of the Inthanon Zone belongs to the Sibumasu Terrane and therefore included the older rocks of the Inthanon Zone within Sibumasu. Although we provisionally accept this conclusion, and accept that both terranes derived from Gondwana (Burrett et al. 1990, 2014; Khin et al. 2014), we are not convinced that the evidence of probably Cambrian siliciclastics and fossiliferous Ordovician limestone is sufficient to place these in Sibumasu as such sequences are found along the early Palaeozoic margin of Gondwana on several terranes (Burrett et al. 2014, 2017; Lin et al. 2013; Thassanapak et al. 2018; Loydell et al. 2019). The age spectrum of zircons from one sample of late Permian sandstone from the NWTR is not only similar to samples from the Inthanon Zone (Dew et al. 2021) but also from the Truong Son Terrane of Indochina suggesting that many terranes received similar-aged zircons when they were arrayed along the Gondwana margin before rifting (Burrett et al. 2014). The uppermost Silurian-Lower Devonian section described by Burrett et al. (1986) from the southern Inthanon Zone is not similar faunally to coeval sections in Sibumasu. Moreover and crucially, the Inthanon Zone lacks the cool-water upper Palaeozoic succession and faunas that are generally characteristic of Sibumasu and the glacial-temperate sediments and faunas of Ridd's (2015a) subdivision of Sibumasu-the Sibuma Terrane. All known Inthanon Zone Carboniferous to Permian limestone faunas and floras are fully tropical (Fontaine et al. 2009). Indeed, in the overthrust (or allochthon) model, the Sibumasu 'basement' of the Inthanon Zone appears to lack autochthonous Permian sedimentary rocks. The western boundary of the Inthanon Zone is defined by strongly contrasting Permian sediments across the MYMS FZ.

The eastern boundary of the Inthanon Zone is taken as the Chiang Rai Line (CRL on Fig. 1) or the Chiang Mai-Chiang Rai Line/Suture (Mitchell 1977; Barr and MacDonald 1991; Metcalfe et al. 2017) which is the putative but cryptic and variably demarcated sutural contact with the Palaeozoic to Norian volcanic arc Sukhothai Terrane. The western boundary was placed by Barr and MacDonald (1991) at or near to the Mae Yuam Fault (also referred to as the Mae Sariang Fault, Mae Hong Son Fault or the Mae Sariang-Mae Hong Son Fault) (Figs. 1–3).

The Mae Yuam Fault is a splay of the transcurrent Mae Ping Fault (Figs. 1, 2(a)) and movement is Cenozoic and, most recently, dextral (Searle and Morley 2011). Earthquake locations show that it is still active (Wiwegwin et al. 2014; Kosuwan et al. 2019) and hot springs and earthquake epicentres follow the north-south fault-trend, in a straight line, 20 km northwards into Myanmar (Fig. 2) (Sarapirome and Khundee 1994). It is difficult to be sure whether or not the Mae Yuam Fault is also a Palaeozoic or Late Triassic fault or suture reactivated in the Cenozoic. Certainly, there are N-S elongated bodies or blocks of a variety of Cambrian to Triassic sedimentary rocks distributed along the length of the fault (Fig. 2) and these are probably fault slices as shown for some of these blocks on Thai geological maps (e.g. Department of Mineral Resources 1999). Gardiner et al. (2016a) interpret the Mae Yuam Fault as a high-angle transcurrent fault and the Mae Sariang Fault as a low-angle thrust zone (Fig. 3). This fault arrangement would account for the numerous kilometre-scale blocks of Palaeozoic-Triassic sedimentary rocks that are found along the Mae Yuam Valley and to the north (Figs. 2, 3) and we accept their interpretation here (Fig. 3). The surface trace of the Mae Sariang thrust fault is parallel to the near-vertical Mae Yuam Fault (Figs. 2, 3) and in three dimensions it is the Mae Sariang Fault that is, therefore, the probable significant structural boundary between Inthanon and Sibumasu (Fig. 3). However, in two-dimensional map view, it is currently impossible to separate the surface traces of these two faults and we refer to them together as the Mae Yuam-Mae Sariang Fault Zone or MYMS FZ. Barr and MacDonald (1991) placed the area, west of the MYMS FZ in their Western Thailand Terrane (equivalent to the West Tectonic Province of Northern Thailand of Bunopas (1982)) and we will adopt their terminology and refer to the area west of the MYMS FZ in Thailand as the Northern West Thailand Region or NWTR.

Several authors have placed the western boundary of the Inthanon Zone a little to the west of the MYMS FZ (Metcalfe et al. 2017, their fig. 2) or several kilometres west of the fault (e.g. Königshof et al. 2012; Gardiner et al. 2016b; Racki et al. 2019). The Gondwana-Palaeotethyan margin was drawn by Myo Min et al. (2001) to include parts of the southern NWTR, to exclude the northern NWTR and to head northwest across Shan State within Myanmar. In this paper, we assess published, unpublished and often neglected German and Thai geological survey reports and present new data from the NWTR on Permian limestones and their microfauna and the geochemistry of Permian and Triassic radiolarian cherts. We suggest that the MYMS FZ is most likely the reactivated boundary between the Inthanon Zone and Sibumasu Terrane as originally proposed by Barr and MacDonald (1991) and is also the palaeobiogeographic boundary between Sibumasu-Baoshan-South Qiangtang and typical Palaeotethyan or 'Cathaysian' fusulinid faunas in Inthanon, Sukhothai and Indochina (Zhang et al. 2020).

Previous regional studies on the NWTR and the Sibumasu Terrane-Inthanon Zone boundary

The NWTR is a relatively high relief, landslide prone and a heavily vegetated region containing few roads or tracks heading west from the Mae Yuam Valley towards the Thailand-Myanmar border. As a result, many of the published papers have been based on sections along or close to the main north-

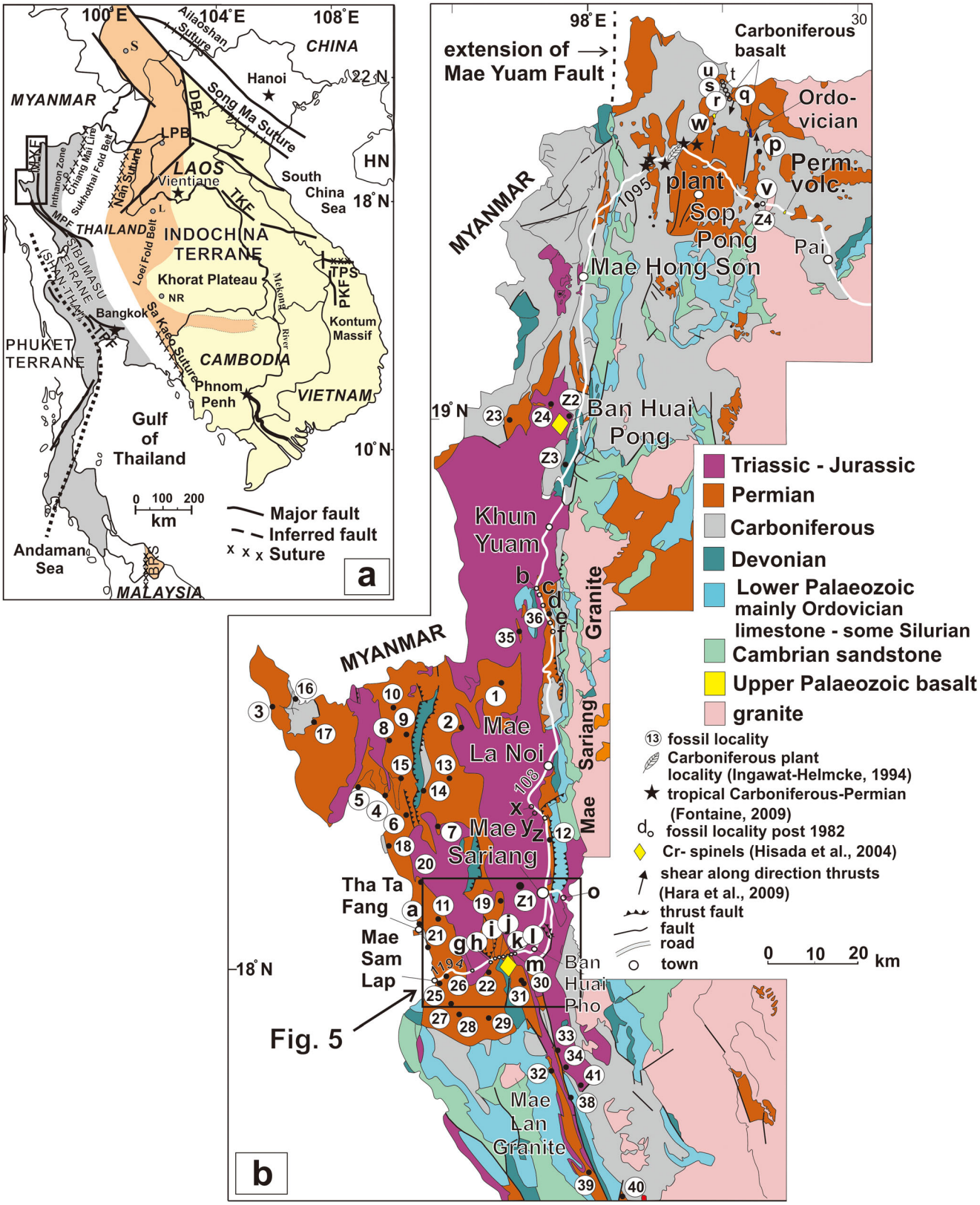

south Highway 108 which follows the flat plain of the Mae Yuam Valley and the area further north (Figs. 2, 4(a, b)). Large areas to the west of Highway 108, both in Thailand and in Myanmar, remain sparsely explored geologically.

Fig. 2 **a** Simplified general map of mainland SE Asia showing terranes and study area in NW Thailand. Orange area is Loei-Phetchabun Terrane which is part of the composite Indochina Terrane (see Khin et al. 2014). Grey is Sibumasu Terrane. The dotted line indicates the eastern margin of the characteristically glacial early Permian Phuket Terrane subdivision of the Sibumasu Terrane (Ridd 2015a). The Chiang Mai Line equals the Chiang Rai line of various authors. *DBF* Dien Bien Phu Fault, *MYF* Mae Yuam Fault, *NS* Nan Suture, *NR* Nakhon Ratchisima (Khorat), *PKF* Poko Fault, *TKF* Thakhek-Sepon Fault Zone, *TPS* Tamky Suture. **b** Simplified geological map of the NWTR (Northern West Thailand Region) and northwest part of the Inthanon Zone compiled and simplified mainly from the Chiang Mai, Chiang Dao and Li 1: 250,000 scale maps of the German Geological Mission (Hess and Koch 1979; von Braun et al. 1981; Baum et al. 1982 von) with some amendments from our fieldwork, Sarapirome and Khundee (1994) and Royal Thai Department of Mineral Resources mapping. Possible extension of the Mae Yuam Fault northwards into Myanmar based on earthquake epicentres mapped in Sarapirome and Khundee 1994, their fig. 3). Numbers in circles are fossil localities from Hahn and Siebenhüner (1982) with their locality numbers and age (*d* Devonian, *h* Carboniferous, *p* Permian, *t* Triassic) in brackets listed below with taxonomic assignments by their colleagues at the German Geological Survey. Limited updating of chronostratigraphic and taxonomic nomenclature has been applied. Stars indicate tropical Viséan to upper Permian coral, fusulinid faunas and diverse calcareous algae found in carbonates in the northwest Inthanon Zone (Fontaine et al. 1993, 2009). (a–z4) are fossil localities described in post-1981 papers and theses in NWTR (other than Hahn and Siebenhüner (1982)) and nearby in the northwest Inthanon Zone. (a) Fusulinid *Monodiexodina shiptoni* from Tha Ta Fang on the Salween River (Ingavat and Douglass 1981). See also Ueno (2006), Kungurian to Roadian (late early Permian to early middle Permian). (b) Radiolarians, middle Triassic Feng et al. (2004a). (c) Radiolarians, early Carboniferous, Feng et al. (2004b). (d) Radiolarians, early Ladinian-late Anisian, Thassanapak (2008). (e) Radiolarians, late Ladinian, Thassanapak (2008). (f) Radiolarians, late Permian (Feng et al. 2004a). (g) Radiolarians in conglomerate clasts mixed Permo-Triassic, Caridroit et al. (1993). (h) Wordian conodonts (*Mesogondolella siciliensis* and *Mesogondolella dicerocarinata*), small foraminifera, fish teeth and calcareous algal tubes—Permian limestone in sample MY04 of samples MY01-MY07 herein. (i) Devonian shark locality of Long and Burrett (1989) and Long (1990). (j) Conodonts Late Devonian (11m section) of Dopieralska et al. (2012), Königshof et al. (2012) and Savage (2013, 2019). (k) Late Devonian fish localities of Long and Burrett (1989), Long (1990). (l) Cr-spinel locality of Hisada et al. (2004). (m) Conodonts, Permian Huai Pho locality herein, samples HP 01-HP 03. (n) Radiolarians, middle Triassic Feng et al. (2004a). (o) Radiolarians middle Triassic, Thassanapak (2008). (p) Bivalves and gastropods probably Carboniferous, Hara et al. (2012). (q, r, s, t, u) Ammonoids and bivalves, probably Carboniferous. (v) Permian radiolarians, Inthanon Zone near Pai, Inthanon Zone-geochemistry discussed in the text. Wonganan and Caridroit (2006). (w) Ammonoids: *Pseudopronorites arkansasensis* (Smith) and *Cravenoceras* ? sp. mid to late Pennsylvanian, Fujikawa and Ishibashi (1999), Inthanon Zone. (x) Radiolarians Late Triassic, early Carnian, *P.triassicus* Zone, Feng et al. (2004a). (y) radiolarians Late Triassic, early Carnian, *P.triassicus* Zone, Feng et al. (2004a) and siliceous limestone Carnian, Thassanapak (2008). (z) Radiolarians, late Anisian (early Middle Triassic), Thassanapak (2008). (z1) Radiolarians, Early to Late Triassic, chert, chert and shale with calcareous beds. Kamata et al. (2002). (z2) Cr-spinels locality of Hisada et al. (2004). (z3) Radiolarians, early Carnian (early Late Triassic) *P.triassicus* Zone, Feng et al. (2004a). (z4) Inthanon Zone, Upper Devonian radiolarian chert at Ban Pang Paek, Pai Province, Sanjit et al. (2014). (1) (47/p2) fusulinids: Verbeekinidae, Schubertellinae, Schwagerinidae, *Sumatrina/Afghanella*, small foraminiferan: *Pachyphloia* sp., late middle Permian. (2) (57/t-p) conodonts: *Mesogondolella* cf *bitteri* (Kozur), *Mesogondolella babcocki*, early late Permian. (3) (49/p2) fusulinids*: Monodiexodina* 'of the *sutchanica* type', late early Permian to early middle Permian—probably *M. shiptoni*, see Ueno (2006). (4) (50/p2) conodonts: *Mesogondolella* cf *bitteri* (Kozur), *Mesogondolella babcocki*. Guadalupian (middle Permian). (5) (43/p2-1) fusulinids: *Monodiexodina* sp., *Pseudofusulina fusiformis*, Staffelidae. Late early Permian to early middle Permian. (6) (52/p2) conodonts, not listed Permian. (7) (41/p1) fusulinids: *Schwagerina*, *Monodiexodina*? early Permian. (8) (46/p2) conodonts: *Mesogondolella babcocki. M.* cf. *idahoensis*, *M.* '*rosenkrantzi*' (Guadalupian (middle Permian). (9) (53/p3-2) conodonts: *Mesogondolella babcocki*, *M.* '*rosenkrantzi*' (Guadalupian. middle Permian). (10) (39/p-h2) ammonoid: ? *Agathiceras* sp., Pennsylvanian—middle Permian. (11) (40/p) brachiopods—probably Permian. (12) (37/ph) ammonoid: *Agathiceras* sp., Pennsylvanian—middle Permian. (13) (36/h1) conodonts: *Gnathodus pseudosemiglaber*, *G. semiglaber*, (Tournaisian 3 to Viséan). (14) (31/h-d) brachiopods: Overtoniidae, Productacea, gastropods (Late Devonian to Carboniferous). (15) (32/h-d) brachiopod: chonetid, ostracodes: *Bythocypris*, *Bairdia*, *Darwinula*, *Polytylites*, *Healdia* (Late Devonian to Carboniferous). (16) (35/h1) conodonts: *Polygnathus inornatus*, *Pseudopolygnathus marginatus*, *Ps. multistriatus Ps. triangulus*, Tournaisian. (17) (34/h1) conodonts: *Polygnathus communis communis*, *P. purus purus*, *Pseudopolygnathus multistriatus* Tournaisian 2. (18) (56/p3) foraminiferans: ?*Ammodiscus*, *Cribopeneria*, *Misselina* (late Permian), *Parafusulina* (early to middle Permian). (19) (54/p2) conodonts: *Mesogondolella bitteri* (Kozur), *Mesogondolella* '*rosenkrantzi*' (Bender and Stoppel), Guadalupian. (20) (38/p-h) foraminiferans *Archaeodiscus*? *Nodosinella*? Palaeotextularidae, Carboniferous-Permian. (21) (51/p2) *Verbeekiella*? (Rugosa—'horn' coral) and brachiopods *Costiferina*, *Phricodothyris*, *Neophricodothyris*, Artinskian. (22) (55/p3-2) *Michelinia*? (Tabulata) brachiopods*: Orthotichia*, *Rhipidomella*, '*Productus*' *opuntia*, *Waagenoconchus waageni*, *Costiferina*, *Spiriferellina cristata* (middle to late Permian?). (23) (44/p) conodonts: *Mesogondolella idahoensis* (Leonardian = Kungurian). (24) (49/p?) foraminifera ?Permian. (25) (39/p2-1) fusulinids: *Parafusulina* (early to middle Permian) (probably very close to the late Permian sandstone and detrital zircon locality of Dew et al. 2021). (26) (29/h1) brachiopods: *Punctospirifer*, *Echinoconchus*, trilobite: Phillipsiidae ?Mississippian. (27) (37/p2-1) early to middle Permian fusulinids. (28) (38/p2-1) early to middle Permian fusulinids. (29) (36/p1?) coral: *Waagenophyllum*, brachiopod: orthothetid, bryozoan: Fenestellidae (early ?Permian). (30) (34/p1). Brachiopod: *Phricodothyris*, ammonoid: *Agathiceras* (Pennsylvanian—early Permian). (31) (27/h) *Ellipsella* (ostracod), ?Carboniferous. (32) (30/p1-h2) brachiopod: Spiriferinidae, ammonoid: ?*Agathiceras* (Pennsylvanian—early Permian). (33) (44/p3-2) fusulinids: *Afghanella*, *Neoschwagerina*, *Sumatrina* (middle to late Permian). (34) (68/h1) conodonts: *Gnathodus girtyi*, '*Spathognathoides*' cf *crassidalata*. Viséan 3c. (35) (48/p2) fusulinids: Schwagerininae, *Sumatrina* (late middle Permian). (36) (46/p2-h2?) bivalve: *Aviculopecten*, ostracod: *Healdia*, ammonoid: *Agathiceras* (Pennsylvanian—middle Permian). (38) (42/p3-2) fusulinids (middle-?late Permian). (39) (35/ph) conodont: *Mesogondolella bisselli*, early Permian. (40) (10/p2) fusulinids: *Schwagerina*, *Neoschwagerina*, *Afghanella* (middle-?late Permian). (41) (43/p2-3) fusulinids: *Schwagerina*, *Neoschwagerina*, *Afghanella* (middle-?late Permian).

The Palaeozoic to Triassic of the NWTR are folded, faulted and, in places, thrusted (Figs. 2–5). Vergence is generally to the west (Hess and Koch 1979; Baum et al. 1982; Caridroit et al. 1993; Morley 2018) (Fig. 3). Outcrops along the Mae Yuam Valley include N-S elongated fault slices of Cambrian to Triassic sedimentary rocks (Figs. 2, 4(b)) and radiolarian cherts on the eastern side of the Mae Yuam Valley are strongly folded and, in places, verge towards the east (Chonglakmani 2011, his fig. 6.4).

Extensive Late Triassic S-type granites of the Central Belt, including the Mae Sariang pluton (Fig. 2), are present in the Inthanon Zone to the east of the MYMS FZ (Putthapiban

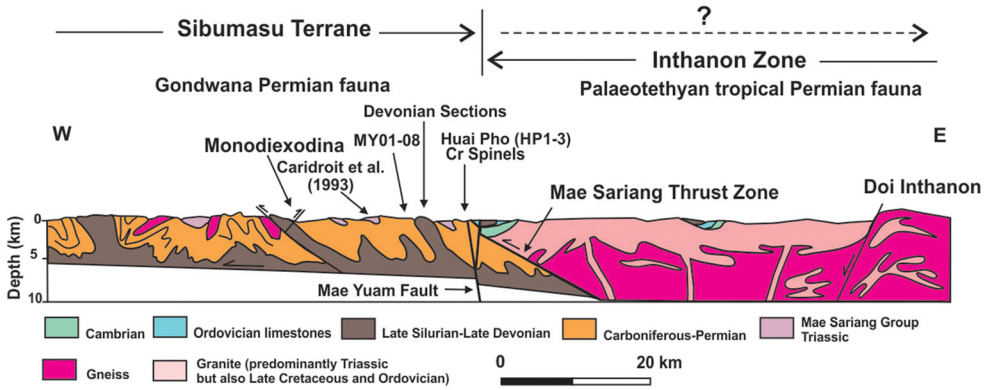

Fig. 3 Diagrammatic cross-section across northwestern Thailand. Based on Gardiner et al. 2016a). Note the still active, near-vertical Mae Yuam Fault Zone and the shallow dipping Mae Sariang Thrust Zone. It is the Mae Sariang Thrust Zone that thrust the Inthanon Zone over the Sibumasu (or Sibuma) Terrane and that is the boundary between temperate Gondwana and the palaeotropical Inthanon Zone. In two-dimensional map view, the surface trace of both the Mae Yuam and Mae Sariang faults is close to and parallel to the Mae Yuam Valley and is therefore combined in the text as the Mae Yuam/Me Sariang Fault Zone or MYMS FZ. Note the abundance of granite and gneiss on the Inthanon Zone and its rarity west of the MYMS FZ. Cool-water or temperate Permian faunas such as *Monodiexodina* characterise the Sibumasu (or Sibuma) Terrane in the NWTR and the contiguous Thitsiphin Limestone Platform of Myanmar to the west whereas the Inthanon Zone is characterised by Visean to Permian palaeotropical (or Palaeotethyan) faunas found in isolated carbonate bodies interpreted as allochthonous, oceanic volcanic seamounts by Ueno and Charoentitirat (2011) and others and as isolated carbonate platforms on horst-graben structures in this paper. The two very different shallow-water carbonate Permian faunas are separated by an approximately 15-km-wide, narrow band of hemipelagic, continental margin radiolarites distributed on either side of the Mae Yuam Valley

2002; Cobbing 2011; Department of Mineral Resources 2014) but, in contrast, only two small granite stocks the Mae Lam and Ban Pasu granites are present within the NWTR. The Cretaceous Mae Lam Granite (Fig. 2) is related to eastward subduction under Myanmar and Thailand (Pitfield 1988; Pitragool and Panupaisal 1979).

Sedimentary rocks in the NWTR range from the Lower Palaeozoic to Jurassic with Cenozoic sediments deposited, particularly along the Mae Yuam Valley (Fig. 2) (Baum et al. 1970; Hahn and Siebenhüner 1982; Charoenprawat et al. 1985; Boriphatkhosal 1990; Jindasut et al. 1990; Bungunphai 2005), but most of the outcropping rocks in the NWTR comprise the mainly siliciclastic Mae Sariang Group of Triassic age (Raksakulwang and Bunopas 1985; Tofke et al. 1993; Srinak et al. 2007; Chonglakmani 2011) (Fig. 2).

Unfossiliferous sandstones and minor shales assumed to be Cambrian in age, outcrop extensively in the southern part of the NWTR but further north are only found as faulted blocks within the Mae Sariang Fault thrust belt (Fig. 2) and to the east within the Inthanon Zone. Ordovician dolomitic limestones assigned to the Hod Limestone of the Inthanon Zone para-autochthon and correlated to the Thung Song Group of southern Thailand follow a similar distributional pattern. Conodonts (Hahn and Siebenhüner 1982) and macrofossils (Ratanasthein et al. 2010) are found in the Ordovician limestone. Silurian and Lower-Middle Devonian shales, sandstones and limestones also yield conodonts. The fossiliferous Devonian limestones mainly occur as fault bound blocks within the NWTR and along the MYMS FZ (Figs. 2, 5) and yield faunas from the Lower to the Upper Devonian (Blieck and Goujet 1978; Hahn and Siebenhüner 1982; Long and Burrett 1989; Savage 2013, 2019).

The 11-m-thick Upper Devonian section (loc. j on Fig. 2 and Figs. 4–6) studied in great detail by Königshof et al. (2012), Racki et al. (2019) and Savage (2013, 2019) is, however, composed mainly of micrites, with hardgrounds, neptunian dykes, both pelagic and benthic fauna and some microstromatolites. Entomozoacean ostracodes are present in this section and they probably indicate '…a nektobenthic lifestyle, in poorly oxygenated, but not necessarily deep environment…' (Casier 2004 p. 73). The faunal and sedimentological features of the Upper Devonian section indicate '…an environment of relatively deep, quiet and poorly oxygenated water in the aphotic zone…' (Königshof et al. 2012 p. 153). The sequence may be interpreted as having been deposited on a platform or ramp margin with the influence of an oceanic water mass a few kilometres to the east.

The condensed Upper Devonian section is close to and is probably included in the folded and faulted Emsian to Famennian section briefly studied by Long and Burrett (1989) (Figs. 2, 5). Long (1990) described abundant Famennian microvertebrates from calciturbidites in this section which, although belonging to widely distributed pelagic fish such as *Jalodus australiensis*, were unlikely to be fully oceanic and are found in shelf carbonates in North Africa and Iran (Ginter et al. 2002). Ginter (2000) compared the 'deep-water' Thailand chondrichthyan assemblage to that found at Buschteich in the Thuringian Slate Mountains of the Variscan orogen. Based on conodont biofacies and sedimentological considerations, Girard et al. (2020) place the Buschteich section in an outer ramp setting.

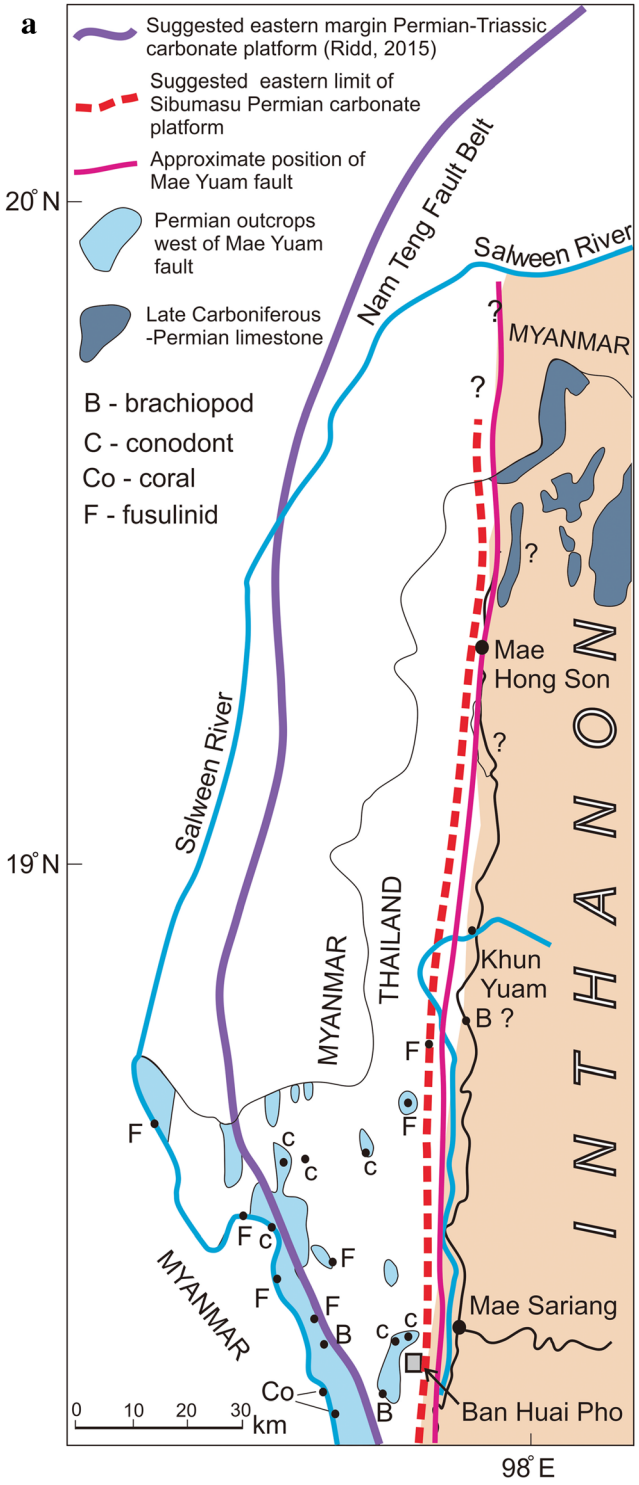

Fig. 4 **a** Suggested trace of the Permian Thitsiphin carbonate platform margin as drawn by Ridd (2015b). However, the distribution of probable mainly shallow water Permian fossils in NWTR limestones suggests the eastern limit of the Sibumasu Permian carbonate platform (shown in light blue) should be drawn closer to the Mae Yuam Fault zone—at least in the southern part of the NWTR. Based on our new data and data collected by the German Geological Survey Mission to Thailand and summarised in Figure 2 (Hahn and Siebenhüner 1982), Permian platform margin limestones are found to within about 9 km of the Mae Yuam Valley and are replaced to the east by outcrops of Permian radiolarites and other siliciclastics closer to and along the Mae Yuam Valley. All data on the Permian carbonates of the Shan State in Myanmar indicate shallow water, platform conditions and there is no evidence of platform margin or slope deposits (Zaw Win et al. 2020; Zhang et al. 2020). The grey shading indicates outcrops of the Doi Chiang Dao Inthanon Zone, shallow marine, palaeotropical limestones ranging from Visean to Permian that are interpreted as capping oceanic seamounts within the Inthanon Zone and extending to the western margin of the Inthanon Zone (Ueno and Charoentitirat 2011) or interpreted by us as remarkably long-lived isolated carbonate platforms on horsts. **b** Map of part of NWTR and the Mae Yuam Valley showing locations of important locations discussed in text. Abbreviations used for selected localities as in Figure 2(b). Eastern limit of Permo-Triassic carbonate platform according to Ridd (2015b). Our data, that of the German Geological Survey and recent studies by Zhang et al. (2020) do not support the platform margin extending westwards and northwestwards into Myanmar. On the contrary, we suggest the platform margin is within 9 km of and parallel to the Mae Yuam Valley—at least in the southern part of the NWTR

Long's (1990) new genus and species *Siamodus janvieri* has a restricted peri-Gondwana and South China distribution and has been found in Morocco, Sardinia, the Carnic Alps and in Thuringia in open marine to deep water but not fully oceanic limestones (Randon et al. 2007; Derycke et al. 2008).

However, Dopieralska et al. (2012) and Racki et al. (2019) using Nd isotopes in conodont apatite (Dopieralska 2003, 2009; Dopieralska et al. 2006) showed that the Late Devonian seawater to the west of Mae Yuam Fault was 'oceanic' and therefore concluded that the Inthanon Zone boundary was at least 9 km to the west of the MYMS FZ and that the Mae Sariang Devonian was on a separate block and positioned within the Palaeotethys Ocean. This position of the Inthanon Zone margin west of the MYMS FZ was accepted by Gardiner et al. (2016b). However, to quote Racki et al. (2019), 'In terms of provenance, the siliciclastic fraction in the MS (Mae Sariang) succession corresponds to continental margin'. On petrographic and faunal evidence, we suggest that the Mae Sariang/Mae Sam Lap, Late Devonian section, was deposited on a deep platform/ramp and was not within an ocean as suggested by Racki et al. (2019) but influenced by oceanic waters from a spreading ocean basin a few kilometres away to the present-day east.

Further north, about 20km north of Mae Sariang in 'Tchop-Ton quarry', Blieck and Goujet (1978) and Blieck et al. (1984) figured an acanthodian fish of the '*Nostolepis* type' and a *Turinia* sp. (thelodont fish) scale considered to belong to *Turinia* sp. cf *Turinia* sp. B from west Yunnan and Australia to be of early Eifelian age (Turner 1997) and of shallow marine ('littoral') origin (Lelievre et al. 1984; Turner 1997). We have only found conodont-bearing Triassic limestone at this locality but the thelodont fish does not indicate oceanic conditions in the early Eifelian. The Carboniferous of the NWTR consists of siltstone, sandstone and thin, conodont-bearing limestone (Figs. 2, 5)

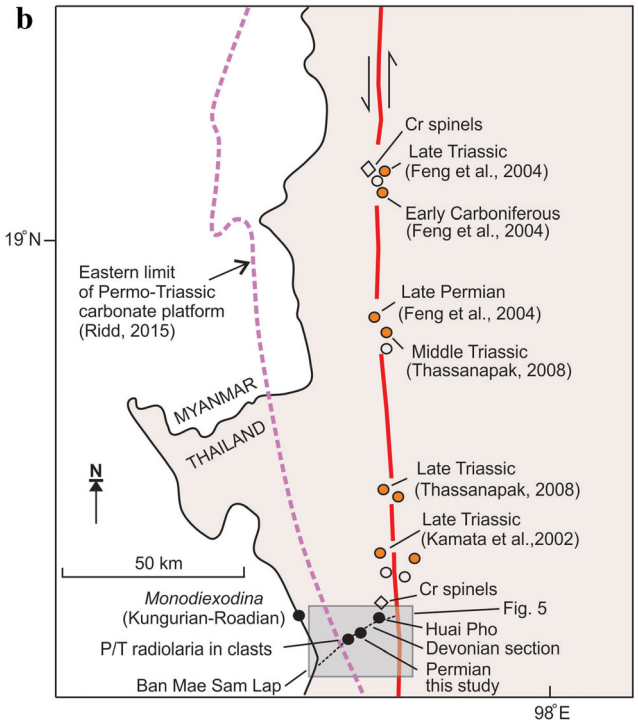

Fig. 4 (continued)

(Sukto et al. 1984; Charoenprawat et al. 1985; Raksakulwang and Bunopas 1985; Raksakulwong and Tantiwant 1986; Jindasut et al. 1990; Bungunphai 2005). The Doi Kong Mu Formation of Bunopas (1982) consists of about 300 m of coarse siliciclastics west of Mae Hong Son which were regarded as Carboniferous because of their apparent position beneath Permian limestone. However, they are overturned (Raksakulwang and Bunopas 1985, p. 18) and unfossiliferous and their age is unknown (Ueno and Charoentitirat 2011, p. 76).

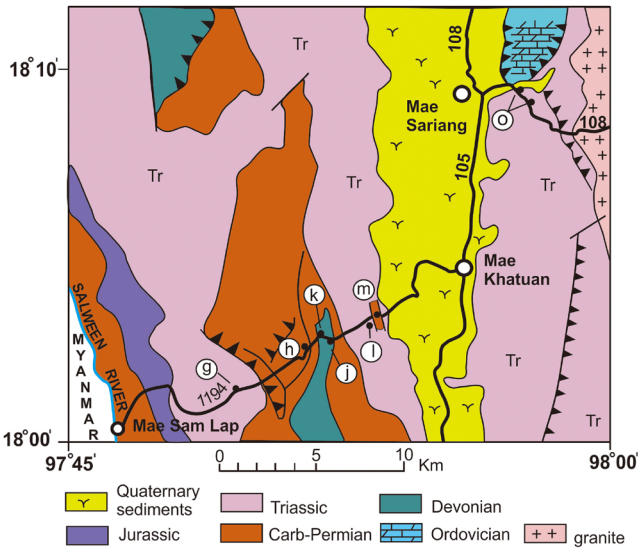

Fig. 5 Simplified geological map of Mae Sariang-Mae Sam Lap area showing localities mentioned in text. Geology adapted from Bungunphai (2005) with additions. Abbreviations used for selected localities as in Figure 2(b). For location, see Figs. 2(b) and 4.

Ridd (2015a) placed a Permian shelf margin to the west of the MYMS FZ and mainly in Myanmar (Figs. 4(a, b)). Ridd's (2015b) placement of this Permian shelf margin follows from his belief that Permian marine platform limestones were not deposited in the NWTR northeast of his shelf margin line (Figs. 4(a, b)). However, such limestones have been mapped and their faunas recorded by Hahn and Siebenhüner (1982) (Fig. 2) who identified several localities containing Permian conodonts, foraminiferans, corals and brachiopods and confirm the Permian age of the mapped strata (Figs. 2–4) and which suggest that Ridd's (2015b) platform margin should be placed further east and much closer to the MYMS FZ Fault as shown in Figure 4(a).

We have examined part of the Permian limestone mapped by Department of Mineral Resources geologists (Bungunphai 2005) and found it to consist of carbonate lithofacies indicating a deep shelf to basinal environment and probably was deposited on or near the Permian platform margin and about 9 km west of the MYMS FZ.

Neither extrusive nor intrusive mafic or ultramafic igneous rocks have been found in the Devonian of the NWTR, making an oceanic (i.e. seawater above ocean crust) environment unlikely. A general lack of Palaeozoic-Triassic volcanic rocks contrasts with their widespread, but areally restricted and scattered presence in the Inthanon Zone (Barr et al. 1990; Panjasawatwong

1999; Panjasawatwong et al. 2003; Phajuy et al. 2005; Barr and Charusuri 2011; Ueno and Charoentitirat 2011; Wang et al. 2017). However, Hisada et al. (2004) collected Triassic Mae Sariang Group sandstones from the Huai Pho and Huai Pong sections, 5 km west of the fault (Figs. 2 and 4(b)) and found detrital Cr spinels which indicated a source from 'ocean floor peridotite, chromitite, and intra-plate basalt' which was removed by erosion and re-deposited during the Triassic. We have re-plotted Hisada et al.'s (2004) data on Kamenetsky et al.'s (2001) spinel discrimination diagrams and find they plot in Ocean Island, or Mid-Ocean Ridge (Or Back Arc) and Island Arc fields with the island arc samples representing lower titanium boninites or tholeiites.

The Triassic Mae Sariang Group in the NWTR has been studied by Raksakulwang and Bunopas (1985), Tofke et al. (1993), Srinak et al. (2007) and Chonglakmani (2011). The group consists of about 900 m of mainly siliciclastics with minor limestones and much of the group was deposited in a submarine fan within a foredeep of a foreland basin receiving clastic sediments from a rising orogen to the east (Srinak et al. 2007; Ridd 2015b). Strongly folded siliciclastic sequences including sandstone, shale and conglomerate exposed along a road-cut at Ban Huai Pho to Mae Sam Lap, west of Mae Sariang (Figs. 4(a, b), 5), contain Permian to Triassic radiolarian-bearing chert clasts suggesting uplift and erosion during the Late Triassic or later (Caridroit et al. 1993). The occurrence of poorly sorted conglomeratic breccia, overlying Upper Triassic chert and underlying a lower Jurassic ammonite/bivalve open marine assemblage to the north of Mae Sot (MS on Fig.1), supports uplift and erosion during the latest Triassic-earliest Jurassic and confirms deposition of radiolarian chert up to the Triassic-Jurassic boundary (Ishida et al. 2006). Triassic cherts are found along and close to the MYMS FZ and are discussed below (Fig. 4(b)).

Permian limestone

Two sections of Permian strata with limestones are described, one at Huai Pho (Figs. 2, 4, locality m, 18° 01′ 58.669″ N, 97° 53′ 03.811″ E) and the other about 4 km to the west and close to the outcrops of Devonian limestones studied by Long and Burrett (1989) and Königshof et al. (2012) (Figs. 2, 4, locality h, 18° 01′ 03.541″ N, 97°, 50′42.454″ E). The thin-bedded limestone at Huai Pho was included in the Triassic Mae Sariang Group by Hisada et al. (2004) but is found to contain only Permian conodonts. These conodont elements belong to *Mesogondolella dicerocarinata* are unbroken and do not suggest reworking. Sections along the Salween River include quartz-sandy limestone, quartz sandstone and shale and contain the fusulinid *Monodiexodina* indicating late early to early middle Permian ages (Ingavat and Douglass 1981; Hahn and Siebenhüner 1982). (Fig. 2, locs. a, 3, 5, 7).

Two main sections of Permian limestone observed at 1 and 4 km west of Huai Pho are the Huai Pho and Mae Yuam sections, respectively (Figs. 3, 6). The Huai Pho section is structurally complex and the limestone is thin but the Mae Yuam section consists of at least 300 m of well-bedded limestones (Figs. 7, 8). Acetic acid residues contain an abundance of silicified calcareous alga tubes and small foraminifera along with abundant silicified ostracodes belonging to at least six species. Conodonts have a CAI of 5 and indicate sub-metamorphic to metamorphic temperatures of between 300 and 480° C (Rejebian et al. 1987; Königshof 2003). The main limestone section probably correlates with the Doi Phawar Formation which was established but loosely defined south of the Mae Ping Fault in western Thailand and is poorly known (Ueno and Chareontitirat 2011, their fig. 5.14).

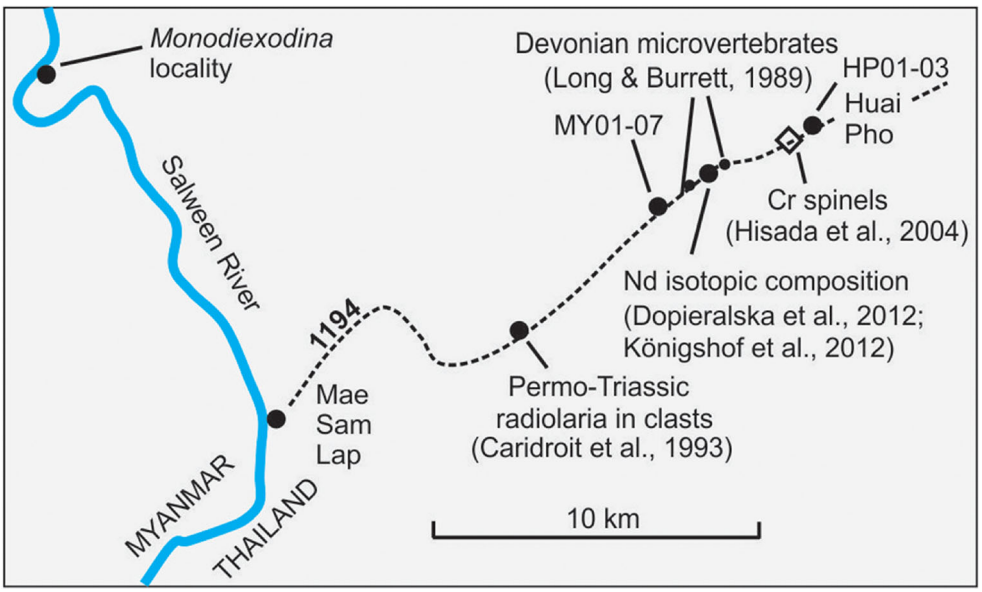

Fig. 6 Important localities discussed in text along road 1194 to Mae Sam Lap. For location, see Fig. 2(a)

Microfacies and palaeoenvironment of Permian limestone

The limestone from the Mae Yuam section along road number 1194 is thin to medium bedded (mainly 10–20 cm thick) with slump structures observed in some intervals (Fig. 8). The limestone is medium to dark grey and dark grey with brown and red pigmentation laminar seams are prominent between the limestone beds (Fig. 8). Fossils are very rarely observed on the limestone surface and only a few solitary rugose corals are observed in the field. The contact of the limestone with over 200m of thin-bedded, unfossiliferous, undated siltstones and shales to the north is obscured by soil cover and vegetation.

More than 30 thin sections of limestones were prepared for microfacies classification using the system of Dunham (1962) with expanded classification by Embry and Klovan (1971) and placed into standard microfacies for environmental interpretation (e.g. Flügel 2004).

MF 1: Nodular microbioclastic wackestone

In the field, this facies type presents as thin-bedded limestone. Under thin section, it consists of fine bioskeletal debris randomly distributed in a micrite matrix. The bioclastic component includes sponge spicules, planktonic foraminifers, thin-shelled ostracods, ammonoid jaw apparatus and shell fragments and other shell debris (Fig. 9). Fine quartz grains, peloids, nodular fabrics and intraclasts are minor components.

Interpretation: Common planktonic foraminifers, sponge spicules and ammonoids suggest an open marine environment (Blendinger et al. 1992). Dispersed fine bioclastic debris with nodular fabrics in a fine matrix support a deep subtidal environment below storm wave base in relatively low-water energy conditions (Flügel 2004).

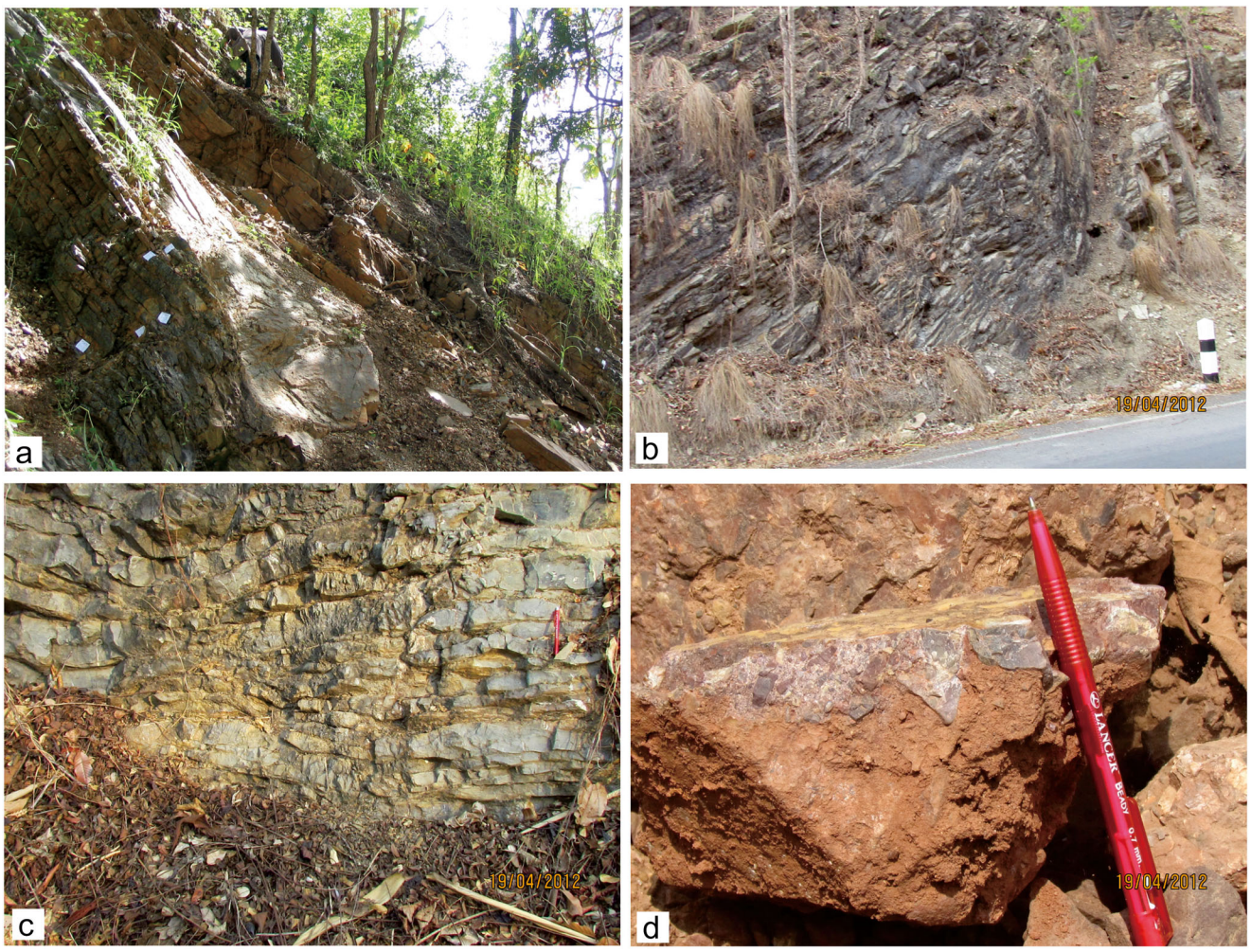

Fig. 7 Photographs of outcrops mentioned in text. (a) The Mae Sariang, Middle Triassic chert section along the highway HW 108, Mae Sariang-Chom Thong route (loc. o on Figs. 2, 5), (b) early Late Triassic chert with thin-bedded limestone intercalation, along HW 108 Mae Sariang-Mae La Noi route (loc. y on Fig. 2), (c) magnification of limestone bed from the same outcrop as (b), containing thin bivalve shell and radiolarian, (d) conglomerate consisting mainly of chert clasts exposed along a road-cut at Ban Huai Pho to Mae Sam Lap, west of Mae Sariang (Figs. 4(a, b), 5).

MF2: Microbioclastic peloidal packstone/grainstone

Skeletal grains are densely packed in a micritic matrix. Bioclastic components are mainly silt-size consisting of shell debris, microconchid (calcareous tubeworm), ostracods, benthic and planktonic foraminifers, sponge spicules, echinoderm fragments, dacyclad algal fragments and larger ammonoid shell and fragments. Lithoclasts include mainly peloids and carbonate lump intraclasts. Fine quartz grains are commonly dispersed throughout the matrix. Skeletal grading, parallel and cross lamination and burrows are common sedimentary features of this facies (Fig. 9).

Interpretation: This microfabric and mixing of faunas can be compared to densely packed calcisiltite of facies zone 3, representing a condensed unit at a deep shelf to toe-of-slope

Fig. 8 Photographs of outcrops mentioned in the text. **a** Thin-bedded limestone with slump structure from Mae Yuam sections, locality h on Fig. 2; **b** thin-bedded limestone with pronounced Fe–Mn hardground crust indicative of a condensed section; **c** folded siliciclastic sequences with chert intercalation to the east of Mae Sam Lap; **d** outcrop of Permian limestone along the creek at the Huai Pho section


a
cm
1
2
3
4
5
6
7
8

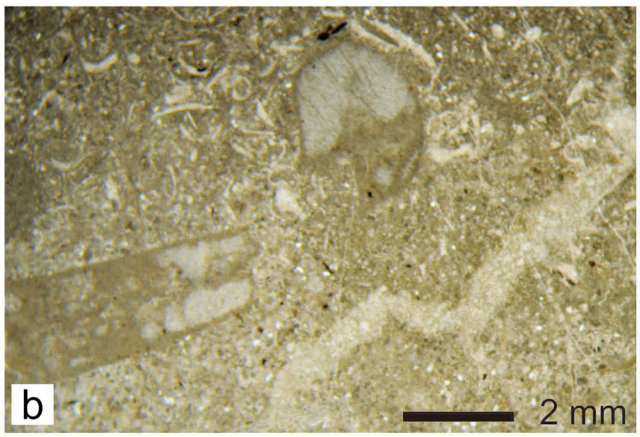
b
2 mm

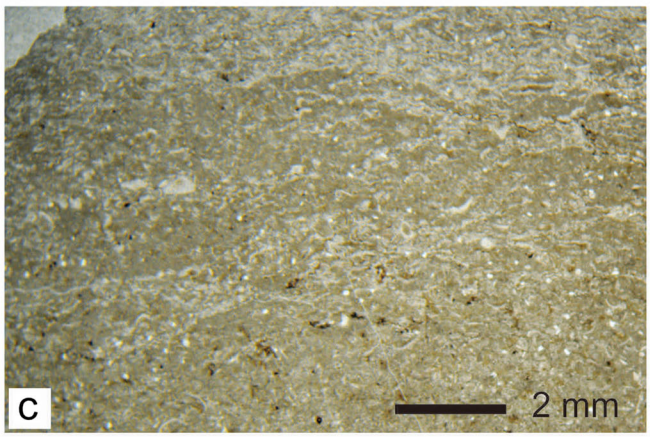
c
2 mm

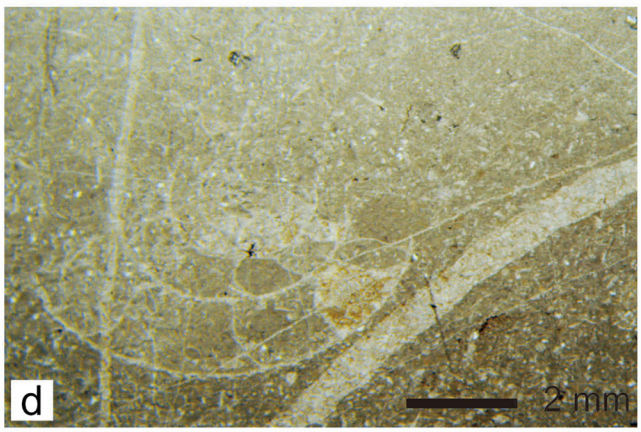
d
2 mm

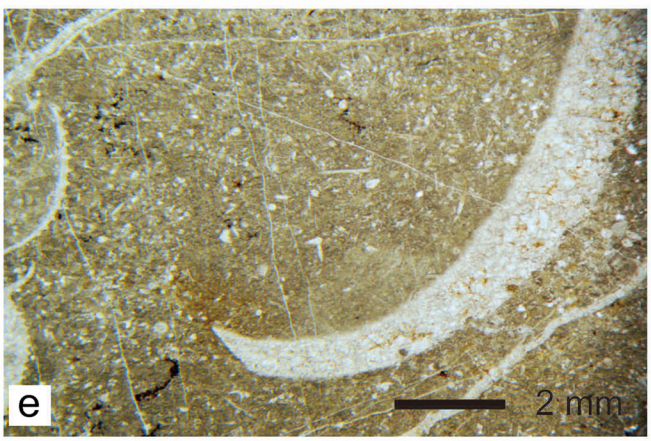
e
2 mm

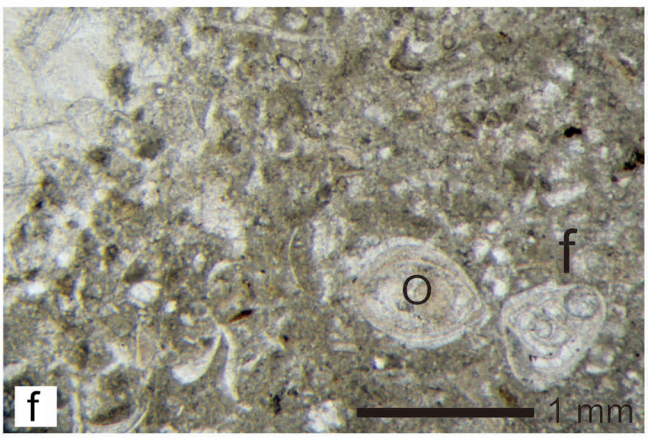
f
O
f
1 mm

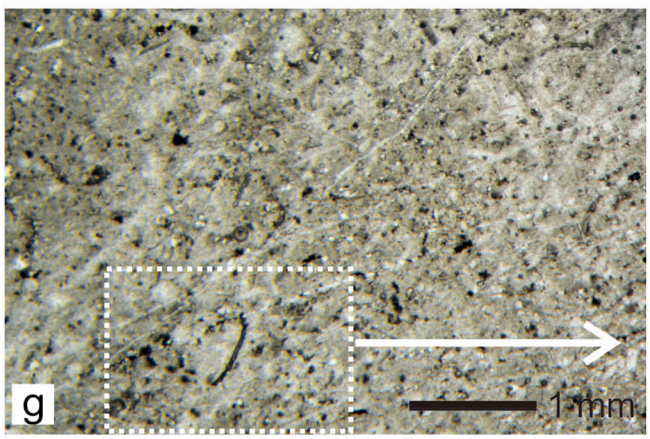
g
1 mm

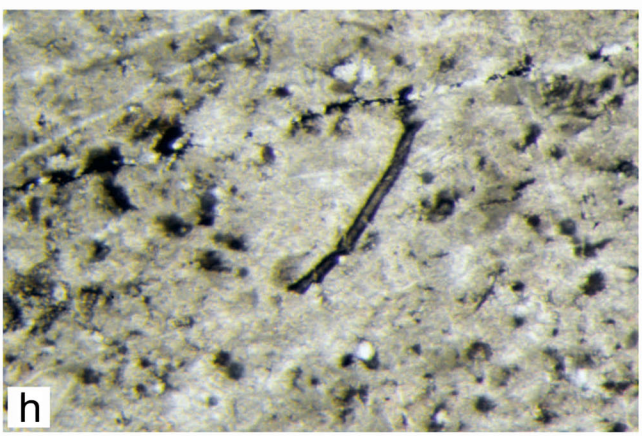
h

◀ **Fig. 9** Photomicrographs of thin sections of Permian limestone microfacies from Mae Yuam section, locality h on Figure 2. **a** Polished slab of thin-bedded packstone/grainstone with normal grading (MF2) underlain and overlain by Fe–Mn laminated crust (MF3); **b**, **f** microbioclastic packstone showing echinoderm fragments, ostracode (*o*) and smaller foram test (*f*) with microbioclastic fragments floating in a micrite matrix (MF2); **c** micritic nodules arranged in parallel in microbioclastic wackestone matrix; **d**, **e** small ammonoid shell and jaw fragments with nodular fabric in microbioclastic wackstone matrix rich in sponge spicules (MF1); **g** microbial mudstone consisting of microbial tube with organic debris dispersed in micritic mud matrix (MF 4); **h** magnification of G showing microbial tube with organic debris

environment (Flügel 2004). The mixture of benthic and planktonic faunas indicates transport of shelf faunas to deeper marine environments. Abundant and well-preserved microconchid tubes suggest a secondary frame-builder in microconchid-algal build-ups in a mud mound up-slope environment (Vinn and Mutvei 2009; Wilson et al. 2011). Fragments of dacyclad green algae support a shallow-marine shelf environment. Gradation of skeletal detritus covered by parallel lamination indicates occasionally high energy or turbiditic events. Quartz grains (Fig. 9) represent terrestrial input to the depositional environment.

MF3: Stromatolitic bindstone

In the field, this facies is characterised as 1–3 cm thick, laminated crust commonly intercalated with thin-bedded limestone (condensed layer). The polished slab of this facies type shows as a black stromatolitic seam with partly brown and dark red pigmentation. The acid-etched surface of the slab shows undulating seams with expansion ridges (tepee structure). Under thin section, the seam is non-sutured with a parallel arrangement to bedding plane including wispy, parallel sets of laminated fabric, dome and horsetail structures. It is intercalated with micrite and nodular fabric layers. The nodular fabric consists of densely packed bioclastic wackestone/packstone. Bioclastic and fine-quartz grains are common, dispersed or embedded in the matrix (Fig. 10). Neptunian dykes a few millimetres wide are common, and truncate the host sediments and the stromatolitic seams with a host sediment infill.

Interpretation: This facies is interpreted as part of a complex hardground which is overlain and underlain by a condensed unit in a submarine slope environment. The dark red impregnated crust of the undulating layer with tepee structure represents Fe–Mn microstromatolites associated with the hardground surface. This non-random strain pigment of Fe–Mn crust indicates syndepositional sedimentation (Lazar et al. 2013; Gradinaru et al. 2019). This red pigmentation suggests bacterial mediation during early diagenesis in which the existence of microstromatolites and filaments in microbial mudstone facies (MF4) suggests the presence of iron bacteria in the environment (e.g. Mamet and Preat 2006). Microbioclastic peloidal packstone/grainstone facies with a hardground couplet indicate a condensed unit with a low sedimentation rate in deeper marine conditions. The hardground is normally formed during maximum flooding surface event at the top of a transgressive system tract (Riding 2000; Catuneanu 2006). Neptunian dykes are interpreted as synsedimentary features formed by differential compaction of the sediment and are common in deep shelf and slope to basin environments.

MF4: microbial mudstone

This facies is characterised by a mud-supported fabric of micritic wall filaments. The fabric consists of thin-walled curved and aligned calcimicrobe tubes of probably calcified cyanobacteria or other microbes, along with a large amount of irregular organic debris loosely dispersed throughout the mud matrix (Fig. 9).

Interpretation: Abundant organic debris is interpreted as disintegrated microorganisms such as cyanobacteria, algae and other microbes. These organisms play an important role as a source of micrite and carbonate mud. This facies is interpreted as part of a microbial mound located in a slope environment of a shallow, warm, well-oxygenated carbonate shelf (e.g. Mamet 1991; Parvizi et al. 2013).

Foraminiferans

The fusuline *Monodiexodina shiptoni* is the only Permian foraminiferan previously described and illustrated from the TWTR (Ingavat and Douglass 1981; Ueno 2006; Department of Mineral Resources 2014, p. 99). It was found in a sequence of about 200 m of interbedded grey limestone and quartzitic sandstone along the Salween River 28 km west of the MYMS FZ (Fig. 2, loc. A, Figs. 4(b), 6) and has also been recorded with *Pseudofusulina* sp. further north along the Salween River and elsewhere in the TWTR by Hahn and Siebenhüner (1982) (Fig. 2, locs. 3, 5, 7). *Monodiexodina* is a palaeogeographically important fusuline genus which Ueno (2006) demonstrated has a bi-hemispheric distribution in the early to middle Permian and was restricted to shallow water, high-energy environments in temperate to subtropical palaeolatitudes. *Monodiexodina* has been described from limestones from above the glacimarine rocks of NW Malaysia (Jasin 1991), by Ueno (2006) from Kanchanaburi in western Thailand and by Zhang et al. (2020) from the Wordian Thitsiphin Fm. limestone of the Shan State of Myanmar. These three areas are on the Sibumasu Terrane (or on the geographically more restricted non-glacial Sibuma Terrane of Ridd 2015a). This genus has not been found in the palaeotropical Inthanon Zone, Indochina terranes or in the South China Terrane but is present in the palaeotemperate Permian (Wordian) of Russian Far East terranes and NE China (Kotlyar et al. 2007). The illustrated Thai and Malaysian *Monodiexodina* have been placed in *M. shiptoni* which ranges from the Kungurian through to the Roadian (Ueno 2006). Smaller foraminiferans are common in the limestones at our new section in the TWTR (Figs. 9, 10).

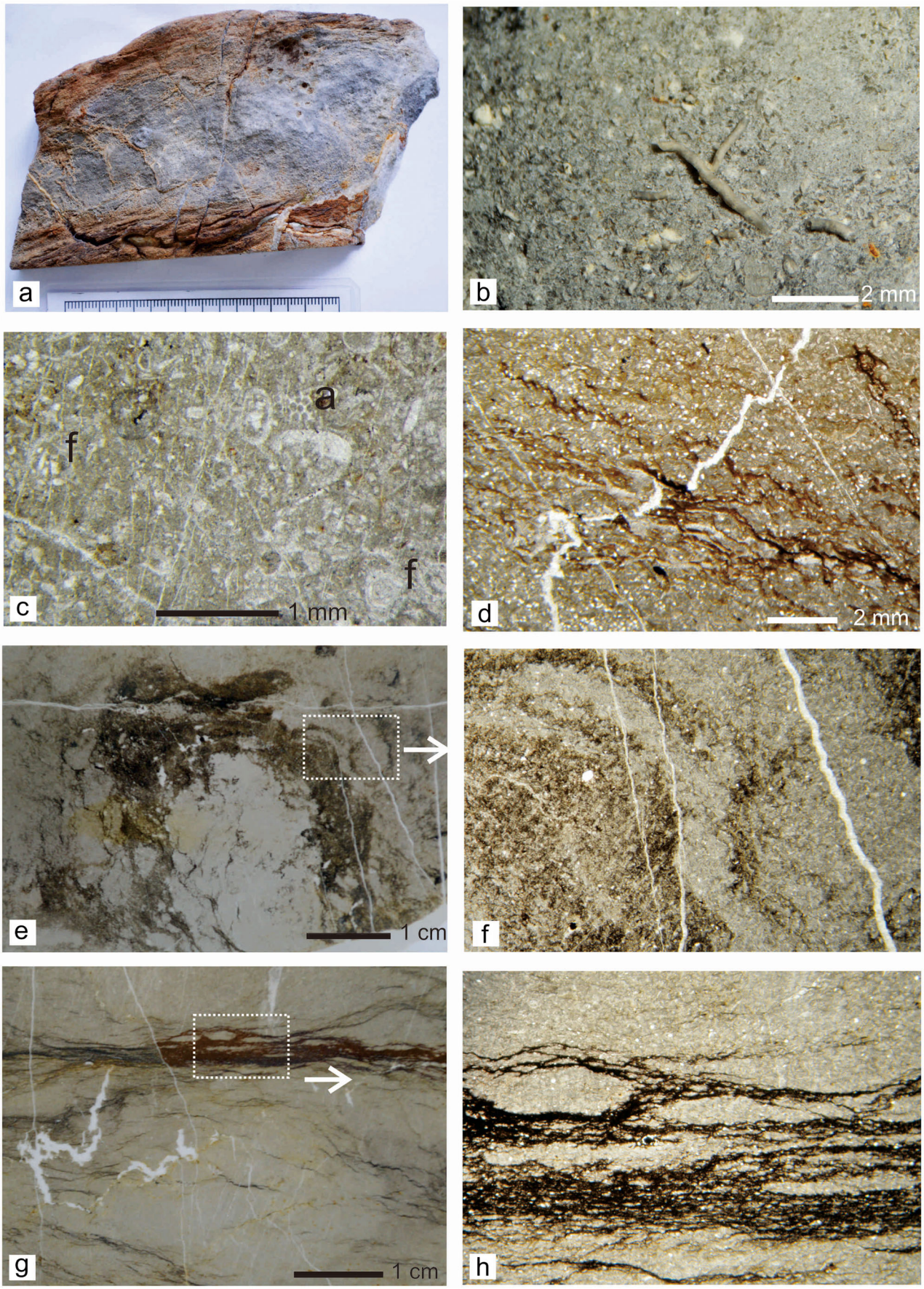
a
b
2 mm
a
f
f
c
1 mm
d
2 mm
e
1 cm
f
g
1 cm
h

◀ **Fig. 10** Photomicrographs of thin sections of Permian limestone microfacies from Mae Yuam sections, locality h on Figure 2. (a) Acid-etched slab of same sample as Fig. 9 a showing details of laminated Fe–Mn crust on bottom and top of the slab with tepee structure on bottom right; (b) magnification of an etched slab showing microconchid tubeworm floating in fine bioclastics and shell debris (MF2); (c) microbioclastic packstone showing smaller foraminifers (*f*) and calcareous green algal fragment (*a*) with microbioclastics floating in micrite matrix (MF2); (d) nodular microbioclastic wackestone (MF 1) with fine quartz grains dispersed in a micrite matrix, (e, g) stromatolitic bindstone (MF 4); (f) magnification of (e) showing intercalation of dark and light bands, (h) magnification of (g) showing nodular fabric and fine-grained particles embedded in a laminated stromatolite layer

Conodonts

Conodont elements from localities at Mae Yuam and Huai Pho (Figs. 2, 6) include *Mesogondolella siciliensis* and *M. dicerocarinata* (Fig. 10). All elements of the gondolellid apparatus are present at locality MY4 are generally unbroken, and suggest little to no reworking. *M. siciliensis* is a widespread conodont and ranges from the late Kungurian through to the Roadian (Henderson 2016; Wang et al. 2016) or to the uppermost Wordian (Kozur and Wardlaw 2010). It has previously been found in Thailand on both the Indochina and Sibumasu terranes (Dill et al. 2004; Burrett et al. 2015) as well as in Laurentia, South China, the Lhasa Terrane and in Oman (Kozur and Wardlaw 2010; Zhang et al. 2010 Yuan et al. 2016). *Mesogondolella dicerocarinata* (Wang and Wang) is a long-ranging species having co-existed and evolved from *M. siciliensis* in the Roadian and Wordian and possibly then survived by itself after the Wordian through to the upper Changhsingian. As *M. dicerocarinata* is known in the uppermost Wordian in Oman and co-occurs with *M. siciliensis*, we, therefore, place our two sections in the Wordian but note that other typical conodonts of the Wordian (Wardlaw and Nestell 2015) are absent in our two TWTR sections.

Systematic Palaeontology

Phylum Chordata Bateson, 1886
Class Conodonta Eichenberg, 1930
Order Ozarkodinida Dzik, 1976
Family Gondolellidae Lindström, 1970
Genus *Mesogondolella* Kozur, 1989
Mesogondolella siciliensis (Kozur, 1975) fig. 7, 7.

Synonymy

For synonymy see Yuan et al. (2016) and Burrett et al. (2015).
Mesogondolella cf. flexibilis (Chernykh and Reshetkova 1987), Dill et al. (2004) figs. 2, 9a-c
?Mesogondolella discedus Sobolev, 1996 in Sobolev and Nakrem (1996). Dill et al. (2004) figs. 2, 11-12.
Mesogondollella siciliensis (Kozur 1975) herein Figure 11 e and g.

M.rosenkrantzi (as *Gondolella rosenkrantzi*) was reported from several localities in the NWTR by Dieter Stoppel (in Hahn and Siebenhüner (1982), localities 8, 9 and 19 in Fig. 2). This species was erected by Bender and Stoppel (1965) on specimens from East Greenland and Sicily. The Sicilian specimens (Bender and Stoppel 1965, figs. 4–6) were placed in a new species, *Gondolella siciliensis* by Kozur (1975). The type of *M. rosenkrantzi* (Bender and Stoppel 1965, plate 14, fig. 11a, b) has a rounded posterior margin a small cusp and parallel sides until tapering anteriorly. The type differs markedly from other specimens referred by the original authors to *G. rosenkrantzi*. The Pa specimen on their plate fig.7a, b is triangular in overall shape whereas plate 14, fig. 10, is triangular, slightly curved, has a straight posterior margin and has prominent expansions of the platform posteriorly. It is this morphotype that was probably identified as *M. rosenkrantzi* by Stoppel (in Hahn and Siebenhüner 1982 *M. rosenkrantzi* is now identified in Greenland and other Laurentian localities as a Lopingian species (Henderson 2016). Subsequent work has shown that a similar 'blunt' and posteriorly expanded morphotype is a minor constituent of typical *M. siciliensis* populations (e.g. Yuan et al. 2016). However, in the Wadi Rustaq section in Oman, Kozur and Wardlaw (2010) found that the blunt, posteriorly expanded morphotype of *M. siciliensis* became dominant up-section and they erected a new species *M. omanensis* which they suggested developed from *M. siciliensis*. *M. rosenkrantzi* 'has a more triangular platform outline, the anterior blade is lower, the posterior denticles are very densely spaced' and 'the cusp is larger' than those in *M. omanensis* Kozur and Wardlaw (2010) p. 226. C. Y. Wang and Z. H. Wang (in Zhao et al. 1981) erected *Neogondolella dicerocarinata* on specimens from the upper Changhsingian of Zhejiang, South China. This species is identical to our triangular *Mesogondolella* and *M. omanensis*. *M. omanensis* is, therefore, a probable junior synonym of *Mesogondolella dicerocarinata*. Thus, *Mesogondolella dicerocarinata* (Wang and Wang) may be a long-ranging species having co-existed and evolved from *M. siciliensis* in the Roadian and Wordian and survived by itself after the Wordian through to the upper Changhsingian. As *M. dicerocarinata* is known in the uppermost Wordian in Oman and co-occurs with *M. siciliensis*, we, therefore, place our two sections in the Wordian but note that other typical conodonts of the Wordian are absent in our two NWTR sections.

Mesogondolella dicerocarinata (C. Y. Wang and Z. H. Wang 1981)
(Figure 11 a–d, i and j.)

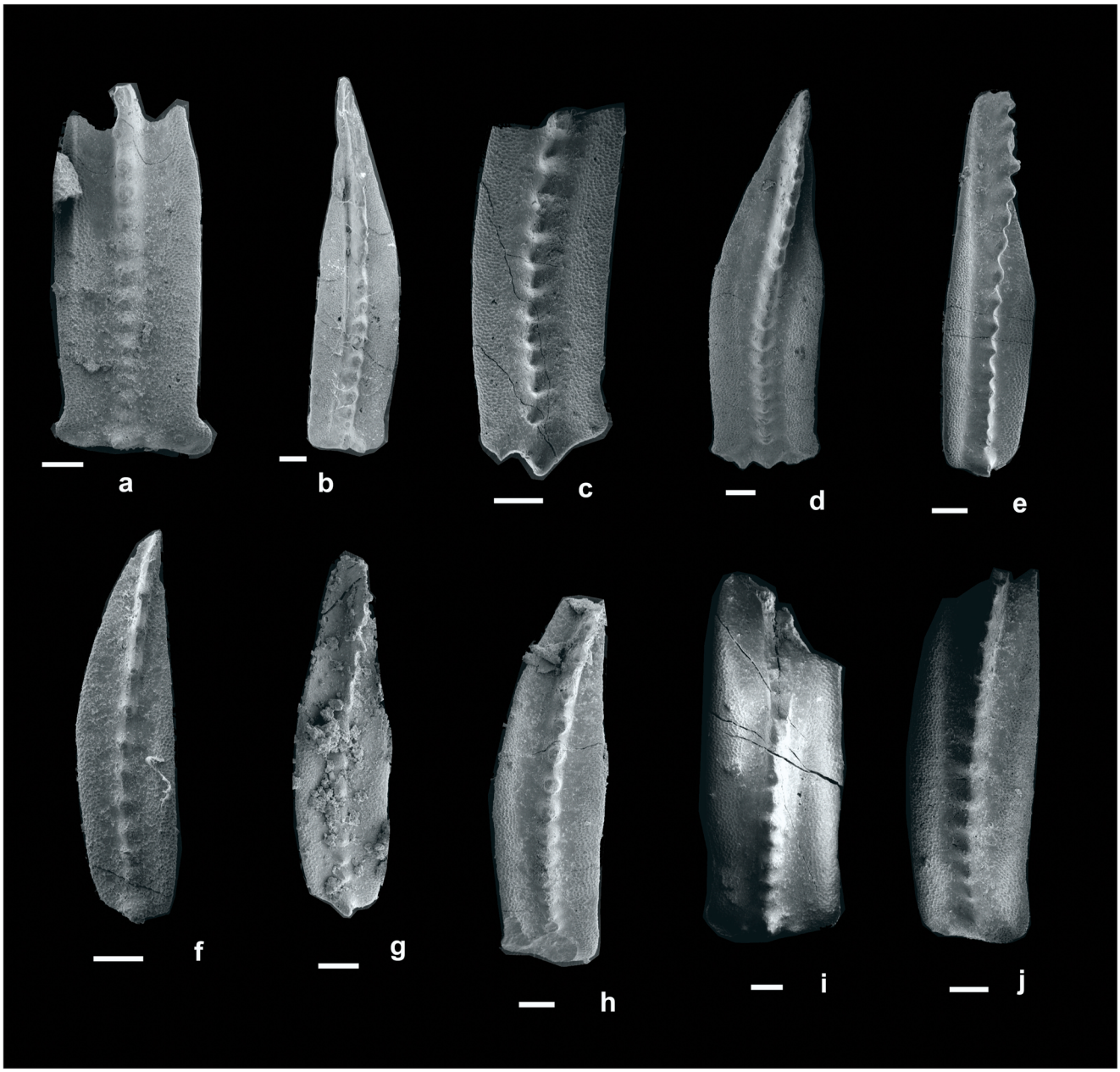

Fig. 11 Conodonts from sample MY 04 at Mae Yuam section, locality h in Figure 2(b). Scale bar = 100 microns. All Pa elements. (a–d, i, j) *Mesogondolella dicerocarinata* (Wang and Wang), (e, g) *M. siciliensis* (Kozur), (f, h) specimens intermediate between *M. siciliensis* and *Mesogondolella dicerocarinata*. Palaeontological Research and Education Centre specimen numbers PRC 609-618. Numerous typical *M. siciliensis* are also present in this sample

Synonymy

Neogondolella dicerocarinata Wang and Wang, 1981 (in Zhao et al. (1981), p.79, plate V., figs.19-20).
Mesogondolella omanensis Kozur and Wardlaw 2010, p. 226, Plate 2, figs. 2, 11, 12, 14-16.
Mesogondolella dicerocarinata (Wang and Wang, 1981) herein Fig. 11 a–d, i and j.

Description: (adapted from Wang and Wang in Zhao et al. (1981))

The platform is wedge-shaped, gradually tapering anteriorly and expanding near the posterior margin forming ear-like processes laterally. The carina is low, becoming node-like near the posterior end of the platform with a node-like transverse ridge. The keel is wide. Its posterior edge is square in outline and bears a pit and a groove. The species is easily distinguished from other gondolellids in having ear-like posterior-lateral processes and a transverse ridge at the posterior end of the carina. As in Oman, some of our specimens are intermediate with *M. siciliensis* (Fig. 11 f, h).

Radiolarian cherts

Previous work on radiolarian cherts in NW Thailand

Several radiolarian faunas from cherts ranging in age from the Mississippian to the Carnian have been described from the Mae Sariang-Mae Hong Son area (Caridroit et al. 1993; Kamata et al. 2002; Feng et al. 2004a, 2004b, 2005; Thassanapak 2008) and Late Devonian to Triassic radiolarites have been described from the Inthanon Zone (Wonganan and Caridroit 2005, 2006; Thassanapak et al. 2011a; Sanjit et al. 2014). Most faunas have been obtained from along or near Highway 108 which generally follows the eastern side of the Mae Yuam River valley (Figs. 2, 4(b)). Radiolarians are also reported in the Frasnian-Famennian limestones described by Königshof et al. (2012) but are rare and were not isolated or identified in our processed samples from that locality. Although radiolarians have been found within clasts in coarse Mesozoic siliciclastics 16 km west of the Mae Yuam Fault (Caridroit et al. 1993) (Figs. 4(b), 6), the farthest west radiolarians have yet been found in bedded chert which is 5 km from the fault (Figs. 2, 4).

The upper Permian radiolarians from 56 km north of Mae Sariang (Fig. 2, loc. f, 4b) (Feng et al. 2004a) are abaillellellids which Xiao et al. (2017) consider indicative of 'intermediate water depths' of between 300 and 1000 m. Such meso- to bathypelagic depths are characteristic of deep shelves or shelf margins, but not of true oceans.

Kamata et al. (2009) studied the chert belts of Thailand and identified two types of radiolarian chert. One type is hemipelagic, has a microcrystalline quartz matrix and contains calcareous organisms including foraminifers. The second type is pelagic, and consists of densely packed radiolarian tests and no terrigenous material and is found in the Inthanon Zone. The Triassic age radiolarian cherts of the NWTR are hemipelagic and were deposited on the eastern margin of the Sibumasu Terrane from the late Early Triassic to the Norian (Kamata et al. 2002; Feng et al. 2004a) and also on the western margin of the Inthanon Zone (Feng et al. 2004a; Thassanapak et al. 2017). The pelagic cherts of the Inthanon Zone Triassic range from the lowermost to the Middle Triassic (Kamata et al. 2009). The work of Kamata et al. (2009), therefore, supports a hemipelagic environment rather than a fully oceanic environment for the NWTR and its western margin during the Triassic.

Middle Triassic radiolarians from NWTR

Several chert sections along the highway HW 108 from Mae Sariang to Mae Hong Son have been studied. They include the Mae Sariang, Mae La Noi and Khun Yuam sections. Middle Triassic (Anisian to Ladinian) radiolarian faunas from these sections are summarised.

Khun Yuam section

The Khun Yuam section is located at km 179 along HW 108 between Mae Sariang and Mae Hong Son (x on Fig. 2). The species observed in the lower part of the section includes *Paroertlispongus chiensis* (Feng), *Cryptostephanidium cornigerum* Dumitrică, *Perispyridium* sp., *Spongostephanidium spongiosum* Dumitrică, *Parasepsagon* sp., *Triassospongosphaera multispinosa* (Kozur and Mostler), *Archaeocenosphaera* sp. and *Acanthosphaera* sp.

The upper part of the section, a few metres above the base, includes *Oertlispongus inaequispinosus* Dumitrică, Kozur and Mostler, *Baumgartneria ambigua* Dumitrică, *Baumgartneria curvispina* Dumitrică, *Baumgartneria retrospina* Dumitrică, *Baumgartneria yehae* Kozur and Mostler, *Falcispongus calcaneum* Dumitrică, *Paroertlispongus chinensis* (Feng), *Paroertlispongus multispinosus* Kozur and Mostler, *Paroertlispongus rarispinosus* Kozur and Mostler, *Pseudoertlispongus mostleri mostleri* Kozur, *Paroertlispongus daofuensis* Feng, *Paroertlispongus* sp. aff. *P. daofuensis* Feng, and other radiolarians.

The existence of advanced from of Oertlispongidae especially *Oertlispongus inaequispinosus*, with a unique long recurved spine, is a typical guide form of the Fassanian. Without having a typical late Ladinian species, the section is not younger than Fassanian. Therefore, the base of this section is late Anisian (Illyrian) and the upper part is early Ladinian (Fassanian).

Mae Sariang section

This section is located to the east of Mae Sariang town at km 99.575 of HW 108 along, the Mae Sariang-Chom Thong route (loc. o on Figs. 2 and 5). Radiolarians from this section are rare and are moderately preserved. The characteristic species are *Eptingium manfredi manfredi* Dumitrică, *Pseudostylosphaera coccostyla coccostyla* (Rüst), *Spongostephanidium* sp. cf. *S. longispinosum* Dumitrică, *Triassocampe deweveri* (Nakaseko and Nishimura), *Triassocampe* sp., *Oertlispongus inaequispinosus* Dumitrică, Kozur and Mostler, *Paroertlispongus multispinosus* Kozur and Mostler, *Pseudoertlispongus mostleri* Kozur, *Paurinella* sp., and *Pararuesticyrtium* sp. Based on the occurrence of the Fassanian guide form *Oertlispongus inaequispinosus* with its characteristic recurved spine as reported in the Khun Yuam section, the age of this section is confirmed as early Ladinian (Fassanian).

Mae La Noi section

This section is located along HW 108 between Mae Sariang and Mae La Noi (z on Fig. 2). Radiolarians are moderately well preserved consisting of *Eptingium manfredi manfredi*

Dumitrică, *Archaeospongoprunum bispinosum* Kozur and Mostler, *A.mesotriassicum mesotriassicum* Kozur and Mostler, *A. mesotriassicum asymmetricum* Kozur and Mostler, *Hindeosphaera spinulosa* (Nakaseko and Nishimura), *Pseudostylosphaera coccostyla coccostyla* (Rüst), *Pseudostylosphaera longispinosa* Kozur and Mostler, *Pseudostylosphaera nazarovi* (Kozur and Mostler), *Spongostylus tricostatus* Kozur, Krainer and Mostler, *Paroertlispongus multispinosus* Kozur and Mostler, *Paroertlispongus rarispinosus* Kozur and Mostler, *Paroertlispongus* sp., *Paurinella* sp., *Hozmadia rotunda* (Nakaseko and Nishimura), *Parasepsagon variabilis* (Nakaseko and Nishimura), *Archaeocenosphaera* sp., *Acanthosphaera nicorae* Kozur and Mostler, *Acanthosphaera* sp., *Astrocentrus* sp., *Annulotriassocampe companilis* Kozur, *Triassocampe coronata* Bragin, *Triassocampe deweveri* (Nakaseko and Nishimura), and *Triassocampe myterocorys* Sugiyama.

Among these species, *Archaeospongoprunum bispinosum* and *A. mesotriassicum mesotriassicum* are Illyrian species, and are typical late Anisian guideforms. *Hindeosphaera spinulosa* also frequently occurred in the late Anisian. Some species such as *Acanthosphaera nicorae* and *Hozmadia rotunda* are restricted to the *Tiborella florida* Subzone of *Spongosilicarmiger transitus* Zone (Kozur and Mostler 1994; Kozur et al. 1996). The age of this assemblage is therefore late Anisian (Illyrian).

Geochemistry of Permian and Triassic radiolarian cherts

The geochemistry of cherts is a powerful tool for elucidating palaeo-depositional environments (e.g. Armstrong et al. 1999; Kato et al. 2002; Murray 1994; Nozaki 2010; Owen et al. 1999; Thassanapak et al. 2011b; Udchachon et al. 2011, 2015). Radiolarian cherts are generally deposited along continental margins or in deep to very deep marine basins. Cherts, siliceous and phosphate rocks containing Middle Triassic radiolarians (radiolarites) were collected from localities near Mae Sariang, Mae La Noi and Khun Yuam (locs. o, d, e on Fig. 2). Permian radiolarites were sampled from the Pai and Khun Yuam sections (locs. v, f on Fig. 2). The Triassic sections are on or near the eastern margin of the NWTR or the western margin of the Inthanon Zone. Triassic radiolarians from these sections are identified and their ages assigned above. Late Permian radiolaria from Khun Yuam were identified by Feng et al. (2004a). The Khun Yuam section may have been on the eastern side of the NWTR or on the western margin of the Inthanon Zone. The radiolarians from the Permian section from Pai in the Inthanon Zone were described by Wonganan and Caridroit (2006) and assigned to the late Permian (late Capitanian to Wuchiapingian).

Analyses of major, minor and rare-earth elements (REEs) were carried out on these Permian and Triassic cherts. The inductively coupled plasma-mass spectrometry (ICP-MS) technique was used for REE analysis using an Agilent 7500a at the State Key Laboratory, China University of Geosciences (Wuhan). The detection limit is 0.003 to 0.1 μg/g for heavier mass elements and 0.01 to 1 μg/g for lighter elements. Analytical precision is generally better than 5% for REEs. The contents of REE abundance are normalised to the North American Shale Composite (NASC) with normalised values as proposed by Gromet et al. (1984). REE contents are also plotted against chondrite (Boynton 1984) to facilitate comparisons (e.g. Armstrong et al. 1999). Cerium anomalies (Ce/Ce*) are calculated from $Ce/Ce^*=Ce_n/(La_n\times Pr_n)1/2$ and europium anomalies (Eu/Eu*) are deduced from $Eu/Eu^*=Eu_n/(Sm_n\times Gd_n)1/2$ (Taylor and McLennan 1985). NASC-normalised Lan/Ybn ratio is used to represent HREE relative to LREE (Chen et al. 2006). The discrimination of chert depositional environment was conducted by using La_n/Ce_n vs. $Al_2O_3/(Al_2O_3+Fe_2O_3)$ ratio (Murray 1994). X-ray fluorescence (XRF) technique was used to analyse major element concentration. This process was carried out using an Oxford ED2000 XRF analyser at Suranaree University of Technology, Thailand.

Major element geochemistry

The silica content of Triassic chert from the Mae La Noi section (MLN) is between 83.21 and 87.98 w%, except for two samples of phosphatic rock which contain 2.70 and 37.96 w% silica and 88.38 and 46.33 w% phosphorus (Table 1). At Mae Sariang (MSR), silica content ranges between 81.77 and 87.57 w%, except for one sample which shows 28.33 w% of phosphorus and 55.22 w% of silica. At Khun Yuam (KYY), SiO_2 concentration ranges between 82.27 and 85.48 w%.

The increasing silica content of the rocks in these sections corresponds to decreasing phosphorus content. Almost all samples in these localities show mostly highly negative correlation coefficients of silica with other elements. This does not include samples from Mae La Noi which show both negative and moderate to high positive correlation with other elements (Tables 2 and 3).

The aluminium concentration from these Triassic rocks is between 0.85 and 2.62 w% at Mae Sariang and between 0.14 and 1.12 w% at Mae La Noi and between 1.44 and 2.10 w% at Khun Yuam. At Mae La Noi, the correlation coefficient of aluminium with titanium and potassium is highly positive (0.93 and 0.94 respectively). From the same locality, aluminium shows a moderately high positive correlation coefficient with iron oxide (0.90). At Mae Sariang, aluminium has a high positive correlation coefficient to iron (0.96) and manganese (1) and shows a moderate positive correlation to titanium (0.86) and potassium (0.86). At Khun Yuam, aluminium has a moderate positive correlation coefficient only with titanium (0.83) and potassium (0.80). Among these three localities, the

highest titanium content is 0.094 w% at Mae Sariang while one sample with a non-detectable value is found at Mae La Noi and ranges up to 0.036 w% but the Khun Yuam locality contains between 0.033 and 0.067 w%. The correlation coefficient of titanium in Mae La Noi is highly positive with respect to aluminium and potassium (0.94). This element has a moderate to high positive correlation coefficient to aluminium, iron, manganese and potassium (0.83 to 0.98) at Mae Sariang. At Khun Yuam, titanium shows a moderate to high positive correlation coefficient to aluminium, iron, calcium and potassium (0.82 to 0.98).

Potassium content at Khun Yuam is the highest, ranging from 0.85 to 1.45 w%. The K content at Mae La Noi and Mae Sariang is 0.24–0.62 w% and 0.43–1.06 w%, respectively. Normally, five samples from each outcrop were selected for geochemical discrimination. However, some samples showing high phosphate content with low silica content (phosphate rock) were separated from cherts for interpretation. On the other hand, samples with low silica concentration were discarded. In the Khun Yuam locality, the correlation coefficients of potassium with titanium, iron and calcium are highly positive (between 0.90 and 0.98) and moderately positive with aluminium (0.80). At Mae La Noi, the correlation coefficient of potassium is highly positive with titanium (0.94) and aluminium (0.92).

The iron concentration at Mae Sariang ranges between 0.31 and 2.74 w%. The correlation coefficient of this element to titanium, aluminium, magnesium and potassium is highly positive (between 0.94 and 0.97). Iron contents at Khun Yuam and Mae La Noi are 0.25–0.63 w% and 0.21–0.49 w%, respectively. The correlation coefficient of iron with titanium, calcium and potassium is

Table 1 Major element content of Permian and Triassic cherts from northern Thailand

	SiO_2	TiO_2	Al_2O_3	Fe_2O_3	MnO	MgO	CaO	Na_2O	K_2O	P_2O_5	Al/(Al+Fe)
Permian											
PI3	82.24	0.053	1.53	1.32	0.085	0.015	5.02		0.82		0.54
PI8	82.89	0.048	1.59	1.68	0.045	0.020	4.43		0.74		0.49
PI15	80.24	0.093	2.69	1.59	0.069	0.108	7.20	0.17	1.76		0.63
PI22	83.82	0.035	1.32	0.61	0.029	0.033	6.03		0.61		0.69
PI27	2.09		0.07	0.05	0.066	0.053	2.76	1.58		91.55	0.59
KY7	68.78	0.022	0.92	0.66	0.764		24.18		0.35		0.58
KY13	76.63	0.013	0.80	0.45	0.288	0.013	16.09	0.50	0.21		0.64
KY20	86.82	0.020	0.94	0.45	0.080	0.035	5.85	0.10	0.31		0.68
KY29	52.63	0.020	0.71	0.98	1.346	0.132	40.33	0.15	0.31		0.42
KY1-4	57.99	0.023	0.84	0.61	0.590	0.051	29.58		0.33		0.58
KY2-3	83.42	0.070	1.63	0.51	0.088		6.88		0.69		0.76
KY3-2	79.75	0.059	2.10	0.71	0.037	0.059	7.79	0.15	1.49		0.75
KY4-4	69.34	0.016	0.81	0.24	0.019		7.28		0.24		0.77
Triassic											
KYY1-5	84.09	0.050	1.82	0.50	0.032	0.026	7.79	2.00	1.14		0.78
KYY2-3	85.48	0.033	1.64	0.25	0.024	0.048	6.98	0.30	0.85		0.87
KYY3-1	84.51	0.042	1.61	0.45	0.054	0.049	8.82		1.13		0.78
KYY3-3	84.93	0.042	1.44	0.47	0.100	0.015	8.21		0.99		0.75
KYY3-5	82.27	0.067	2.01	0.63	0.045	0.042	9.69		1.46		0.76
MLN1-7	37.96	0.019	0.75	0.21	0.017	0.015	12.79		0.41	46.33	0.78
MLN1-13	87.87	0.016	0.75	0.30	0.035	0.026	7.03	0.07	0.24		0.71
MLN2-6	87.98	0.036	1.14	0.38	0.017		6.21		0.60		0.75
MLN2-12	83.21	0.031	1.20	0.49	0.065	0.022	9.53	0.33	0.62		0.71
MLN3-3	2.70		0.14	0.04	0.068		4.64	2.73		88.38	0.77
MSR1-5	87.57	0.024	0.98	0.45	0.072	0.125	6.28		0.45		0.68
MSR2-7	55.22	0.028	0.85	0.31	0.019	0.078	12.14	0.25	0.43	28.33	0.73
MSR3-4	85.74	0.040	2.22	1.49	0.358	0.514	5.56	0.21	0.57		0.60
MSR4-1	85.86	0.016	1.04	0.53	0.058	0.061	5.57		0.46		0.66
MSR5-1	81.77	0.094	2.62	2.74	0.413	0.643	6.47		1.06		0.49

Table 2 Concentration of trace elements from Permian and Triassic cherts from northern Thailand

	Sc	V	Cr	Co	Ni	Cu	Zn	Ga	Rb	Sr	Y	Zr	Nb	Mo	Sn	Cs	Ba	Hf	Ta	W	Tl	Pb	Th	U	Total (ppm)
Permian																									
PI3	4.23	42.7	12.2	95.4	2.85	6.94	3.95	5.65	49.7	36.9	4.62	32.2	2.47	1.35	0.89	12.1	822	1.00	0.95	16.2	0.54	9.38	3.68	2.88	1171.19
PI8	2.63	13.9	11.6	116	9.70	15.4	3.63	3.72	27.1	39.8	4.95	30.8	1.85	0.44	0.72	8.02	724	0.86	0.48	22.9	0.19	12.1	2.24	1.69	1055.17
PI15	2.13	12.5	6.69	87.0	2.08	8.78	2.58	3.60	25.4	41.0	3.73	27.0	1.77	0.38	0.74	7.46	932	0.72	0.49	18.7	0.20	8.32	2.07	0.86	1195.99
PI22	1.74	8.78	5.62	136	1.58	4.26	5.42	2.43	18.1	38.6	2.79	15.3	0.40	0.26	0.53	6.43	874	0.42	0.25	9.73	0.19	5.46	1.38	0.37	1139.97
PI27	4.62	40.7	17.4	45.2	2.45	13.7	5.37	7.49	63.2	34.8	7.55	44.5	4.08	0.34	1.36	11.6	865	1.17	0.55	6.47	0.53	4.72	4.72	1.82	1189.51
Avg	**3.07**	**23.73**	**10.71**	**95.90**	**3.73**	**9.81**	**4.19**	**4.58**	**36.72**	**38.23**	**4.73**	**29.94**	**2.11**	**0.55**	**0.85**	**9.12**	**843.55**	**0.83**	**0.54**	**14.79**	**0.33**	**8.00**	**2.82**	**1.53**	**1150.37**
KY7	1.96	9.08	5.56	148	13.5	16.2	4.20	2.35	14.9	13.1	3.32	10.9	0.96	0.36	0.43	1.97	61.0	0.31	0.73	20.2	0.18	3.13	0.95	0.35	333.47
KY13	0.98	4.22	4.05	135	4.12	6.04	5.81	1.40	10.5	9.69	1.57	7.01	0.29	0.31	0.23	1.35	57.1	0.19	0.37	13.1	0.085	2.32	0.56	0.15	266.96
KY20	1.11	4.28	5.31	85.5	4.34	11.7	5.77	1.59	10.5	7.17	1.34	10.1	0.69	0.25	0.27	1.32	67.9	0.28	0.43	11.1	0.069	2.05	0.67	0.18	233.94
KY29	1.23	5.24	4.30	218	5.28	7.54	12.3	1.50	11.8	22.1	2.35	8.45	0.37	2.40	0.33	1.39	67.1	0.24	0.62	8.21	0.091	2.47	0.66	0.17	384.05
Avg	**1.32**	**5.71**	**4.80**	**146.67**	**6.82**	**10.37**	**7.03**	**1.71**	**11.93**	**13.00**	**2.14**	**9.12**	**0.58**	**0.83**	**0.31**	**1.51**	**63.28**	**0.25**	**0.54**	**13.16**	**0.11**	**2.49**	**0.71**	**0.21**	304.61
Triassic																									
KYY1-5	3.19	9.50	9.85	90.9	2.45	5.11	5.31	4.16	31.0	11.2	10.4	32.6	2.33	0.63	0.64	6.31	128	0.75	0.89	10.9	0.20	11.3	2.15	0.69	380.53
KYY2-3	2.76	6.46	4.15	98.4	1.93	3.15	2.70	3.09	23.1	7.84	6.77	18.8	0.88	0.36	0.40	3.05	136	0.48	0.47	8.59	0.15	6.76	1.22	0.72	338.08
KYY3-1	2.99	11.3	8.36	57.5	3.68	5.69	4.07	3.65	29.1	8.69	7.06	30.4	1.59	0.30	0.62	4.65	119	0.67	0.62	6.83	0.18	1.73	1.86	0.72	311.46
KYY3-3	2.76	10.6	8.25	82.0	3.42	5.49	4.44	3.28	27.2	9.02	6.11	20.4	1.42	0.21	0.59	4.35	131	0.51	0.79	9.03	0.17	1.73	1.82	0.62	334.83
KYY3-5	3.38	14.7	11.9	72.0	4.71	7.88	6.64	4.60	41.0	10.5	7.77	24.4	2.34	0.19	0.75	5.77	127	0.72	0.73	8.09	0.23	2.19	2.40	0.52	360.04
Avg	**3.01**	**10.52**	**8.50**	**80.16**	**3.24**	**5.46**	**4.63**	**3.76**	**30.30**	**9.45**	**7.62**	**25.34**	**1.71**	**0.34**	**0.60**	**4.82**	**128.04**	**0.63**	**0.70**	**8.69**	**0.19**	**4.74**	**1.89**	**0.65**	**344.99**
MLN1-7	2.80	8.59	8.79	58.3	5.92	9.15	6.59	2.76	18.5	17.0	8.11	19.2	1.27	0.19	0.49	2.60	76.5	0.48	0.78	7.28	0.17	5.20	1.97	1.29	263.97
MLN1-13	3.10	12.8	9.12	52.3	5.54	11.6	9.20	3.46	22.7	15.4	6.60	20.5	1.56	0.20	0.54	2.91	76.4	0.49	0.70	5.73	0.17	5.96	1.78	0.78	269.47
MLN2-6	2.21	12.1	16.3	128	3.91	9.67	4.83	2.73	16.4	13.3	5.22	13.9	1.23	0.22	0.66	2.16	92.5	0.38	0.74	9.78	0.11	4.53	1.42	0.86	343.23
MLN2-12	2.45	9.38	11.7	210	4.90	6.38	6.63	2.75	18.9	12.2	4.01	13.2	1.33	0.35	0.53	2.06	92.1	0.39	1.45	15.5	0.15	8.64	1.32	1.34	427.85
MLN3-3	1.40	7.50	9.86	67.1	5.39	12.3	11.2	1.46	8.67	11.6	2.64	8.81	0.60	0.73	0.44	1.52	60.1	0.27	0.58	6.11	0.090	5.15	1.03	0.51	224.95
Avg	**2.39**	**10.07**	**11.14**	**103.19**	**5.13**	**9.81**	**7.68**	**2.63**	**17.05**	**13.90**	**5.32**	**15.12**	**1.20**	**0.34**	**0.53**	**2.25**	**79.51**	**0.40**	**0.85**	**8.88**	**0.14**	**5.90**	**1.51**	**0.95**	**305.89**
MSR1-5	8.10	52.4	29.6	17.6	9.46	22.2	290	10.8	75.1	9.79	15.7	75.8	7.63	0.76	1.81	5.26	675	2.19	0.71	162	0.31	245	6.96	1.16	1725.83
MSR2-7	2.95	18.1	11.1	32.2	6.18	10.3	119	4.03	27.8	8.07	7.30	27.2	2.39	0.18	0.62	2.50	445	0.73	0.54	295	0.16	19.8	2.36	0.51	1044.88
MSR3-4	4.32	22.8	15.8	28.0	7.11	16.5	208	5.52	29.6	6.93	8.63	42.2	3.92	0.32	0.87	4.23	296	1.12	0.55	251	0.13	30.7	3.48	0.91	988.38
MSR4-1	1.46	3.47	3.52	257	2.90	6.54	81.6	2.01	13.6	5.97	3.55	9.43	0.26	0.64	0.86	0.82	328	0.30	0.31	746	0.061	32.6	1.26	1.09	1503.58
MSR5-1	1.62	6.03	5.14	67.8	2.11	18.1	31.5	2.31	14.9	6.75	3.58	12.8	0.61	1.41	0.50	0.89	131	0.36	0.50	436	0.13	31.3	1.48	0.80	777.15
Avg	**3.69**	**20.56**	**13.03**	**80.56**	**5.55**	**14.74**	**146.09**	**4.93**	**32.22**	**7.50**	**7.76**	**33.51**	**2.96**	**0.66**	**0.93**	**2.74**	**374.92**	**0.94**	**0.52**	**378.02**	**0.16**	**71.97**	**3.11**	**0.89**	**1207.97**

Table 3 Concentration of rare earth elements (REE) from Permian and Triassic cherts from northern Thailand

REE	PI3	PI8	PI15	PI22	PI27	KY7	KY13	KY20	KY29	KYY1-5	KYY2-3	KYY3-1
La	6.58	6.59	5.19	2.83	12.0	2.98	2.12	1.79	2.02	10.43	4.85	7.87
Ce	15.9	19.2	13.0	6.85	33.7	10.2	7.48	5.34	7.34	23.00	10.83	15.66
Pr	1.76	1.95	1.31	0.71	3.12	0.86	0.64	0.49	0.65	2.91	1.47	2.21
Nd	6.52	7.36	4.56	2.44	11.2	3.40	2.38	1.90	2.51	11.13	5.77	8.27
Sm	1.11	1.33	0.70	0.43	1.96	0.74	0.52	0.36	0.61	2.28	1.29	1.70
Eu	0.29	0.31	0.22	0.20	0.43	0.17	0.12	0.090	0.15	0.46	0.27	0.32
Gd	0.80	0.85	0.48	0.36	1.23	0.72	0.42	0.27	0.56	1.93	1.11	1.28
Tb	0.14	0.13	0.084	0.062	0.19	0.12	0.059	0.043	0.085	0.30	0.18	0.20
Dy	0.79	0.83	0.57	0.42	1.26	0.66	0.32	0.23	0.44	1.73	1.07	1.23
Ho	0.17	0.17	0.13	0.096	0.26	0.12	0.054	0.048	0.082	0.36	0.22	0.26
Er	0.53	0.55	0.43	0.30	0.86	0.34	0.16	0.15	0.21	1.11	0.64	0.75
Tm	0.080	0.090	0.066	0.046	0.13	0.049	0.022	0.024	0.030	0.16	0.09	0.11
Yb	0.60	0.58	0.45	0.31	0.88	0.32	0.13	0.15	0.18	1.08	0.61	0.70
Lu	0.095	0.083	0.070	0.045	0.13	0.045	0.021	0.022	0.026	0.16	0.09	0.10
ΣREE(ppm)	**35.37**	**40.05**	**27.24**	**15.10**	**67.40**	**20.73**	**14.46**	**10.91**	**14.89**	**57.05**	**28.50**	**40.65**
Chondrite normalised												
Ce/Ce*	1.11	1.28	1.19	1.15	1.31	1.52	1.53	1.35	1.53	0.99	0.97	0.89
Eu/Eu*	1.01	0.96	1.23	1.64	0.89	0.75	0.86	0.93	0.81	0.71	0.75	0.72
La/Yb	7.44	7.66	7.87	6.13	9.24	6.32	11.24	8.19	7.61	6.56	5.38	7.64
La/Ce	1.08	0.90	1.04	1.08	0.93	0.76	0.74	0.88	0.72	1.19	1.17	1.31
NASC normalised												
Ce/Ce*	1.09	1.25	1.16	1.21	1.27	1.52	1.55	1.18	1.77	0.91	0.88	0.82
Eu/Eu*	1.42	1.35	1.73	2.31	1.28	1.11	1.27	1.52	1.26	0.96	1.00	0.97
La/Yb	1.10	1.13	1.16	1.17	1.95	1.52	2.62	1.49	1.31	0.94	0.77	1.09
La/Ce	0.89	0.74	0.86	0.83	0.80	0.62	0.62	0.85	0.50	1.03	1.02	1.15

REE	KYY3-3	KYY3-5	MLN1-7	MLN1-13	MLN2-6	MLN2-12	MLN3-3	MSR1-5	MSR2-7	MSR3-4	MSR4-1	MSR5-1
La	7.13	7.48	11.52	7.08	4.79	3.77	2.96	20.04	7.63	10.04	4.33	4.12
Ce	14.17	14.64	28.27	15.52	10.17	7.93	7.06	42.98	17.20	22.29	9.41	9.22
Pr	2.05	2.01	3.07	1.92	1.36	1.08	0.86	4.68	1.99	2.42	1.06	0.95
Nd	7.60	7.18	11.40	7.14	5.20	4.18	3.38	17.94	7.47	9.56	3.94	3.48
Sm	1.52	1.39	2.18	1.52	1.15	0.92	0.67	3.28	1.51	1.84	0.85	0.69
Eu	0.29	0.27	0.42	0.28	0.24	0.19	0.13	0.65	0.31	0.32	0.17	0.16
Gd	1.23	1.11	1.72	1.30	1.01	0.78	0.55	2.72	1.32	1.42	0.64	0.56
Tb	0.19	0.18	0.27	0.20	0.16	0.12	0.08	0.43	0.21	0.23	0.11	0.10
Dy	1.07	1.12	1.43	1.16	0.95	0.68	0.46	2.74	1.28	1.46	0.63	0.57
Ho	0.21	0.24	0.28	0.22	0.19	0.14	0.09	0.59	0.25	0.31	0.14	0.13
Er	0.62	0.73	0.75	0.63	0.55	0.40	0.28	1.68	0.70	0.91	0.33	0.34
Tm	0.09	0.11	0.11	0.09	0.07	0.06	0.04	0.24	0.09	0.12	0.05	0.05
Yb	0.60	0.76	0.68	0.59	0.53	0.40	0.27	1.70	0.64	0.79	0.35	0.35
Lu	0.09	0.11	0.10	0.09	0.08	0.06	0.04	0.25	0.09	0.12	0.06	0.05
ΣREE(ppm)	**36.86**	**37.33**	**62.20**	**37.77**	**26.45**	**20.71**	**16.87**	**99.93**	**40.70**	**51.83**	**22.05**	**20.77**
Chondrite normalised												
Ce/Ce*	0.88	0.90	1.13	1.00	0.95	0.94	1.05	1.06	1.05	1.08	1.05	1.11
Eu/Eu*	0.70	0.70	0.71	0.65	0.73	0.74	0.71	0.71	0.72	0.65	0.75	0.82
La/Yb	8.06	6.63	11.43	8.08	6.13	6.39	7.35	7.98	8.02	8.60	8.39	8.06
La/Ce	1.31	1.33	1.06	1.19	1.23	1.24	1.09	1.22	1.16	1.18	1.20	1.17
NASC normalised												
Ce/Ce*	0.99	0.82	1.04	0.92	0.87	0.86	0.96	0.97	0.96	0.98	0.96	1.01
Eu/Eu*	0.94	0.94	0.96	0.88	0.98	0.99	0.96	0.96	0.97	0.87	1.01	1.11
La/Yb	1.15	0.95	1.63	1.16	0.88	0.91	1.05	1.14	1.15	1.23	1.20	1.15
La/Ce	1.15	1.17	0.93	1.04	1.07	1.09	0.96	1.06	1.01	1.03	1.05	1.02

moderate to high positive (0.87 to 0.93) at the Khun Yuam and moderately positive with aluminium (0.90) at Mae La Noi.

Normally, phosphate content for all samples is under the detection limit, except for two samples of phosphate rock from Mae La Noi and a sample of phosphatic chert from Mae Sariang. Phosphate rock samples show 46.33 and 88.38 w% phosphate content, while the phosphatic chert contains 28.33 w% phosphate.

The Permian cherts show high Si as 80.24–83.84 w% from the Pai section (PI) and relatively low in the Khun Yuam section (KY) as 52.63–86.82 w%. Phosphate rock from Pai shows 2.09 w% of silica content with 91.55 w% phosphorus content (Table 1).

The aluminium content ranges from 1.32 to 2.69 w% and 0.71 to 2.10 w% from Pai and Khun Yuam, respectively. Correlation coefficients of aluminium with titanium and potassium are high (0.91 to 0.99), but low with other elements (Table 3).

The potassium content of Permian chert ranges from 0.61 to 1.76 w% and 0.21 to 1.49 w% from Pai and Khum Yuam, respectively. It shows a very high positive correlation coefficient with titanium (0.99) and aluminium (0.99) in Pai. These correlation coefficients are 0.80 and 0.96, respectively, in Khun Yuam. The iron content of chert from Pai is high and ranges between 0.61 and 1.68 w% which is highest compared to rocks from all sections analysed in this study. However, a phosphate rock from this section has 0.07 w% Fe. Iron content from chert and siliceous rocks from Khun Yuam range from 0.24 to 0.98 w%. Generally, iron content exhibits a low correlation coefficient with other elements. Four samples from Khun Yuam show high calcium content (16.09–40.33 w%).

Trace elements

The concentration of trace elements is presented in Table 4. For the Triassic rocks, in most cases, Co, Rb, Zr and Ba have significant concentrations above other trace elements. At Khun Yuam, there are 80.16, 30.30, 25.34 and 128.04 ppm average contents of Co, Rb, Zr and Ba, respectively. At Mae La Noi, the average concentration of Co, Rb, Zr and Ba is 103.19, 17.05, 15.12 and 79.51 ppm, respectively. The average content of these elements in Mae Sariang is 80.56, 32.22, 33.51 and 374.92 ppm, respectively. Other significant content is observed in W (average 378.02 ppm) and Zn (146.09 ppm) at Mae Sariang. Concentrations of other trace elements in these localities are low and variable. They are less than 1 ppm in some elements and up to a few tens ppm in others.

Correlation coefficients of some trace element including Cr, Rb, Zr, Nb, Hf, Ta and Th with major element contents are shown in Table 2. At Khun Yuam, titanium and potassium show a good correlation to some trace elements (Cr, Rb and Th) with 0.92 to 0.99 in both cases. Aluminium shows a variable positive correlation to trace elements (0.35 to 0.82) and the highest positive correlation with Rb. However, MgO has mostly a low negative correlation to these elements.

At Mae La Noi, titanium and aluminium have high positive correlations only with Cr but show a high negative correlation with most selected trace elements. Magnesium shows high positive value with almost all these trace elements. At Mae Sariang, most correlation coefficients between given major and trace elements show a negative or poor relationship.

For the Permian rocks, correlation coefficients of these trace elements with most major elements being low for the Pai samples. However, titanium and potassium from the Khun Yuam samples show moderate to high correlation coefficients with these trace elements (0.70–0.88 and 0.74–0.94, respectively). Aluminium shows high correlation values with Cr (0.88) and Nb (0.81) (Table 3).

Rare earth elements

The concentration of rare earth elements (REEs) from Permian and Triassic sections are shown in Table 5 and Figures 12 and 13. For the Triassic cherts, total REE at Mae Sariang is relatively high compared to other samples (20.77 to 99.93 ppm). This value ranges from 28.50 to 57.05 ppm and 16.87 to 62.20 ppm at Khun Yuam and Mae La Noi, respectively. Most of the positive and high values are observed in LREE. HREE is relatively low (less than 1) in most cases.

The REE distribution pattern in relation to NASC (North American Shale Composite normalisation value from Gromet et al. 1984) in all localities is generally flat. It shows a slightly low HREE in Mae La Noi and Mae Sariang (average of La_n/Yb_n =1.13 and 1.17, respectively) with the lowest in Khun Yuam (average of ratio La_n/Yb_n =0.98). Most samples from Khun Yuam show pronounced negative Ce and Nd patterns with slightly negative Nd patterns observed from other sections.

La abundance at Mae Sariang is the highest of the three sections. It ranges from 4.12 to 20.04 ppm. At Mae La Noi and Khun Yuam, it ranges from 2.96 to 11.52 ppm and 4.85 to 10.43 ppm, respectively (Table 5). Ce anomalies in most samples from all sections are slightly negative and close to 1 with only two samples showing slightly low positive anomaly (Fig. 12). La_n/Ce_n values in all sections are low with slightly positive values for most of the samples. It ranges from 1.02 to 1.17, 0.93 to 1.09 and 1.01 to 1.06 in Khun Yuam, Mae La Noi and Mae Sariang, respectively. Most Eu anomalies in all sections are slightly negative and close to 1. It lies from 0.94 to 1.00 in Khun Yuam. In Mae La Noi and Mae Sariang, it ranges from 0.88 to 0.99 and 0.87 to 1.11, respectively.

For chondrite normalised REE (Table 5), the distribution pattern exhibits clear high LREE and low HREE

in all samples. They show a slightly negative Ce anomaly in Khun Yuam. All sections have pronounced negative Eu with slightly positive Gd (Fig. 12).

For the Permian samples, the total REE of most samples from the Pai section is high (15.10 to 67.40 ppm). It is lowest at Khun Yuam (10.19 to 20.73 ppm) compared to all Permian and Triassic sections in this study. The LREE content is high and higher than that of HREE content. All HREE are lower than 1 ppm (Table 5). The average of La_n/Yb_n from Pai and Khun

Table 4 Correlation coefficients of major and trace elements from Triassic chert from northern Thailand

Section code = KYY

	SiO_2	TiO_2	Al_2O_3	Fe_2O_3	MnO	MgO	CaO	K_2O	Cr	Rb	Zr	Nb	Hf	Ta	Th
SiO_2	1														
TiO_2	−0.99	1													
Al_2O_3	−0.85	0.83	1												
Fe_2O_3	−0.90	0.93	0.59	1											
MnO	0.10	−0.05	−0.60	0.26	1										
MgO	−0.09	−0.02	0.33	−0.26	−0.66	1									
CaO	−0.84	0.82	0.48	0.87	0.29	0.10	1								
K_2O	−0.99	0.98	0.80	0.92	−0.05	0.11	0.90	1							
Cr	−0.90	0.93	0.63	0.99	0.18	−0.24	0.83	0.93	1						
Rb	−1.00	0.99	0.82	0.92	−0.04	0.06	0.87	0.99	0.92	1					
Zr	−0.32	0.32	0.35	0.42	−0.25	0.05	0.27	0.41	0.52	0.32	1				
Nb	−0.85	0.88	0.75	0.89	−0.10	−0.20	0.63	0.86	0.94	0.85	0.67	1			
Hf	−0.74	0.74	0.73	0.74	−0.30	0.07	0.57	0.79	0.81	0.74	0.87	0.93	1		
Ta	−0.42	0.51	0.22	0.70	0.33	−0.75	0.30	0.44	0.73	0.45	0.53	0.77	0.60	1	
Th	−0.90	0.92	0.66	0.98	0.12	−0.23	0.80	0.92	1.00	0.91	0.56	0.96	0.85	0.75	1

Section code = MLN

	SiO_2	TiO_2	Al_2O_3	Fe_2O_3	MnO	MgO	CaO	K_2O	Cr	Rb	Zr	Nb	Hf	Ta	Th
SiO_2	1														
TiO_2	0.40	1													
Al_2O_3	0.53	0.93	1												
Fe_2O_3	0.71	0.69	0.90	1											
MnO	0.42	0.13	0.48	0.78	1										
MgO	0.97	−0.05	0.20	0.51	0.55	1									
CaO	−0.92	−0.36	−0.35	−0.43	−0.03	−0.99	1								
K_2O	0.18	0.94	0.92	0.68	0.25	−0.27	−0.05	1							
Cr	0.76	0.86	0.80	0.67	0.08	0.72	−0.79	0.65	1						
Rb	0.66	−0.39	−0.15	0.27	0.50	0.99	−0.53	−0.52	0.02	1					
Zr	0.64	−0.43	−0.30	0.03	0.15	0.89	−0.67	−0.64	0.08	0.93	1				
Nb	0.84	−0.14	0.08	0.44	0.49	1.00	−0.73	−0.32	0.29	0.96	0.91	1			
Hf	0.77	−0.27	−0.09	0.27	0.36	0.97	−0.71	−0.47	0.20	0.97	0.97	0.98	1		
Ta	0.23	0.41	0.68	0.81	0.91	0.15	0.16	0.59	0.16	0.10	−0.27	0.13	−0.03	1	
Th	0.85	−0.12	0.01	0.30	0.24	0.97	−0.85	−0.37	0.38	0.89	0.95	0.96	0.97	−0.12	1

Section code = MSR

	SiO_2	TiO_2	Al_2O_3	Fe_2O_3	MnO	MgO	CaO	K_2O	Cr	Rb	Zr	Nb	Hf	Ta	Th
SiO_2	1														
TiO_2	0.07	1													
Al_2O_3	0.36	0.86	1												
Fe_2O_3	0.29	0.95	0.96	1											
MnO	0.39	0.83	1.00	0.94	1										
MgO	0.31	0.87	0.99	0.95	0.99	1									
CaO	−0.99	−0.12	−0.44	−0.37	−0.46	−0.37	1								
K_2O	0.20	0.98	0.86	0.97	0.82	0.85	−0.26	1							
Cr	0.21	−0.33	−0.29	−0.36	−0.21	−0.20	−0.07	−0.41	1						
Rb	0.20	−0.35	−0.39	−0.42	−0.33	−0.31	−0.05	−0.41	0.98	1					
Zr	0.24	−0.33	−0.27	−0.35	−0.19	−0.19	−0.10	−0.41	1.00	0.97	1				
Nb	0.22	−0.34	−0.28	−0.37	−0.21	−0.20	−0.08	−0.42	1.00	0.97	1.00	1			
Hf	0.26	−0.34	−0.29	−0.37	−0.22	−0.21	−0.12	−0.41	1.00	0.98	1.00	1.00	1		
Ta	−0.03	0.03	−0.05	−0.08	0.02	0.07	0.15	−0.10	0.89	0.85	0.89	0.89	0.87	1	
Th	0.29	−0.33	−0.30	−0.35	−0.22	−0.21	−0.14	−0.38	0.99	0.99	0.99	0.99	1.00	0.86	1

Yuam are 1.30 and 1.73, respectively, and are higher than those of the Triassic samples Table 6.

The REE distribution pattern in relation to NASC from both sections is generally flat with pronounced positive Ce and Eu anomalies in Khun Yuam and Pai, respectively (Fig. 13).

La abundance at Khun Yuam is higher than that of Pai. It ranges from 2.83 to 12.00 ppm and 1.79 to 2.98 ppm at Khun Yuam and Pai, respectively (Table 5). Ce anomalies of these Permian samples are positive and more than 1 which is higher than all analysed Triassic samples. La_n/Ce_n values of all Permian samples are low and lower than all Triassic samples and range from 0.74 to 0.89 and 0.50 to 0.85 at Pai and Khun Yuam, respectively. The Eu anomaly from Pai is highly positive for most samples ranging from 1.28 to 2.31 and lies between 1.11 and 1.52 for the Khun Yuam samples. Chondrite normalised REE distribution patterns show a high LREE with low HREE in all samples. They display a slightly positive Ce anomaly as well as positive Eu in Khun Yuam and Pai, respectively (Fig. 13).

Interpretation of the origin and depositional environment of chert and siliceous rocks

The Al–Fe–Mn diagram was developed by Adachi et al. (1986) and Yamamoto (1987) to discriminate the differentiate cherts as either hydrothermal or non-hydrothermal.

Table 5 Correlation coefficients of major and trace elements from Permian chert from northern Thailand

Section code = PI

	SiO_2	TiO_2	Al_2O_3	Fe_2O_3	MnO	MgO	CaO	K_2O	Cr	Rb	Zr	Nb	Hf	Ta	Th
SiO_2	1														
TiO_2	−0.99	1													
Al_2O_3	−0.95	0.99	1												
Fe_2O_3	−0.64	0.62	0.56	1											
MnO	−0.68	0.56	0.42	0.52	1										
MgO	−0.81	0.88	0.94	0.26	0.17	1									
CaO	−0.60	0.66	0.72	−0.17	0.06	0.90	1								
K_2O	−0.96	0.99	0.99	0.51	0.47	0.94	0.76	1							
Cr	0.06	−0.17	−0.30	0.56	0.50	−0.61	−0.82	−0.31	1						
Rb	−0.18	0.04	−0.13	0.31	0.84	−0.38	−0.41	−0.07	0.78	1					
Zr	−0.45	0.36	0.23	0.86	0.74	−0.12	−0.44	0.22	0.86	0.73	1				
Nb	−0.53	0.42	0.27	0.78	0.87	−0.07	−0.33	0.28	0.81	0.84	0.97	1			
Hf	−0.35	0.24	0.09	0.74	0.79	−0.25	−0.51	0.09	0.91	0.85	0.98	0.98	1		
Ta	−0.31	0.17	0.00	0.40	0.90	−0.27	−0.34	0.05	0.76	0.99	0.79	0.89	0.89	1	
Th	−0.23	0.10	−0.07	0.41	0.86	−0.35	−0.43	−0.03	0.81	0.99	0.80	0.89	0.90	1.00	1

Section code = KY

	SiO_2	TiO_2	Al_2O_3	Fe_2O_3	MnO	MgO	CaO	K_2O	Cr	Rb	Zr	Nb	Hf	Ta	Th
SiO_2	1														
TiO_2	0.44	1													
Al_2O_3	0.54	0.91	1												
Fe_2O_3	−0.53	0.15	0.11	1											
MnO	−0.82	−0.36	−0.49	0.79	1										
MgO	−0.58	0.16	−0.01	0.82	0.57	1									
CaO	−0.90	−0.40	−0.52	0.74	0.96	0.55	1								
K_2O	0.36	0.80	0.96	0.27	−0.35	0.12	−0.36	1							
Cr	0.35	0.73	0.88	−0.20	−0.22	−0.44	−0.35	0.81	1						
Rb	−0.39	0.70	0.26	0.36	0.46	−0.22	0.40	0.74	0.58	1					
Zr	0.16	0.86	0.76	0.02	−0.02	−0.26	−0.16	0.92	0.98	0.65	1				
Nb	0.22	0.74	0.81	−0.12	−0.11	−0.48	−0.22	0.83	0.97	0.74	0.96	1			
Hf	0.09	0.88	0.71	0.07	0.05	−0.25	−0.08	0.94	0.96	0.72	1.00	0.97	1		
Ta	−0.63	0.84	0.04	0.66	0.71	0.16	0.63	0.83	0.48	0.93	0.62	0.61	0.69	1	
Th	−0.14	0.78	0.53	0.18	0.24	−0.33	0.15	0.85	0.81	0.95	0.85	0.92	0.89	0.85	1

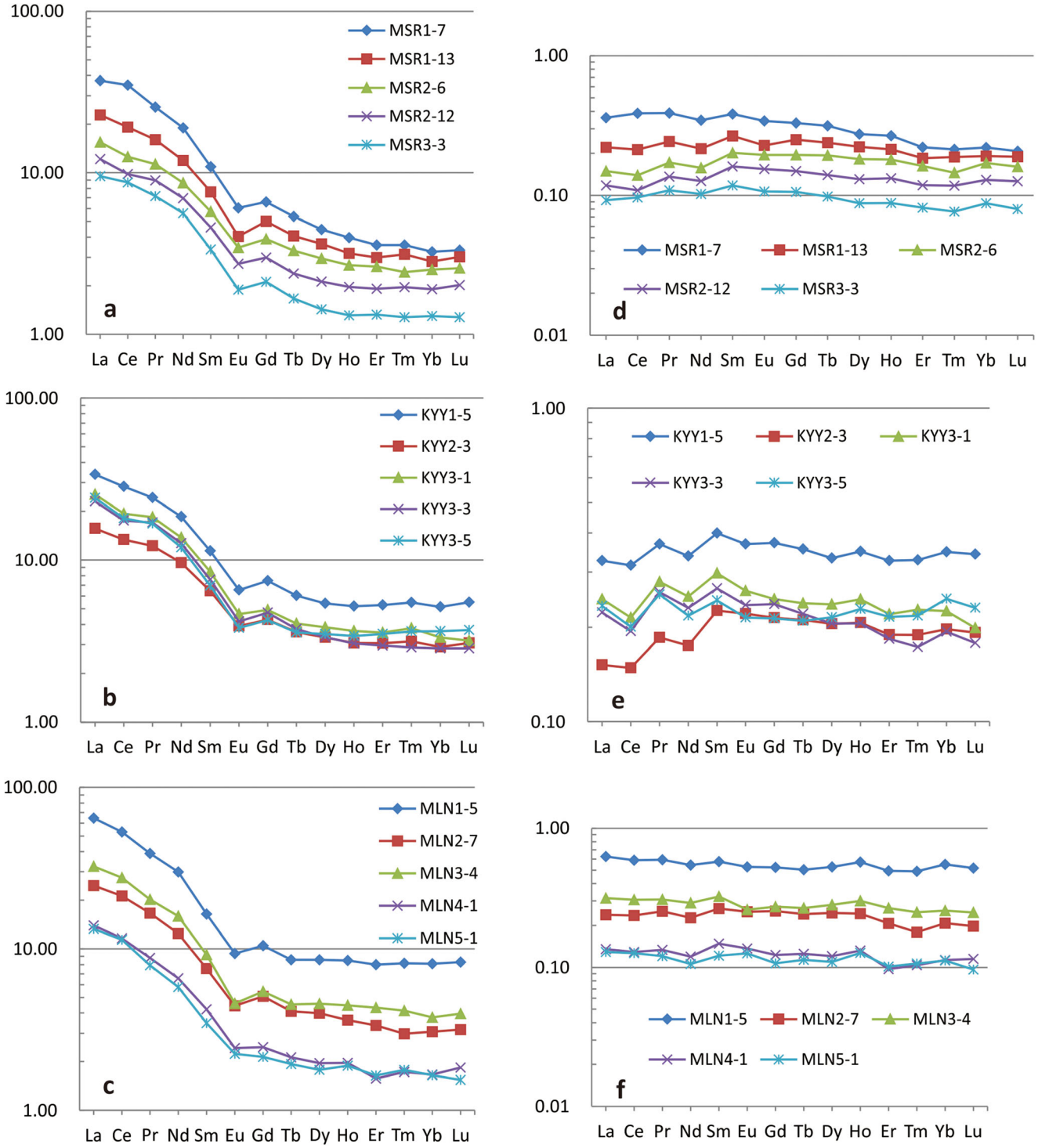

Fig. 12 REE distribution diagrams of Triassic cherts from the study sections along the route HW 108 in Mae Sariang and nearby, northwest Thailand. **a–c** Chondrite normalised; **c–f** *NASC* normalised; *MSR* Mae Sariang; *KYY* Khun Yuam; *MLN* Mae La Noi. *LREE* enrichment indicates a significant proportion of terrigenous particles deposited on a continental margin. A slightly negative Ce anomaly in some samples from *KYY* indicates the influence of open-ocean seawater. Slightly negative *HREE* supports a continental margin setting to a transition zone between continental margin and open ocean

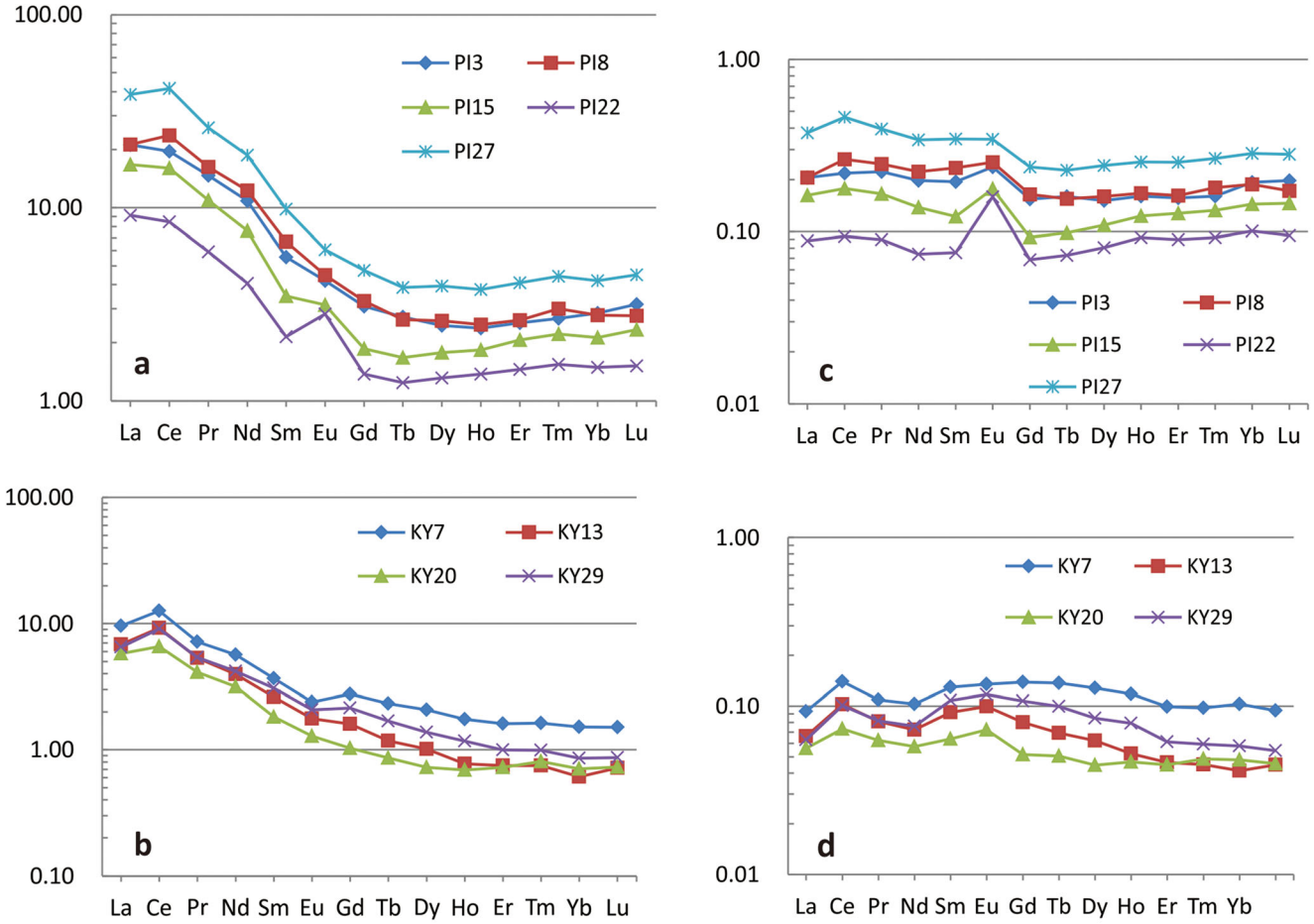

Fig. 13 *REE* distribution diagrams of Permian cherts from Khun Yuam (*KY*) along the route HW 108 in Mae Sariang and the Pai (PI), northwest Thailand. **a**, **b** Chondrite normalised; **c**, **d** NASC normalised. REE pattern with a distinctively positive Ce anomaly supports large terrigenous input. A positive Eu anomaly in some samples indicates an interval of higher supply of detrital feldspar from a nearby andesitic arc

Hydrothermal chert contains high Mn concentrations (several thousand ppm) and is related to mafic volcanic rocks. Based on the Al–Fe–Mn diagram, all analysed Triassic and Permian samples are non-hydrothermal with very low Mn content compared to those of hydrothermal origin (Fig. 14).

The Al/(Al+Fe+Mn) ratio in marine chert is a good marker for determining its origin (Bostrom and Peterson 1969). This ratio varies from 0.01 (pure hydrothermal chert) to 0.60 (pure biogenic chert) (Adachi et al. 1986; Yamamoto 1987).

However, due to diagenetic alteration of Mn, the Al/(Al+Fe) is used instead to represent proximity to land and/or oceanic ridges. $Al_2O_3/Al_2O_3+Fe_2O_3$ ratios of chert from mid-oceanic ridge, pelagic and continental margin settings range from 0.05 to 0.40, 0.40 to 0.70 and 0.55 to 0.90, respectively (Murray 1994). The ratio ranges of our analysed Triassic samples correspond clearly to a continental margin environment. Additionally, the ratios from the Mae Sariang section (0.49–0.73) suggest a greater distance from a continental supply source of Al than the others (0.71–0.87 and 0.75–0.87 for Mae La Noi and Khun Yuam, respectively) (Table 1). The Permian samples from Pai and Khun Yuam range from 0.49 to 0.69 and 0.42 to 0.77, respectively. These ratios suggest these areas were deposited between pelagic and continental margin environments (Table 1).

There are slightly positive Eu/Eu* among Mae La Noi, Mae Sariang and Khun Yuam (Table 3). However, NASC-normalised REE distribution diagrams show a relatively smooth pattern without a pronounced Eu concentration. This suggests a lower hydrothermal input in comparison to a typical hydrothermal chert or lower supply of weathered mafic volcanic rocks (Chen et al. 2006). The Eu source of the Mae Sariang, Mae La Noi and Khun Yuam samples is of non-hydrothermal origin and supports the Al–Fe–Mn plot (Fig. 15). In general, Eu occurs in a strongly reduced environment and is related to magmatic processes within the lower crust.

Positive average values of La_n/Yb_n abundances at Mae Sariang and gradually decreasing values through Mae La Noi and Khun Yuam indicate a relatively high LREE content compared with HREE. The decreasing ratio indicates decreasing hydrothermal influences or increasing influences of seawater

Table 6 Comparison of REE indices from different types of environments to this study and from previous work from Triassic and Devonian chert from terranes in northern Thailand

	Murray et al. (1990)			Hara et al. (2013)	Thassanapak et al. (2011b)			This study				
	Pacific-type	Atlantic-type	SHL-type	Chiang Dao	CD	LP	DC	KYY	MSR	MLN	PI	KY
Chondrite normalised												
Ce/Ce*	0.11–0.51	0.68–1.01	0.95–1.13	0.69–1.13	0.95–1.14	0.81–1.07	0.88–0.99	0.88–0.99	0.94–1.13	1.05–1.11	1.11–1.31	1.35–1.53
Eu/Eu*	0.67–1.17	0.68–0.83	0.55–0.62	0.55–0.72	0.61–0.71	0.64–0.74	0.56–0.76	0.70–0.75	0.65–0.74	0.65–0.82	0.89–1.23	0.75–0.93
Lan/Ybn	3.75–7.87	6.0–14.68	10–12.25	3.90–16.37	4.15–5.50	3.56–13.02	3.49–5.18	5.38–8.06	6.13–11.43	7.98–8.60	6.13–9.24	0.72–0.88
NASC normalised												
Ce/Ce*	<1 (cluster at 0.5)	0.19–0.61	*c*.1	0.63–1.20	0.87–1.05	0.74–0.92	0.81–0.91	0.82–0.99	0.86–1.04	0.96–1.01	1.09–1.27	1.18–1.77
Eu/Eu*	0.97–1.23	0.97–1.63	*c*.0.8	0.74–0.97	0.83–0.96	0.91–0.99	0.76–1.00	0.94–1.00	0.88–0.99	0.87–1.11	1.28–2.31	1.11–1.52
Lan/Ybn	0.8–1	0.82–1.86	1.27–1.45	0.56–2.34	0.59–0.79	0.51–0.96	0.50–0.74	0.77–1.15	0.88–1.63	1.14–1.23	1.10–1.95	1.31–2.62
Lan/Cen	1.66–5.49	1.30–2.48	0.66–1.33	0.90–1.92	0.86–1.07	0.85–1.26	1.03–1.10	1.02–1.17	0.93–1.09	1.01–1.06	0.80–0.89	0.50–0.85

along this trend. However, as mentioned above, the Al–Fe–Mn diagram and Eu anomalies indicate a non-hydrothermal origin. The La_n/Yb_n ratio can only be used for correlating the relative influences of seawater among these localities.

Based on the La_n/Ce_n vs. $Al_2O_3/(Al_2O_3+Fe_2O_3)$ diagram (La and Ce NASC normalised) (Fig. 15), Triassic samples from all three localities plot in the continental margin field. Distribution diagrams of all samples from Mae La Noi are compatible and located in a continental margin environment. Samples from Mae Sariang are separated into three groups because of different $Al_2O_3/(Al_2O_3+Fe_2O_3)$ ratios. The majority of samples are located in the continental margin and between continental margin and pelagic fields (Fig. 15). One sample is located outside of these fields because of a low $Al_2O_3/(Al_2O_3+Fe_2O_3)$ ratio. However, it is more closely related to the continental margin than any other as indicated by the low La_n/Ce_n ratio. At Khun Yuam, the distribution diagram presents a good distribution pattern of the data and also indicates the continental margin field. In summary, all of the chert and siliceous sediment geochemical data from the three localities indicate a non-hydrothermal origin and deposition at a continental margin. High phosphate values in some samples (MLN1-7, MLN3-3, MSR2-7) suggest an upwelling margin. This is supported by the report of black shales with phosphatic nodules at the Khun Yuam Mississippian radiolarian locality (Loc. c, Fig. 2) (Feng et al. 2004b, p. 378).

Most of the Permian samples plot outside the La_n/Ce_n vs. $Al_2O_3/(Al_2O_3+Fe_2O_3)$ diagram, in which only three samples have high Al/(Al+Fe) ratios and fall in the continental margin field. The remainder of the samples shows moderate ratios (Fig. 15). Due to a low ratio of La/Ce, we interpret the Permian samples from Pai (Inthanon Zone) and Khun Yuam as continental margin deposits. A flat REE pattern with a distinctively positive Ce anomaly from Khun Yuam, and a slightly positive Ce value from Pai supports a relative short suspension time of REE, deposited with proximity to land. A striking positive Eu anomaly in some samples from Pai suggests proximity to a volcanic source such as a volcanic arc rather than hydrothermal activity in an oceanic ridge setting. Detrital feldspar from an andesitic arc has been inferred as the source contributing Eu concentrations into sediments (e.g. Taylor and McLennan 1985; Owen et al. 1999; Udchachon et al. 2011). From other reports, hydrothermal systems are also regarded as major sources of Eu anomalies in sediments (e.g. Murray et al. 1990). Sediments accumulated in a hydrothermal regime generally display LREE enrichment (compared with the typical LREE-depleted pattern of seawater) along with a positive Eu anomaly (Michard 1989; Douville et al. 1999; German et al. 1990, 1999). Although large volumes of hydrothermal fluid were recharged to the ocean, only rare positive Eu anomalies and REE-enriched patterns are well documented in the geological record (Murray et al. 1990).

However, in our study, the Al/(Al+Fe) ratios fall within the area between pelagic and continental margin and a high positive Ce anomaly (more than 1) is detected in both the Pai and Khun Yuam Permian samples. Therefore, we interpret the depositional environment of both chert sections as deposited on Permian continental margins (Fig. 15). A slightly enhanced La/Yb ratio in the Permian samples (e.g. compared to the Triassic samples) could be due to embryonic arc spreading and weathering of mafic volcanics during the Permian in a continental margin setting. Some trace elements including Cr, Zr, Hf, Rb, Th and in part V are mainly associated with terrigenous particles (Marchig et al. 1982; Halamić et al. 2001).

In our analysed Permian samples, most Cr, Zr, Hf, Rb and Th values from Khun Yuam show a good correlation to Ti and Al which is regarded as evidence of continental input. By contrast, these trace elements show a low to negative correlation to Ti and Al in Pai, but they display a good correlation with Fe and Mn. This suggests andesitic arc materials were periodically supplied to the basin in Pai during the Permian. The ratios of Al/(Al+Fe) and La_n/Ce_n as well as Ce anomaly support Khun Yuam as closer to a continent than Pai during the Permian. The plot of Eu/Ce anomalies of both sections exhibits the same pattern indicating a similar type of sedimentary source region. A volcanic influence is common in northern Thailand as well-known volcaniclastic intercalations in the sedimentary successions of the Carboniferous Dan Lan Hoi Group and the Permian Ngao Group in the Sukhothai Volcanic Arc Terrane as well as a few occurrences within the Inthanon Zone.

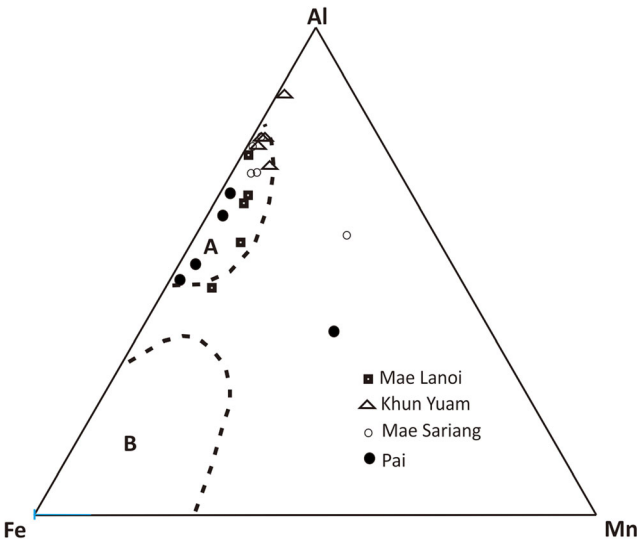

Fig. 14 Al–Fe–Mn diagram of chert and siliceous rocks from study sections along highway HW 108 in Mae Sariang and nearby along the Mae Yuam Valley and from Pai in the Inthanon Zone, northwest Thailand. *A* non-hydrothermal or biogenic field, *B* hydrothermal field. (Hydrothermal and non-hydrothermal fields from Adachi et al. 1986). It suggests a biogenic/non-hydrothermal origin for both Permian and Triassic cherts and siliceous rocks from these sections

We have further compared both chondrite and NASC-normalised REE ratios from Permian and Triassic cherts in this study with REE indices from the different environmental settings proposed by Murray (1994). The main settings include the Pacific type of large ocean with limited terrigenous input and the Atlantic type of moderate basin flanked by passive margins with more terrigenous influence than the Pacific type and the Southern High Latitude (SHL) type of continental margin setting. The NASC-normalised REE indices are most useful to discriminate these environmental settings. Our results are most correlative to the SHL type and partly to the Atlantic type. This situation is also observed in the Devonian chert from the Inthanon terrane (Hara et al. 2012) and the Triassic chert from Inthanon and the Sukhothai terranes (Thassanapak et al. 2011a). These terrigenous influenced signatures suggest areas close to continental margins.

Discussion and regional correlations

The Permian limestone successions in the NWTR contrasts strongly to that of the Inthanon Zone. In the northwest Inthanon Zone, a thick succession of limestones ranges from the early Visean to the late Permian (Fontaine et al. 2009; Ueno and Charoentitirat 2011) and continues possibly into the Early Triassic. The Inthanon Zone limestones are typical shallow-water limestones containing oolites, oncolites, abundant and diverse calcareous algae, diverse fusulinids and often

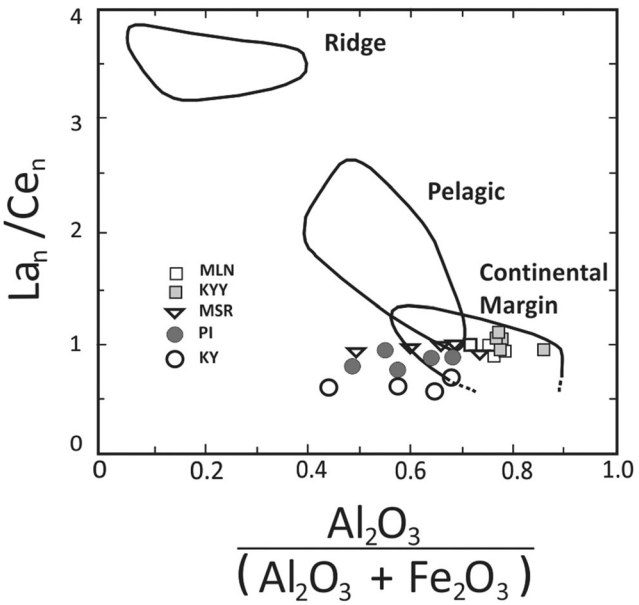

Fig. 15 La_n/Ce_n vs. $Al_2O_3/(Al_2O_3+Fe_2O_3)$ diagram (La and Ce NASC normalised). Most of the samples are restricted to the continental margin field which indicates a deeper part of the continental margin depositional environment with minimal terrestrial influx

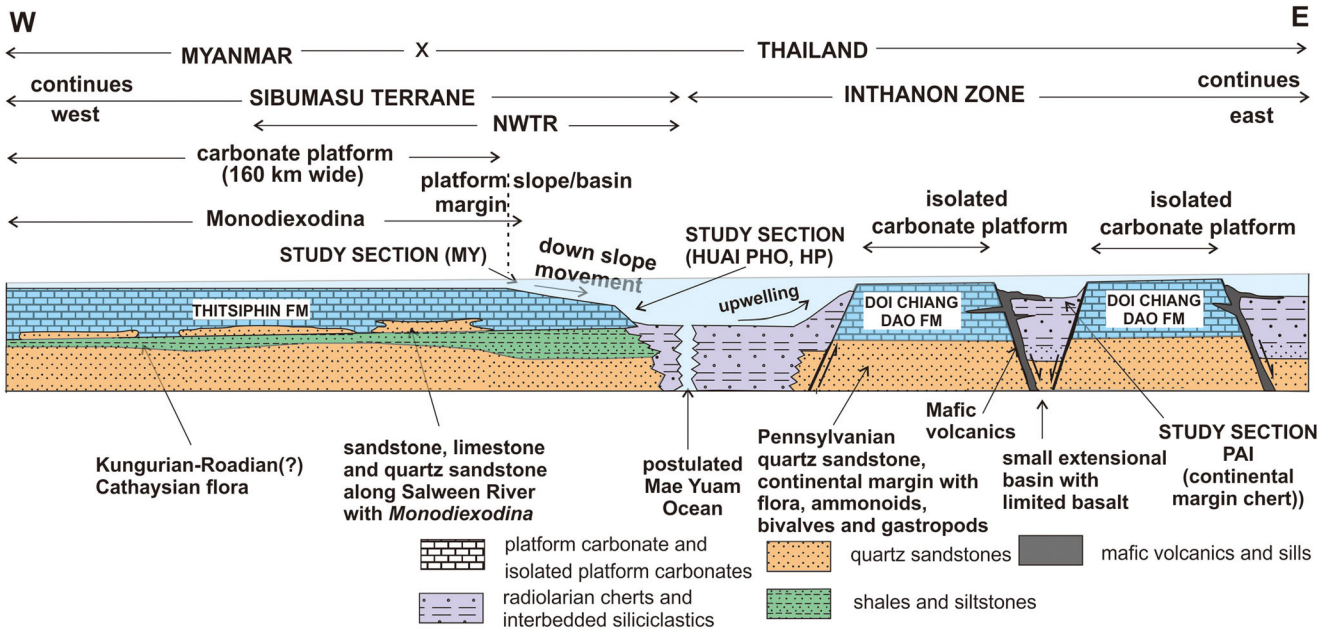

Fig. 16 Diagram showing proposed hypothesis for NW Thailand and adjacent areas of Myanmar for mid-Permian (Wordian) time. Diagrammatic section from Shan State in Myanmar in the west to the northwestern Inthanon Zone in NW Thailand. Not to scale. The Thitsiphin Formation carbonate platform and fusulinids in Myanmar and in the NWTR are based on Hahn and Siebenhüner (1982), Ingavat and Douglass (1981), Zaw Win et al. (2017) and Zhang et al. (2020). A Cathaysian flora in Shan State is from Zhou et al. (2020). Passive continental margin Carboniferous sandstone in Inthanon is from Hara et al. (2012) and contained fossils from Hara et al. (2012) (gastropods and bivalves), Fujikawa and Ishibashi (1999) (ammonoids) and Ingavat-Helmcke (1994) (plants). This model for the Inthanon Zone with small isolated carbonate platforms (Fontaine et al. 2009) separated by small basins with non-pelagic radiolarian cherts basins ranging from the Devonian (e.g. Hara et al. 2010) to the Triassic (e.g. Thassanapak et al. 2011a, 2011b) is presented as a possible alternative hypothesis to the widely accepted allochthonous/overthrust model (e.g. Barber et al. 2011)

large hermatypic corals typical of faunas (shown as stars on Fig.2) and floras previously described from the composite Indochina Terrane, South China and other palaeotropical Tethyan or 'Cathaysian' localities. The Permian corals of the northwest Inthanon Zone are quite unlike those of southern Thailand, western Thailand and the Shan State of Myanmar (Smith 1941; Fontaine and Suteethorn 1988; Fontaine et al. 1993, 2009, 2012). Fontaine et al. (2009) note that the Carboniferous sandstone-shale succession lies conformably beneath the limestone. This sandstone-shale succession contains ammonoids, bivalves and gastropods (Hara et al. 2009, 2012). The ammonoids *Pseudopronorites arkansasensis* and *?Cravenoceras* described by Fujikawa and Ishibashi (1999) from locality w in Fig. 2 were assigned to the lower to middle Pennsylvanian. Ingavat-Helmcke (1994) and Fontaine et al. (2009) mentioned a flora from the 'Carboniferous sandstone-shale' succession shown as a leaf symbol on Fig. 2. Other fossils listed from the Carboniferous siliciclastics of NW Inthanon include Mississippian and Pennsylvanian conodonts, fusulinids and smaller foraminiferans (Hahn and Siebenhüner 1982). The Carboniferous sandstone-shale succession is geochemically and petrographically typical of a passive continental margin and (Hara et al. 2009, 2012) suggests it was derived from the Indochina Terrane and bi-passing the Sukhothai Volcanic Arc. Hara et al. (2012) also recognise sandstones within mélange beneath the massive limestones, suggest a possible Permo-Triassic age for the mélange and show that the clasts were derived mainly from a volcanic arc source. Hara et al. (2009, 2012) interpret these mélanges as being part of allochthonous oceanic subduction zones with the sandstones derived from the Sukhothai Volcanic Arc. Only three small outcrops of mafic igneous rocks are mapped in the northwestern Inthanon Zone region shown in Fig.2 and only one of these is adjacent to a large limestone outcrop. Geochemical analyses of Middle Triassic radiolarian chert in the NWTR area, as well as in the Inthanon Zone, suggest continental margin depositional environments (Thassanapak et al. 2011a). Differences of key faunas between the terranes on opposite sides of the Mae Yuam Valley suggest the MYMS FZ is a reactivated divide consisting of marginal Palaeotethyan sediments separating Gondwanan from tropical sediments as suggested by Ferrari et al. (2008).

Conclusions

A long-lasting belt of radiolarian cherts, coincident with the Mae Yuam Valley (Feng et al. 2004a) separates Pennsylvanian to

Permian palaeotropical limestones of the Inthanon Zone to the east from Permian limestones in the west (NWTR) containing a temperate marine fauna in the Roadian and a biogeographically distinctive fusulinid fauna in the Wordian. Devonian faunas found in condensed sequences of the NWTR were deposited in a deep platform or ramp environment. A lack of basalts in the NWTR does not suggest oceanic environments for any Palaeozoic sequence within the NWTR and a paucity of basalts in the northwestern part of the Inthanon Zone also does not provide good evidence of an oceanic realm. Indeed, 'continental margin' Carboniferous sandstones appear to underlie the palaeotropical limestones and their plant fossils and their benthonic faunas do not suggest oceanic conditions in the northwestern Inthanon Zone. We, therefore, suggest that an autochthonous or para-autochthonous Inthanon Zone origin for these Carboniferous sandstones is more likely than deposition within a subducting Palaeotethyan Ocean.

A strong contrast between the 'temperate' Permian limestones of the NWTR and the tropical limestones of the Inthanon Zone further emphasises the MYMS FZ as a reactivated oceanic boundary between Gondwana and 'Cathaysia' and is supported by the oceanic lithosphere origin of the detrital Cr spinels in the Triassic foreland basin siliciclastics of the NWTR. The limestones of the Inthanon Zone range from Visean to Permian and possibly Triassic and were deposited in shallow, tropical seas for over 90 million years. This longevity is either not possible or highly unlikely for shallow marine carbonates on volcanic seamounts supported on subducting (and therefore cooling and sinking) ocean crust (Huppert et al. 2020) but is possible on isolated carbonate platforms on continental crust separated by narrow basins with limited volcanism. Carboniferous sandstones and Devonian-Permian radiolarian cherts from the Inthanon Zone are continental marginal and are neither pelagic nor oceanic and are interpreted as deposited in extensional, deeper basins between the isolated carbonate platforms.

We suggest an alternative hypothesis to the overthrust/allochthon model where the NWTR is the eastern platform margin of the Sibumasu Terrane from the Devonian through to the Triassic and separated from the Inthanon Terrane by an ocean in the position of the MYMS FZ (Fig. 16). It is suggested that Inthanon rifted from Gondwana in the Early Devonian and the NWTR, as part of the Sibumasu Terrane, rifted off in the early Permian. As the Inthanon Terrane ribbon continent drifted northwards, the continental crust thinned and extended and small rift basins allowed basalts to be extruded associated with deep-water, continental margin, hemipelagic, non-hydrothermal radiolarian oozes. Isolated carbonate platforms were established on Carboniferous sandstone bases and were separated by deep-water but non-pelagic extensional basins. Turbidites originating on the carbonate highs supplied carbonate clasts containing Devonian through Permian conodonts, to the adjacent basins (Udchachon et al. 2018). We provisionally suggest that the Sukhothai Terrane rifted with Inthanon with its older siliciclastic successions of the Siluro-Devonian (?) Khao Kieo Formation and the unconformably overlying Carboniferous (Dan Lan Hoi Group) (Bunopas 1982; Ueno and Charoentitirat 2011) supplying siliciclastic and volcaniclastic debris to the Inthanon Zone. This hypothesis is broadly in accord with Dew et al.'s (2018) 'explanation A' for the crustal geochemistry of the northern Thailand terranes. In the early Permian (Kungurian), Sibumasu was probably in cool to temperate seas but by the middle Permian, the NWTR had rifted from Gondwana and was in the southern hemisphere tropics (13° ± 2° S, Zhao et al. 2020). Terrane collision occurred during the Triassic (Ishida et al. 2006; Mitchell et al. 2012 Cai et al. 2017; Hara et al. 2021) with the establishment of a thrust front along the Mae Sariang Thrust Zone and the deposition of the mainly siliciclastic Mae Sariang Group on the NWTR within a foreland basin.

Acknowledgements This study was supported by grants from Mahasarakham University. We thank the staff of the State Key Laboratory of Geological Processes and Mineral Resources, China University of Geosciences, for their help with geochemical analyses. We thank Professor Chongpan Chonglakmani and the staff of Suranaree University of Technology, Thailand, for their suggestions and technical support. We also thank colleagues from the Department of Mineral Resources, Bangkok, for their logistic support. This paper is part of our contribution to IGCP-700 Carbonate Build-ups in SE Asia. We thank Dr. Michael Ridd and an anonymous reviewer for their very useful comments that substantially improved the manuscript.

Availability of material All specimens and petrographic slides are deposited in the collections of the Palaeontological Research and Education Centre, Mahasarakham University, Maha Sarakham, Thailand, and given PRC collection numbers.

Author contribution All authors contributed to the writing and checking of the paper. Thassanapak and Udchachon collected the chert, assessed the radiolarian taxonomy and with Feng carried out the chert geochemistry. Geochemical data analyses and interpretation were conducted by Thassanapak and Udchachon. Petrographic analyses were carried out by Udchachon on Devonian and Permian limestones collected by Burrett and Udchachon. Burrett assessed the taxonomy of the conodonts.

Declarations

Conflict of interest The authors declare that they have no conflict of interest.

References

Adachi, M., Yamamoto, K., & Sugisaki, R. (1986). Hydrothermal chert and associated chert from the Northern Pacific, their geological significance as indicators of ocean ridge activity. *Sedimentary Geology, 47*, 125–148.

Angiolini, L., Crippa, G., Muttoni, G., & Pignatti, J. (2013). Guadalupian (Middle Permian) paleobiogeography of the Neotethys Ocean. *Gondwana Research, 24*, 173–184.

Armstrong, H. A., Owen, A. M., & Floyd, J. D. (1999). Rare earth geochemistry of Arenig Cherts from the Ballantrae Ophiolite and

Leadhills Imbricate Zone, Southern Scotland: implications for origin and significance to the Caledonian Orogeny. *Journal of the Geological Society of London, 156*, 549–560.

Baird, A., Dawson, O., & Vachard, D. (1993). New data on biostratigraphy of the Permian Ratburi Limestone from north peninsular Thailand. In T. Thanasuthipitak (Ed.), *International Symposium on the Biostratigraphy of Mainland Southeast Asia* (pp. 243–260). Facies and Paleontology.

Barber, A. J., Ridd, M., & Crow, M. J. (2011). The origin, movement and assembly of pre-Tertiary tectonic units of Thailand. In M. F. Ridd, A. J. Barber, & M. J. Crow (Eds.), *The Geology of Thailand* (pp. 507–538). Geological Society.

Barr, S. M., & Charusuri, P. (2011). Volcanic rocks. In M. F. Ridd, A. J. Barber, & M. J. Crow (Eds.), *The Geology of Thailand* (pp. 415–439). Geological Society.

Barr, S. M., & MacDonald, A. S. (1991). Toward a Late Paleozoic-Early Mesozoic tectonic model for Thailand. *Journal of Thai Geosciences, 1*, 11–22.

Barr, S. M., Tantisukrit, C., Yaowanoiyothin, W., & Macdonald, A. S. (1990). Petrology and Tectonic implications of upper Paleozoic volcanic rocks of Chiang Mai Belt, northern Thailand. *Journal of Southeast Asian Earth Sciences, 4*, 37–47.

Bateson, W. (1886). The ancestry of the Chordata. *Quarterly Journal of Microscopical Science, 26*, 218–571.

Baum, F., von Braun, E., Hess, A., Koch, K. E., Kruse, G., Quarch, H., & Siebenhüner, M. (1970). On the Geology of northern Thailand. *Beihefte zum Geologischen Jahrbuch, 102*, 1–23.

Baum, F., von Braun, E., Hess, A., & Koch, K. E. (1982). *Geological Map of Northern Thailand, Chiang Mai Sheet,1:250,000*. Bundesandstalt fur Geowissenschaften und Rohstoffe.

Bender, H., & Stoppel, D. (1965). Perm-Conodonten. *Geologisches Jahrbuch, 82*, 331–364.

Blieck, A., & Goujet, D. (1978). A propos de nouveau matériel de Thélodontes (Vertébrés, Agnathes) d'Iran et de Thaïlande: aperçu sur la répartition géographique et stratigraphique des Agnathes des "régions gondwaniennes" au Paléozoïque moyen. Apports récents à la géologie du Gondwana (Séance spéc. GFEG-SGN, Villeneuve d'Ascq, 1977). *Annales de la Société Géologique du Nord, 98*, 363–372.

Blieck, A., Goujet, D., Janvier, P., & Lelievre, H. (1984). Microrestes de vertebres du Siluro-Devonien d'Algerie, de Turquie et de Thailande. *Geobios, 17*, 851–856.

Boriphatkhosal, S. (1990*). Investigation report of the geology of Amphoe Khun Yuam and Ban Mae La Luang*. Unpublished report of the Royal Thai Department of Mineral Resources, Geological Survey Division, 1-85. [in Thai]

Bostrom, K., & Peterson, M. N. A. (1969). The origin of Al-poor ferromanganoan sediments in areas of high heat flow on the East Pacific Rise. *Marine Geology, 7*, 427–447.

Boynton, W. V. (1984). Geochemistry of Rare Earth Elements: Meteorite Studies. In P. Henderson (Ed.), *Rare Earth Element Geochemistry* (pp. 63–114). Elsevier. https://doi.org/10.1016/B978-0-444-42148-7.50008-3.

Braun, E. von, Hahn, L., & Maronde, H. (1981). *Geological map of Northern Thailand, Li Sheet, 1:250,000*. Bundesandstalt fur Geowissenschaften und Rohstoffe.

Blendinger, W., Furnish, W. M., & Glenister, B. F. (1992). Permian cephalopod limestones, Oman Mountains: evidence for a Permian seaway along the northern margin of Gondwana. *Palaeogeography, Palaeoclimatology, Palaeoecology, 93*, 13–20.

Bungunphai, N. (2005). *Tawraneewittaya rawang amphoe mae sariang (4545 II), Geology of part of Amphoe Mae Sariang (map 4545 II, 1: 50,000 scale),* Royal Thai Department of Mineral Resources Bangkok, Report 19/2548, 1–127. ISBN 974-226-302-7. [in Thai]

Bunopas, S. (1982). Palaeogeographic History of Western Thailand and Adjacent parts of South-East Asia. *Geological Survey Division, Department of Mineral Resources, Bangkok, Thailand Paper, 5*, 1–801.

Bunopas, S., & Vella, P. (1983). Tectonic and geologic evolution of Thailand. In P. Nutalaya (Ed.), *Proceedings of the Workshop on the stratigraphic correlation of Thailand and Malaysia,* Tech. Paper 1, 307–323.

Burrett, C., Carey, S., & Wongwanich, T. (1986). A Siluro-Devonian carbonate sequence in Northern Thailand. *Journal of Southeast Asian Earth Sciences, 1*, 215–220.

Burrett, C., Long, J., & Stait, B. (1990). Early-Middle Palaeozoic biogeography of Asian terranes derived from Gondwana. In W. S. McKerrow & C. R. Scotese (Eds.), *Palaeozoic Palaeogeography and Biogeography* (12th ed., pp. 163–174). Geological Society Memoir.

Burrett, C., Zaw, K., Meffre, S., Lai, C. K., Khositanont, S., Chaodumrong, P., Udchachon, M., Ekins, S., & Halpin, J. (2014). The configuration of Greater Gondwana-evidence from LA ICPMS, U-Pb geochronology of detrital zircons from the Palaeozoic and Mesozoic of Southeast Asia and China. *Gondwana Research, 26*, 31–51.

Burrett, C., Udchachon, M., Thassanapak, H., & Chitnarin, A. (2015). Conodonts, Radiolarians and Ostracodes in the Permian E-Lert Formation, Loei Foldbelt, Indochina Terrane, Thailand. *Geological Magazine, 152*, 106–145.

Burrett, C., Udchachon, M., & Thassanapak, H. (2017). Palaeozoic correlations and the Palaeogeography of the Sibumasu (Shan-Thai) Terrane - a brief review. *Research and Knowledge, 2*(2), 1–17. https://doi.org/10.14456/randk.2016.12.

Cai, F., Ding, L., Yao, W., Laskowski, A., Xu, Q., Zhang, J., & Sein, K. (2017). Provenance and tectonic evolution of Lower Paleozoic-Upper Mesozoic strata from Sibumasu terrane, Myanmar. *Gondwana Research, 41*, 325–336.

Caridroit, M., Bohlke, D., Lumjuan, A., Helmcke, D., & De Wever, P. (1993). A mixed radiolarian fauna (Permian/Triassic) from clastics of the Mae Sariang area, northwestern Thailand. In T. Thanusuthipitak (Ed.), *International Symposium on the Biostratigraphy of Mainland Southeast Asia:* Facies and Paleontology. 402–413.

Caridroit, M., Vachard, D., & Fontaine, H. (1992). Radiolarian age datings (Carboniferous, Permian and Triassic) in NW Thailand. Evidence of nappes and olistostromes. *Comptes Rendus - Academie des Sciences, Serie II, 315*, 515–520.

Casier, J.-G. (2004). The mode of life of Devonian entomozoacean ostracods and the Myodocopid Mega-Assemblage proxy for hypoxic events. *Bulletin de l'Institut Royal des Sciences Naturelles de Belgique, Sciences de la Terre, 74*(*suppl*), 73–80.

Catuneanu, O. (2006) Principles of Sequence Stratigraphy. Elsevier B.V, 387 p.

Charoenprawat, A., Dhamdusdi, V., Sripongpan, P., & Paksamut, N. (1985). *Geology of Sheet Mae Hong Son (4547 1) and Huai Pong (4547 2) scale 1;50,000,* unpublished Report Royal Thai Geological Survey Division, Department of Mineral Resources Bangkok, 1–24. (in Thai).

Chen, D., Qing, H., Yan, X., & Li, H. (2006). Hydrothermal venting and basin evolution (Devonian, South China): Constraints from rare earth element geochemistry of chert. *Sedimentary Geology, 183*, 203–216.

Chernykh, V. V., & Reshetkova, N. P. (1987). Biostratigraphy and conodonts of the boundary beds of the Carboniferous and Permian in the western slopes of southern and Central Urals. In B. I. Chuvashov (Ed.), *Biostratigrafiya i litholigiya verkhnego paleozoya Urala.* Sbornik Nauchnykh Trudov, PISO Ural AN SSSR, p. 45. [in Russian]

Chonglakmani, C. (2011). Triassic. In M. F. Ridd, A. J. Barber, & M. J. Crow (Eds.), *The Geology of Thailand* (pp. 137–150). Geological Society.

Cobbing, E. (2011). Granitic Rocks. In M. F. Ridd, A. J. Barber, & M. J. Crow (Eds.), *The Geology of Thailand* (pp. 441–457). Geological Society.

Department of Mineral Resources (1999). *Geological Map of Thailand 1: 1,000,000.* Department of Mineral Resources, Ministry of Natural Resources and Environment

Department of Mineral Resources (2014). *Geology of Thailand.* Department of Mineral Resources, Ministry of Natural Resources and Environment, 508pp.

Derycke, C., Spalletta, C., Perri, M., & Corradino, C. (2008). Famennian chondrichthyan microremains from Morocco and Sardinia. *Journal of Paleontology, 82*, 984–995.

Dew, R. E., Collins, A. S., Glorie, S., Morley, C. K., Blades, M., Nachtergaele, S., & King, R. (2018). Probing into Thailand's basement: new insights from U-Pb geochronology, Sr, Sm-Nd, Pb and Lu-Hf isotopic systems from granitoids. *Lithos, 320*, 332–354. https://doi.org/10.1016/j.lithos.2018.09.019.

Dew, R. E., Collins, A. S., Morley, C. K., King, R. C., Evans, N. J., & Glorie, S. (2021). Coupled detrital zircon U-Pb and Hf analysis of the Sibumasu Terrane: from Gondwana to northwest Thailand. *Journal of Asian Earth Sciences, 211*, 1–20. 104709. https://doi.org/10.1016/j.jseaes.2021.104709. accessed 12/12/2020

Dill, H., Luppold, F., Techmer, A., Chaodumrong, P., & Phoonphun, S. (2004). Lithology, micropaleontology and chemical composition of calcareous rocks of Paleozoic through Cenozoic age (Surat Thani Province, central Peninsular Thailand): implications concerning the environment of deposition and the economic potential of limestones. *Journal of Asian Earth Sciences, 23*, 63–89.

Dopieralska, J. (2003). *Neodymium isotopic composition of conodonts as a palaeoceanographic proxy in the Variscan ocean*. Ph.D.Thesis, Justus-Liebig-University, Giessen, pp. 111. http://geb.unigiessen.de/geb/volltexte/2003/1168/

Dopieralska, J. (2009). Reconstructing seawater circulation on the Moroccan shelf of Gondwana during the Late Devonian: evidence from Nd isotope composition of conodonts. *Geochemistry, Geophysics, Geosystems, 10*, Q03015.

Dopieralska, J., Belka, Z., & Haack, U. (2006). Geochemical decoupling of water masses in the Variscan oceanic system during Late Devonian times. *Palaeogeography, Palaeoclimatology, Palaeoecology, 240*, 108–119.

Dopieralska, J., Belka, Z., Königshof, P., Racki, G., Savage, N., Lutat, P., & Sardsud, A. (2012). Nd isotopic composition of Late Devonian seawater in western Thailand: geotectonic implications for the origin of the Sibumasu terrane. *Gondwana Research, 22*, 1102–1109.

Douville, E., Bienvenu, P., Charlou, J. L., Donval, J. P., Fouquet, Y., Appriou, P., & Gamo, T. (1999). Yttrium and rare earth elements in fluids from various deep-sea hydrothermal systems. *Geochimica et Cosmochimica Acta, 63*, 627–643.

Dunham, R. J. (1962). Classification of carbonate rocks according to depositional texture. In W.E. Ham (Ed.), Classification of Carbonate Rocks. *American Association of Petroleum Geologists Memoir, 1,* 108–121.

Dzik, J. (1976). Remarks on the evolution of Ordovician conodonts. *Acta Palaeontologica Polonica, 36*, 265–323.

Eichenberg, W. (1930). Conodonten aus dem Culm des Harzes. *Palaontologisches Zeitschrift, 12*, 177–182.

Embry, A. F., & Klovan, J. E. (1971). A late Devonian reef tract on northeastern Banks Island, NWT. *Bulletin of Canadian Petroleum Geology, 19*, 730–781.

Feng, Q., Chonglakmani, C., Helmcke, D., & Ingavat-Helmcke, R. (2004a). Long-lived Paleotethyan pelagic remnant inside Shan-Thai Block: evidence from radiolarian biostratigraphy. *Science in China (Series D), 47*, 1113–1119.

Feng, Q., Helmcke, D., Chonglakmani, C., Ingavat-Helmcke, R., & Liu, B. (2004b). Early Carboniferous Radiolarians from north-west Thailand: Palaeogeographical Implications. *Palaeontology, 47*, 377–393.

Feng, Q., Malila, K., Wonganan, N., Chonglakmani, C., Helmcke, D., Ingavat-Helmcke, R., & Caridroit, M. (2005). Permian and Triassic Radiolaria from Northwest Thailand: paleogeographical implications. *Revue de Micropaleontologie, 48*, 237–255.

Feng, Q., Yang, W., Shen, S., Chonglakmani, C., & Kitsana, M. (2008). The Permian seamount stratigraphic sequence in Chiang Mai, North Thailand and its tectogeographic significance. *Science in China Series D Earth Sciences, 51*, 1768–1775.

Ferrari, O. M., Hochard, C., & Stampfli, G. M. (2008). An alternative plate tectonic model for the Palaeozoic-Early Mesozoic Palaeotethyan evolution of Southeast Asia (Northern Thailand-Burma). *Tectonophysics, 451*, 346–365.

Flügel, E. (2004). *Microfacies of carbonate rocks*. Springer.

Fontaine, H., & Suteethorn, V. (1988). Late Paleozoic and Mesozoic fossils of west Thailand and their environments. *Coordinating Committee for Geoscience Programmes in East and Southeast Asia, CCOP Technical Bulletin, 20*, 1–107.

Fontaine, H., Suteethorn, V., & Vachard, D. (1993). Carboniferous and Permian limestones in Sop Pong area: unexpected lithology and fossils. In T. Thanasuthipitak (Ed.), *International Symposium on the Biostratigraphy of Mainland Southeast Asia* (pp. 319–336). *Facies and Paleontology*.

Fontaine, H., Hoang Thi Than, Juanngam, S., Kavinate, S., Salypongse, S., Suteethorn, V., & Vachard, D. (2009). *Paleontology and stratigraphy of the northwest Thailand: paleogeographical implications*. Department of Mineral Resources, 208pp.

Fontaine, H., Kavinate, S., Hoang, T. T., & Vachard, D. (2012). Permian limestone of peninsular Thailand in Khao Yoi, Cha-am and Thong Pha Phum. *Natural History Bulletin of the Siam Society, 58*, 39–47.

Fujikawa, M., & Ishibashi, T. (1999). Carboniferous and Permian ammonoids from northern Thailand. *Memoir of the Faculty of Science Kyushu University, Series D. Earth and Planetary Sciences, 30*, 91–110.

Gardiner, N. J., Roberts, N. M., Morley, C. K., Searle, M. P., & Whitehouse, M. (2016a). Did Oligocene crustal thickening precede basin development in northern Thailand? A geochronological reassessment of Doi Inthanon and Doi Suthep. *Lithos, 240-243*, 69–83.

Gardiner, N. J., Searle, M. P., Morley, C. K., Whitehouse, M. P., Spencer, C. J., & Robb, L. J. (2016b). The closure of Palaeo-Tethys in Eastern Myanmar and Northern Thailand: new insights from zircon U-Pb and Hf isotope data. *Gondwana Research, 39*, 401–422.

German, C. R., Klinkhammer, G. P., Edmond, J. M., Mitra, A., & Elderfield, H. (1990). Hydrothermal scavenging of rare-earth elements in the ocean. *Nature, 345*, 516–518.

German, C. R., Hergt, J., & Palmer, M. R. (1999). Geochemistry of a Hydrothermal Sediment Core from the OBS Ventfield, 218N East Pacific Rise. *Chemical Geology, 155*, 65–75.

Ginter, M. (2000). Late Famennian pelagic shark assemblages. *Acta Geologica Polonica, 50*, 369–386.

Ginter, M., Hairapetian, V., & Klug, C. (2002). Famennian chondrichthyans from the shelves of north Gondwana. *Acta Geologica Polonica, 52*, 169–215.

Girard, C., Cornee, J.-J., Joachimski, M., Charruault, A.-L., Dufour, A.-B., & Reneau, S. (2020). Paleogeographic differences in temperature, water depth and conodont biofacies during the Late Devonian. *Palaeogeography, Palaeoecology, Palaeoclimatology, 549*, 108852. https://doi.org/10.1016/j.palaeo.2018.06.046.

Gradinaru, M., Lazar, I., Ducea, M. N., & Petrescu, L. (2019). Microaerophilic Fe-oxidizing micro-organisms in Middle Jurassic ferruginous stromatolites and the paleoenvironmental context of their formation (Southern Carpathians, Romania). *Geobiology.* https://doi.org/10.1111/gbi.12376.

Gromet, L. P., Dymek, R. F., Haskin, L. A., & Korotev, R. L. (1984). The "North American Shale Composite", its compilation, major and

trace element characteristics. *Geochimica et Cosmochimica Acta, 48*, 2469–2482.

Hahn, L., & Siebenhüner, M. (1982*). Explanatory notes on the geological maps of northern and western Thailand 1:250,000.* Institut fur Geowissenschaften und Rohstoffe, 3–76.

Halamić, J., Marchig, V., & Goričan, S. (2001). Geochemistry of Triassic radiolarian cherts in north-western Croatia. *Geologica Carpathica, 52*(*6*), 327–342.

Hara, H., Wakita, K., Ueno, K., Kamata, Y., Hisada, K., Charusiri, P., Charoentitirat, T., & Chaodumrong, P. (2009). Nature of accretion related to Paleo-Tethys subduction recorded in northern Thailand: constraints from mélange kinematics and illite crystallinity. *Gondwana Research, 16*, 310–320.

Hara, H., Kurihara, T., Kuroda, J., Adachi, Y., Kurita, H., Wakita, K., Hisada, K., Charusiri, P., Charoentitirat, T., & Chaodumrong, P. (2010). Geological and geochemical aspects of a Devonian siliceous succession in northern Thailand: implications for the opening of the Paleo-Tethys. *Palaeogeography, Palaeoclimatology Palaeoecology, 297*, 452–464.

Hara, H., Kunii, M., Hisada, K., Ueno, K., Kamata, Y., Srichan, W., Charusiri, P., Charoentitirat, T., Watarai, M., Adachi, Y., & Kurihara, T. (2012). Petrography and geochemistry of clastic rocks within the Inthanon zone, northern Thailand: Implications for Paleo-Tethys subduction and convergence. *Journal of Asian Earth Sciences, 61*, 2–15.

Hara, H., Tokiwa, T., Kurihara, T., Charoentitirat, T., & Sardsud, A. (2021). Advance online publication. Revisiting the tectonic evolution of the Triassic Palaeo-Tethys convergence zone in northern Thailand inferred from detrital zircon U-Pb ages. *Geological Magazine*. https://doi.org/10.1017/S0016756820001028.

Henderson, C. (2016). Permian conodont biostratigraphy. In S. Lucas, & S. Z. Shen (Eds.), *The Permian Timescale.* Geological Society, Special Publications, 450, 119–142. https://doi.org/10.1144/SP450.9

Hess, A., & Koch, K. E. (1979). *Geological Map of Northern Thailand, Chiang Dao Sheet, 1:250,000,* Bundesandstalt fur Geowissenschaften und Rohstoffe.

Hisada, K., Sugiyama, M., Ueno, K., & Charusiri, P. (2004). Missing ophiolitic rocks along the Mae Yuam Fault as the Gondwana-Tethys divide in north-west Thailand. *Island Arc, 13*, 119–127.

Huppert, K. L., Perron, J. T., & Royden, L. H. (2020). Hotspot swells and the lifespan of volcanic ocean islands. *Science Advances, 6*, 1–8 eaaw6906.

Hutchison, C. S. (1975). Ophiolites in Southeast Asia. *Geological Society of America Bulletin, 86*, 797–806.

Ingavat, R., & Douglass, R. C. (1981). Fusuline Fossils from Northwest Thailand Part XIV.: the Fusulinid Genus Monodiexodina from Northwest Thailand. In T. Kobayashi, R. Toriyama, & W. Hashimoto (Eds.), *Geology and Palaeontology of Southeast Asia* (Vol. 22, pp. 23–34). The University of Tokyo Press.

Ingavat-Helmcke, R. (1994). Paleozoic paleontological evidence of Thailand. In P. Anguswathana, T. Wongwanich, & W. Tansathein (Eds.), *Proceedings of the International Symposium on Stratigraphic Correlations of Southeast Asia* (pp. 43–54). Department of Mineral Resources.

Ishida, K., Nanba, A., Hirsch, F., Kozai, T., & Meesook, A. (2006). New micropalaeontological evidence for a Late Triassic Shan-Thai orogeny. *Geosciences Journal, 10*, 181–194.

Jasin, B. (1991). Significance of *Monodiexodina* (Fusulininacea) in geology of Peninsular Malaysia. *Geological Society of Malaysia Bulletin, 29*, 171–181.

Jindasut, S., Tantiwanich, W., Kistudasima, S., & Waser, M. (1990). *Geology of the Ban Kong Soom Area*. Royal Thai Department of Mineral Resources Bangkok, *Geological Survey Report 0146*, 1–24.

Kamata, Y., Sashida, K., Ueno, K., Hisada, K., Nikonsri, N., & Charusiri, P. (2002). Triassic radiolarian faunas from the Mae Sariang area Northern Thailand, and their paleogeographic significance. *Journal of Asian Earth Sciences, 20*, 491–506.

Kamata, Y., Ueno, K., Hara, H., Ichise, M., Charoentitirat, T., Charusiri, P., Sardsud, A., & Hisada, K. (2009). Classification of the Sibumasu and Paleo-Tethys Tectonic Division in Thailand using Chert Lithofacies. *Island Arc, 18*, 21–31.

Kamenetsky, V., Crawford, A. J., & Meffre, S. (2001). Factors controlling chemistry of magmatic spinel: an empirical study of associated olivine, Cr-spinel and Melt inclusions in Primitive Rocks. *Journal of Petrology, 42*, 655–671.

Kato, Y., Nakao, K., & Isozaki, Y. (2002). Geochemistry of Late Permian to Early Triassic Pelagic cherts from southwest Japan: implication for an oceanic redox change. *Chemical Geology, 182*, 15–34.

Khin, Z., Meffre, S., Lai, C. K., Burrett, C., Santosh, M., Graham, I., Manaka, T., Salam, A., Kamvong, T., & Cromie, P. (2014). Tectonics and metallogeny of mainland Southeast Asia - a review and contribution. *Gondwana Research, 26*, 5–30.

Königshof, P. (2003). Conodont deformation patterns and textural alteration in Paleozoic conodonts: examples from Germany and France. *Senckenbergiana lethaea, 83*, 149–156.

Königshof, P., Savage, N., Lutat, P., Sardsud, A., Dopieralska, J., Belka, Z., & Racki, G. (2012). Late Devonian sedimentary record of the Paleotethys Ocean - the Mae Sariang section, northwestern Thailand. *Journal of Asian Earth Sciences, 52*, 146–157.

Kosuwan, S., Takashima, I., & Charusiri, P. (2019). *Active fault zones in Thailand*. Website Department of Mineral Resources www.dmr.go.th/.

Kotlyar, G., Shen, S. Z., Kossvaya, O., & Zhuravlev, A. (2007). Middle Permian (Guadalupian) biostratigraphy in South Primorye, Russian Far East and correlation with Northeast China. *Palaeoworld, 16*, 173–189.

Kozur, H. (1975). Beitrage zur Conodontenfauna des Perm. *Geologisch - Palaontologische Mitteilungen, 5*, 1–44.

Kozur, H. (1989). The taxonomy of the gondolellid conodonts in the Permian and Triassic. *Courier Forschunginstitut Senckenberg, 117*, 409–469.

Kozur, H., & Mostler, H. (1994). Anisian to middle Carnian radiolarian zonation and description of some stratigraphically important radiolarians. *Geologisch-Paläontologische Mitteilungen Innsbruck, Sonderband, 3*, 39–255.

Kozur, H., & Wardlaw, B. (2010). The Guadalupian conodont fauna of Rustaq and Wadi Wasit, Oman and a West Texas connection. *Micropaleontology, 56*, 213–231.

Kozur, H., Krainer, K., & Mostler, H. (1996). Radiolarians and facies of the Middle Triassic Loibl Formation, South Alpine Karawanken Mountains (Carinthia Austria). *Geologisch-Paläontologische Mitteilungen Innsbruck, Sonderband, 4*, 195–278.

Lazar, I., Gradinaru, M., & Petrescu, L. (2013). Ferruginous microstromatolites related to Middle Jurassic condensed sequences and hardgrounds (Bucegi Mountains, Southern Carpathians, Romania). *Facies, 59*, 359–390.

Lelievre, H., Janvier, P., Goujet, D., & Blieck, A. (1984). Microrestes de vertébrés du Siluro-Devonien d'Algerie, de Turquie et de Thaïlande. *Geobios, 17*, 851–856.

Lin, Y. L., Yeh, M., Lee, T., Chung, S., Iizuka, Y., & Charusiri, P. (2013). First evidence of the Cambrian basement in Upper Peninsula of Thailand and its implication for crustal and tectonic evolution of the Sibumasu Terrane. *Gondwana Research, 24*, 1031–1037.

Lindström, M. (1970). A suprageneric taxonomy of the conodonts. *Lethaia, 3*, 427–445.

Long, J. A. (1990). Late Devonian chondrichthyans and other microvertebrate remains from northern Thailand. *Journal of Vertebrate Paleontology, 10*, 59–71.

Long, J. A., & Burrett, C. (1989). Fish from the Upper Devonian of the Shan-Thai terrane indicate proximity to east Gondwana and south China terranes. *Geology, 17*, 811–813.

Loydell, D., Udchachon, M., & Burrett, C. (2019). Llandovery (lower Silurian) graptolites from the Sepon Mine, Truong Son Terrane, central Laos and their palaeogeographical significance. *Journal of Asian Earth Science, 170*, 360–374. https://doi.org/10.1016/j.jseaes.2018.11.013.

Mamet, B. L. (1991). Carboniferous calcareous algae. In R. Riding (Ed.), *Calcareous algae and stromatolites* (pp. 370–451). Springer.

Mamet, B., & Preat, A. (2006). Iron-bacterial mediation in Phanerozoic red limestones: state of the art. *Sedimentary Geology, 185*, 147–157. https://doi.org/10.1016/j.sedgeo.2005.12.009.

Marchig, V., Gundlach, H., Möller, P., & Schley, F. (1982). Some geochemical indicators for discrimination between diagenetic and hydrothermal metalliferous sediments. *Marine Geology, 50*, 241–256.

Metcalfe, I. (1984). Stratigraphy, palaeontology and palaeogeography of the Carboniferous of Southeast Asia. *Memoires Société Géologique France (New Series), 147*, 107–118.

Metcalfe, I., Henderson, C., & Wakita, K. (2017). Lower Permian conodonts from Palaeo-Tethys Ocean Plate Stratigraphy in the Chiang Mai-Chiang Rai Suture Zone, northern Thailand. *Gondwana Research, 44*, 54–66.

Michard, A. (1989). Rare earth element systematics in hydrothermal fluids. *Geochimica et Cosmochimica Acta, 53*, 745–750.

Mitchell, A. H. G. (1977). Tectonic settings for emplacement of Southeast Asian tin granites. *Geological Society of Malaysia Bulletin, 9*, 123–140.

Mitchell, A. H. G., Chung, S., Oo, T., Lin, T., & Hung, C. (2012). Zircon U-Pb ages in Myanmar: magmatic-metamorphic events and the closure of a neo-Tethys ocean? *Journal of Asian Earth Sciences, 56*, 1–23. https://doi.org/10.1016/j.jseaes.2012.04.019.

Morley, C. K. (2018). Understanding Sibumasu in the context of ribbon continents. *Gondwana Research, 64*, 184–215.

Murray, R. W. (1994). Chemical criteria to identify the depositional environment of chert: general principles and applications. *Sedimentary Geology, 90*, 213–232.

Murray, R. W., Buchholtz ten Brink, M. R., Jones, D. L., Gerlach, D. C., & Russ, G. P. (1990). Rare earth elements as indicators of different marine depositional environments in chert and shale. *Geology, 18*, 268–271.

Min, M., Lin, K. K., Fang, Q., Chonglakmani, C., & Helmcke, D. (2001). Tracing disrupted outer margin of Paleoeurasian continent through Union of Myanmar. *Journal of China University of Geosciences, 12*, 201–206.

Nozaki, Y. (2010). Rare earth elements and their isotopes in the ocean. In K. K. Turekian (Ed.), *Marine Chemistry and Geochemistry* (pp. 39–51). Academic Press.

Owen, A. W., Armstrong, H. A., & Floyd, J. D. (1999). Rare earth element geochemistry of Upper Ordovician cherts from the southern uplands of Scotland. *Journal of Geological Society of London, 156*, 191–204.

Panjasawatwong, Y. (1999). Petrology and tectonic setting of eruption of basaltic rocks penetrated in well GTE-1, San Kam Phaeng geothermal field, Chiang Mai, northern Thailand. In B. Ratanasthein & S. L. Rieb (Eds.), *Proceedings of the International Symposium on Shallow Tethys (ST) 5, Chiang Mai, Thailand, February 1999* (pp. 242–264). Chiang Mai University.

Panjasawatwong, Y., Phajuy, B., & Hada, S. (2003). Tectonic setting of the Permo-Triassic Chiang Khong volcanic rocks, northern Thailand based on petrochemical characteristics. *Gondwana Research, 6*, 743–755.

Parvizi, T., Rashidi, K., & Vachard, D. (2013). Middle Permian calcareous algae and microproblematica (Dalan Formation, Dena Mountain, High Zagros, SW Iran). *Facies, 59*, 149–177. https://doi.org/10.1007/s10347-012-0357-6.

Phajuy, B., Panjasawatwong, Y., & Osataporn, P. (2005). Preliminary geochemical study of volcanic rocks in the Pang Mayao area, Phrao, Chiang Mai, northern Thailand: tectonic setting of formation. *Journal of Asian Earth Sciences, 24*, 765–776.

Pitfield, P. (1988). Report on the geochemistry of the granites of Thailand. *NERC, British Geological Survey Overseas Directorate Report, WC/88/6,* 1–17.

Pitragool, S., & Panupaisal, S. (1979). Tin and tungsten mineralization of the Mae Lama mining district NW Thailand. *Geological Society of Malaysia Bulletin, 11*, 267–281.

Putthapiban, P. (2002). Geology and geochronology of the igneous rocks of Thailand. In N. Montajit (Ed.), *Symposium on the Geology of Thailand*. 261–283.

Racki, G., Königshof, P., Belka, Z., Dopieralska, J., & Pisarzowska, A. (2019). Diverse depositional and geochemical signatures of the Frasnian-Famennian global event in western Thailand reveal palaeotethyan vs. Western Australian geotectonic affinities. *Journal of Asian Earth Sciences X, 2*, 100010. https://doi.org/10.1016/j.jaesx.2019.100010.

Randon, C., Derycke, C., Blieck, A., Perri, M., & Spalletta, C. (2007). Late Devonian - Early Carboniferous vertebrate microremains from the Carnic Alps, Italy. *Geobios, 40*, 809–827.

Raksakulwang, L., & Bunopas, S. (1985). *Stratigraphy and tectonic evolution in the Mae Hong Son Province, north western Thailand.* Unpublished report of the Royal Thai Department of Mineral Resources. 1–39.

Raksakulwong, L., & Tantiwant, W. (1986). *Investigation report on the Geology of Sheet Ban Huai Pha and Ban Mae La Na*. Unpublished report of the Royal Thai Department of Mineral Resources 1–32. [in Thai]

Ratanasthein, B., Kotcha, K., & Nualngam, S. (2010). Ordovician fossils at Ban Don Sa-ngud, Mae Sariang district, Mae Hong Son, Thailand. In R. Somana, M. Udchachon, K. Lauprasert, P. Lutat, & H. Thassanapak (Eds.), *Abstracts of the 2nd International Conference on Palaeontology of Southeast Asia* (p. 11). Mahasarakham University.

Rejebian, V., Harris, A., & Huebner, J. (1987). Conodont color and textural alteration: an index to regional metamorphism, contact metamorphism and hydrothermal alteration. *Geological Society of America Bulletin, 99*, 471–479.

Ridd, M. F. (1971). Southeast Asia as part of Gondwanaland. *Nature, 234*, 531–533.

Ridd, M. F. (1980). Possible Palaeozoic drift of SE Asia and Triassic collision with China. *Journal of the Geological Society, 137*, 635–640.

Ridd, M. F. (2015a). Should Sibumasu be renamed Sibuma? The case for a discrete Gondwana-derived block embracing western Myanmar, upper Peninsular Thailand and NE Sumatra. *Journal of the Geological Society, 173*, 249–264.

Ridd, M. F. (2015b). East flank of the Sibumasu block in NW Thailand and Myanmar and its possible northward continuation into Yunnan: a review and suggested tectono-stratigraphic interpretation. *Journal Asian Earth Sciences, 104*, 160–174.

Riding, R. (2000). Microbial carbonates: the geological record of calcified bacterial-algal mats and biofilms. *Sedimentology, 47*, 179–214. https://doi.org/10.1046/j.1365-3091.2000.00003.x.

Sanjit, P., Wonganan, N., & Thasod, Y. (2014). Devonian Radiolarian Faunas in Pai Area, Mae Hong Son Province, Northern Thailand: Paleogeographic Implication. *Journal of Science and Technology Mahasarakham University, Thailand, 33*(6), 393–402.

Sarapirome, S., & Khundee, S. (1994). *Preliminary study of the neotectonics of the Mae Hong Son- Khun Yuam Valley* (pp. 1–13.). Bangkok: Report Geological Survey Division, Department of Mineral Resources.

Savage, N. (2013). *Late Devonian conodonts from Northwestern Thailand* (pp.1-48). Eugene, Oregon: Bourland Printing, Trinity Press.

Savage, N. (2019). Frasnian-Famennian transition in western Thailand: conodonts, biofacies, eustatic changes, extinction. *Journal of Paleontology, 93*(*3*), 476–495. https://doi.org/10.1017/jpa.2018.96.

Searle, M., & Morley, C. K. (2011). Tectonic and thermal evolution in the regional context of SE Asia. In M. F. Ridd, A. J. Barber, & M. J. Crow (Eds.), *The Geology of Thailand* (pp. 539–572). Geological Society.

Shi, G., & Archbold, N. (1995). Permian brachiopod faunal sequence of the Shan-Thai terrane. *Journal of Southeast Asian Earth Sciences, 11*, 177–187.

Smith, S. (1941). Some Permian corals from the Plateau Limestone of the Southern Shan States. *Palaeontologica Indica, New Series, 30*(*2*), 1–21.

Sobolev, N. N., & Nakrem, H. A. (1996). Middle Carboniferous-Lower Permian Conodonts of Novaya Zemlya. *Norsk Polarinstitut Skrifter, 199*, 1–129.

Srinak, N., Hisada, K., Kamata, Y., & Charusiri, P. (2007). Stratigraphy of the Mae Sariang Group of Northwestern Thailand: Implication for Paleoenvironments and Tectonic Setting. *The Natural History Journal of Chulalongkorn University, 7*(*2*), 87–108.

Stauffer, P. H. (1974). Malaya and Southeast Asia in the pattern of continental drift. *Geological Society of Malaysia Bulletin, 7*, 89–138.

Sukto, P., Suteethorn, V., Boripatgosol, S., Meesook, A., & Sareerat, S. (1984). *Geologic map of Moulmein 1:250,000.* Geological Survey Division, Department of Mineral Resources Bangkok.

Taylor, S. R., & McLennan, S. M. (1985). *The Continental Crust: Its Composition and Evolution*. Blackwell.

Thassanapak, H. (2008*). The Triassic Radiolarian Cherts from northern Thailand: implications for Palaeoenvironment and Tectonic Setting*. Unpublished Ph.D., thesis (pp. 1-280). Nakhon Ratchasima, Thailand: Suraneree University of Technology.

Thassanapak, H., Feng, Q., Grant-Mackie, J., Chonglakmani, C., & Thanee, N. (2011a). Middle Triassic radiolarian faunas from Chiang Dao, Northern Thailand. *Palaeoworld, 20*, 179–202.

Thassanapak, H., Udchachon, M., Chonglakmani, C., & Feng, Q. (2011b). Geochemistry of Middle Triassic Radiolarian Cherts from Northern Thailand: Implication for Depositional Environment. *Journal of Earth Science, 22*, 688–703.

Thassanapak, H., Udchachon, M., Feng, Q., & Burrett, C. (2017). Middle Triassic radiolarians from cherts/silicified shales in an extensional basin in the Sukhothai Fold Belt, Northern Thailand. *Journal of Earth Science, 28*(*1*), 29–50.

Thassanapak, H., Udchachon, M., & Burrett, C. (2018). Silurian radiolarians from the Sepon Mine, Truong Son Terrane, central Laos and their palaeogeographic and tectonic significance. *Geological Magazine, 155*, 1621–1640.

Thassanapak, H., Udchachon, M., Chareonmit, J., & Burrett, C. (2020). Early Permian radiolarians from Southern Thailand, the deglaciation of Gondwana and the age of the basal Ratburi Group. *Palaeoworld, 29*, 552–567.

Tofke, T., Lumjuan, A., & Helmcke, D. (1993). Triassic syn-orogenic siliciclastics from the area of Mae Sariang (northwestern Thailand). In T. Thanasuthipitak (Ed.), *International Symposium on Biostratigraphy of Mainland Southeast Asia: Facies and Paleontology*, pp. 391-400.

Turner, S. (1997). Sequence of Devonian thelodont scale assemblages in East Gondwana. *Geological Society of America Special Paper, 321*, 1–45.

Udchachon, M., Thassanapak, H., Feng, Q., & Chonglakmani, C. (2011). Geochemical constraints on the depositional environment of Upper Devonian radiolarian cherts from Loei, North Eastern Thailand. *Frontiers of Earth Science, 5*, 178–190.

Udchachon, M., Thassanapak, H., Feng, Q., & Burrett, C. (2015). Palaeoenvironmental Implications of Geochemistry and Radiolarians from Late Devonian Chert/Shale Sequences of the Truong Son Foldbelt, Laos. *Geological Journal, 52*, 154–173. https://doi.org/10.1002/gj.2743.

Udchachon, M., Thassanapak, H., & Burrett, C. (2018). Reworked conodonts from the Lower Permian carbonate turbidites in the Inthanon Terrane, Northern Thailand and their tectonic significance. GeoBonn. p267. (Abstract)

Ueno, K. (1999). Gondwana/Tethys divide in East Asia: solution from Late Paleozoic foraminiferal paleobiogeography. In B. Ratanasthein and S.L. Rieb (Eds.), *Proceedings of the International Symposium on Shallow Tethys (ST) 5*, pp. 45-54.

Ueno, K. (2003). The Permian fusulinoidean faunas of the Sibumasu and Baoshan blocks: their implication for the paleogeographic and paleoclimatologic reconstruction of the Cimmerian continent. *Palaeogeography, Palaeoclimatology, Paleoecology, 193,* 1-24.

Ueno, K. (2006). The Permian antitropical fusulinoidean genus Monodiexodina: distribution, taxonomy, paleobiogeography and paleoecology. *Journal of Asian Earth Sciences, 26*, 380–404.

Ueno, K., & Charoentitirat, T. (2011). Carboniferous and Permian. In M. F. Ridd, A. J. Barber, & M. J. Crow (Eds.), *The Geology of Thailand* (pp. 71–136). Geological Society.

Ueno, T., & Hisada, K. (2001). The Nan-Uttaradit-Sa Kaeo Suture as a main Paleo-Tethyan suture in Thailand; is it real? *Gondwana Research, 4*(*4*), 804–806. https://doi.org/10.1016/S1342-937X(05)70590-6.

Vinn, O., & Mutvei, H. (2009). Calcareous tubeworms of the Phanerozoic. *Estonian Journal of Earth Sciences, 58*, 286–296.

Wang, D., Jiang, H., Gu, S., & Yan, J. (2016). Cisuralian-Guadalupian conodont sequence from the Shaiwa section Ziyun, Guizhou, South China. *Palaeogeography, Palaeoclimatology, Palaeoecology, 457*, 1–22.

Wang, Y.-J., He, H.-Y., Zhang, Y.-Z., Srithai, B., Feng, Q.-L., & Cawood, P. A. (2017). Origin of Permian OIB-like basalts with two differentiation trends in NW Thailand and implication on the Paleotethyan Ocean. *Lithos, 274-275*, 93–105.

Wardlaw, B. R., & Nestell, M. K. (2015). Conodont faunas from a complete basinal succession of the upper part of the Wordian (Middle Permian, Guadalupian, West Texas). *Micropaleontology, 61*, 257–292.

Wilson, M. A., Vinn, O., & Yancey, T. E. (2011). A new microconchid tubeworm from the Lower Permian (Artinskian) of central Texas, USA. *Acta Palaeontologica Polonica, 56*, 785–791. https://doi.org/10.4202/app.2010.0086.

Win, Z., Shwe, K.K. & Yin, O.S. (2017). Sedimentary facies and biotic associations in the Permian-Triassic limestones on the Shan Plateau, Myanmar. In A. J. Barber, Khin Zaw, M.J. Crow (Eds.), *Myanmar: Geology, Resources and Tectonics. Geological Society, London, Memoirs, 48*, 343-363, https://doi.org/10.1144/M48.15

Wiwegwin, W., Hisada, K.-I., Charusiri, P., Kosuwan, S., Pailoplee, S., Saitong, P., Kaowisat, K., & Won-In, K. (2014). Paleoearthquake investigations of the Mae Hong Son Fault, Northern Thailand. *Journal of Earthquake and Tsunami, 8*(*2*), 14500007. https://doi.org/10.1142/S1793431114500079.

Wonganan, N., & Caridroit, M. (2005). Middle and Upper Devonian radiolarian faunas from Chiang Dao area, Chiang Mai Province, northern Thailand. *Micropaleontology, 51*(*1*), 39–57.

Wonganan, N., & Caridroit, M. (2006). Middle to Upper Permian radiolarian faunas from chert blocks in Pai area, northwestern Thailand. *Eclogae Geologica Helvetica, 99*(*supplement 1*), S133–S139.

Xiao, Y., Suzuki, N., & He, W. (2017). Water depths of the latest Permian (Changhsingian) radiolarians estimated from correspondence analysis. *Earth Science Reviews, 173*, 141–158.

Yamamoto, K. (1987). Geochemical characteristics and depositional environments of cherts in the Franciscan and Shimanto Terranes. *Sedimentary Geology, 52*, 65–108.

Yuan, D., Zhang, Y., Shen, S., Henderson, C., Zhang, Y., Zhu, T., An, X., & Feng, H. (2016). Early Permian conodonts from the Xainza area,

central Lhasa Block, Tibet, and their palaeobiogeographical and palaeoclimatic implications. *Journal of Systematic Palaeontology, 14*, 365–383.

Zhang, N., Henderson, C., Xia, W., Wang, G., & Shang, H. (2010). Conodonts and radiolarians through the Cisuralian-Guadalupian boundary from the Pingxiang and Dachongling sections, Guangxi region, South China. *Alcheringa, 34*, 135–160.

Zhang, Y.-C., Aung, K. P., Shen, S.-Z., Zhang, H., Zaw, T., Ding, L., Cai, F.-L., & Sein, K. (2020). Middle Permian fusulines from the Thitsipin Formation of Shan State, Myanmar and their palaeobiogeographical and palaeogeographical implications. *Papers in Palaeontology, 2020*, 1–35. https://doi.org/10.1002/spp2.1298.

Zhao, J., Huang, B., Yan, Y., Bai, Q., Dong, Y., Win, Z., Aung, H. H., & Yang, X. (2020). A palaeomagnetic study of the Middle Permian and Middle Triassic limestones from Shan State, Myanmar: Implications for collision of the Sibumasu Terrane and Indochina Terrane. *Geological Journal, 55*, 1179–1194. https://doi.org/10.1002/gj.3482.

Zhao, J., Sheng, J., Yao, Z., Liang, X., Chen, C., Hui, L., & Liao, Z. (1981). The Changhsingian and Permian-Triassic boundary of South China. *Bulletin Nanjing Institute of Geology and Palaeontology, 2*, 1–131.

Zhou, W.-M., Aung, K. P., Liu, L., Zhang, Y.-C., Zaw, T., Wang, J., & Shen, S.-Z. (2020). First record of Cisuralian-Guadalupian plant fossils from the Shan Plateau, eastern Myanmar. *Palaeoworld, 29*, 108–116.